AEROSOL LIGHTNING ENHANCEMENT OVER NORTHERN ALABAMA:

PREDICTIONS, MECHANISMS, AND SIMULATIONS

A Dissertation

by

TONG REN

Submitted to the Office of Graduate and Professional Studies of
Texas A&M University
in partial fulfillment of the requirements for the degree of

DOCTOR OF PHILOSOPHY

Chair of Committee,	Anita D. Rapp
Co-Chair of Committee,	Sarah D. Brooks
Committee Members,	Robert L. Korty
	Huiyan Sang
Head of Department,	Ping Yang

December 2018

Major Subject: Atmospheric Sciences

ABSTRACT

Satellite aerosol retrievals, ground-based radar and lightning detections, and model simulations are used to study the impact of aerosols on lightning and the usefulness of knowing the aerosol state in predicting enhanced lightning over northern Alabama. The results show that the Moderate Resolution Imaging Spectroradiometer (MODIS) aerosol optical depth (AOD) retrievals are less useful in predicting enhanced lightning flash rate (FR) for lightning-producing storms than the forecasts of other meteorological variables that are more closely linked to the intensification of convective storms. However, when relatively weaker convective available potential energy (CAPE) is forecast, the probability of enhanced lightning FR increases in a more polluted environment, making the knowledge of aerosols more useful in lightning inference in such CAPE regimes. The FR shows a stronger correlation with the optical depth of absorbing aerosols than that of non-absorbing aerosols, particularly in a low CAPE regime, suggestive of a potentially stronger regulation of storms by absorbing aerosols. The presence of absorbing aerosols may lead to the accumulation of CAPE, as suggested by an increased correlation between AOD and CAPE in the presence of absorbing aerosols. The optical depth of absorbing aerosols shows a weak negative correlation with the planetary boundary layer height (PBLH), suggesting that the interaction between absorbing aerosols and turbulent mixing may contribute to the regulation of lightning-producing storms. Aerosol enhancement of lightning may be associated with enhanced convergence in the boundary layer and secondary convection, which appears to result from a synthesis of multiple mechanisms related to both microphysical and radiative effects of aerosols. The impact of absorbing aerosols on deep convection is sensitive to the height of aerosol layer. A sensitivity modeling study suggests that a daytime heating layer

above the PBL suppresses deep convection in the early afternoon and enhances nighttime storms when the accumulated CAPE is released. A daytime heating layer within the PBL delays the onset of the enhanced nighttime storms and may result in a faster development of the storms at night; the enhanced evaporation of cloud and rain water droplets right before the onset of nighttime storms may contribute to the onset delay.

ACKNOWLEDGEMENTS

I would like to thank my committee chair, Dr. Rapp, co-chair, Dr. Brooks, and my committee members, Dr. Korty and Dr. Sang, for their guidance and support throughout the course of this research.

Thanks also go to my friends and colleagues and the department faculty and staff for making my time at Texas A&M University a great experience.

CONTRIBUTORS AND FUNDING SOURCES

This work was supervised by a dissertation committee consisting of advisor Professor Anita Rapp, co-advisor Professor Sarah Brooks, and Professor Robert Korty of the Department of Atmospheric Sciences and Professor Huiyan Sang of the Department of Statistics. All work for the dissertation was completed independently by the student who was supported by NSF Grant AGS-1261392.

TABLE OF CONTENTS

Page

LIST OF FIGURES

Page

LIST OF TABLES

Page

1. INTRODUCTION

The largest uncertainty in global climate change estimation is contributed by aerosol and cloud interactions (Boucher et al. 2013). Aerosols can interact with clouds and hence impact weather and climate through both their microphysical and radiative effects. The aerosol impact on clouds by acting as cloud condensation nuclei (CCN) and ice nuclei (IN) is called the microphysical effect. Some aerosols in the atmosphere are good sunlight absorbers and called absorbing aerosols. Absorbing aerosols can heat the atmosphere and cool the surface by absorbing solar radiation. The impact of absorbing aerosols on clouds by adjusting the thermodynamics is called the radiative effect.

Increased aerosol particles generally have increased CCN and may lead to increased cloud water droplets and optical depth, reflecting more solar radiation back to space and resulting in a cooling effect at the top of atmosphere (Twomey 1977). This cooling effect is called the first aerosol indirect effect or the cloud albedo effect (Solomon et al. 2007). In addition, the resultant increased and smaller cloud water droplets may slow down the droplet collection growth and prolong the lifetime of the cloud (Albrecht 1989). The longer-lived clouds can also cause a cooling effect at the top of atmosphere, which is called the second aerosol indirect effect or the cloud lifetime effect (Solomon et al. 2007). If the suppression of precipitation by increased CCN is during the warm rain phase of a convective cloud, then there will be more supercooled water lifted above the freezing level as the convective cloud grows deeper, resulting in convection invigoration though the release of additional latent heat (e.g. Rosenfeld et al. 2008). When the focus shifts from individual clouds to an ensemble of clouds, modeling studies have suggested that increased CCN result in stronger downdrafts and secondary

convection through enhancing the evaporative cooling (e.g. Tao et al. 2007). Moreover, when the time and spatial scales of the studied system increase, the aerosol-induced changes in different parts and/or stages of the system may be compensated or cancelled, which is called the buffered effect (Stevens and Feingold 2009). Although observational studies have suggested that the presence of ice-nucleating aerosols lower the glaciation temperature of clouds (e.g. Sassen et al. 2003), most studies of the IN impact on clouds rely on models and are far from conclusive (Fan et al. 2016).

Absorbing aerosols can interact with turbulent mixing within the planetary boundary layer (PBL). The presence of absorbing aerosols can affect static stability and may enhance the evaporation of cloud droplets (Hansen, Sato, and Ruedy 1997), which is called the aerosol semi-direct effect (Solomon et al. 2007). The heating of a layer of absorbing aerosols may lead to a capping inversion that suppresses convection, resulting in a gradual accumulation of convective available potential energy (CAPE) and stronger convection when it occurs later (Wang et al. 2013). The suppression of turbulent mixing within the PBL by absorbing aerosols may enhance low-level vertical wind shear (LLVWS) that may play a role in regulating convective systems (Saide et al. 2015). In addition, absorbing aerosols can interact with large-scale flows, causing a spatiotemporal redistribution of precipitation (Lau et al. 2008). Although numerous studies have focused on each of the different ways by which aerosol impact on clouds, whether and how the interactions between aerosols and clouds impact different weather systems remains unclear (Fan et al. 2016). This study aims at gaining more knowledge on aerosol and cloud interactions with a focus on the impact of aerosols on lightning and associated convection. The related mechanisms are highlighted in Figure 1.

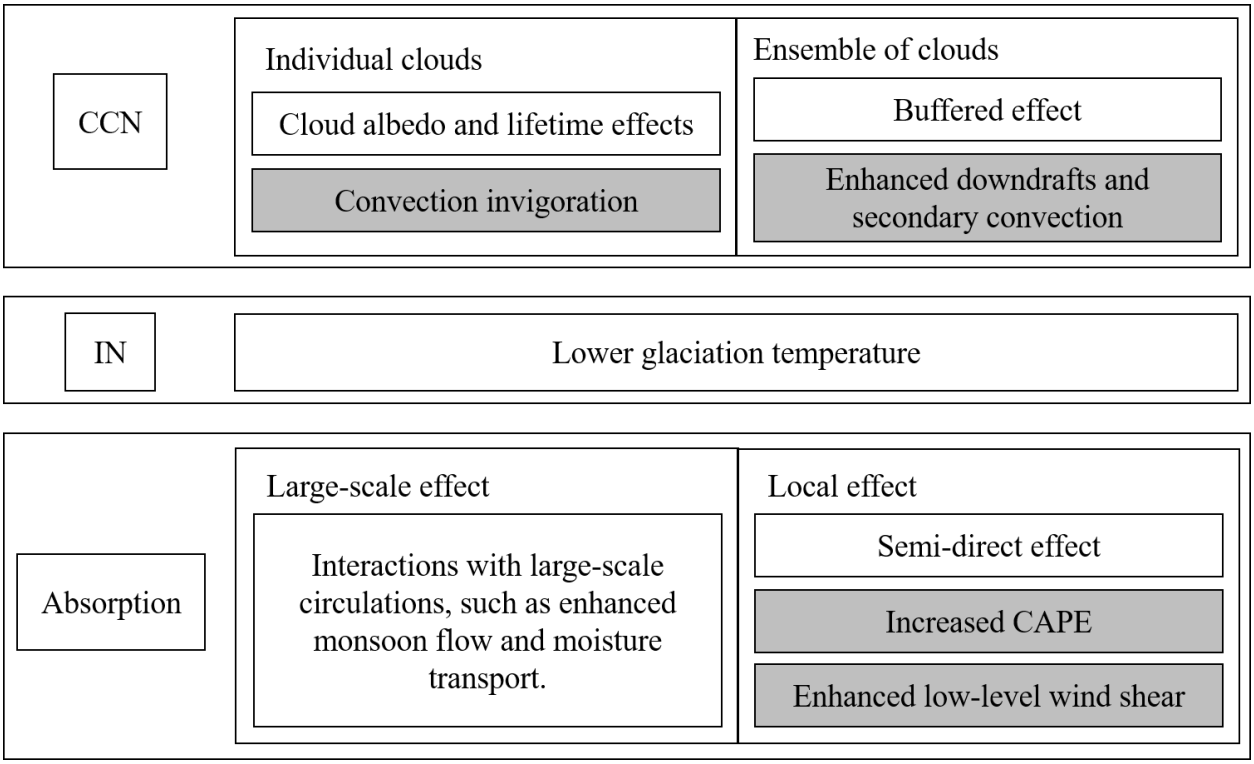

Figure 1. Diagram of different ways by which aerosols impact clouds.

First, satellite aerosol optical depth (AOD) retrievals are correlated with lightning flash rates detected by the Northern Alabama Lightning Mapping Array (NALMA) to study whether the awareness of the aerosol state is useful in predicting enhanced lightning. Then, lightning and associated convection features in the presence of absorbing aerosols are described and analyzed with a focus on examining which of the mechanisms highlighted in Figure 1 may be valid. The observational data of aerosols used are the satellite AOD retrievals, which cannot resolve the vertical distribution of aerosols. However, the response of storms to absorbing aerosols is sensitive to the height of aerosol layer (e.g. Koch and Del Genio 2010). Therefore, at last, model sensitivity experiments of the response of deep convection to daytime aerosol heating at different heights and with different aerosol concentration perturbations are performed. All the three parts

of the study focus on the storms over northern Alabama where long-term lightning observations are available.

2. USEFULNESS OF KNOWING THE AEROSOL STATE IN PREDICTING ENHANCED LIGHTNING FOR LIGHTNING-PRODUCING STORMS OVER NORTHERN ALABAMA[*]

2.1. Introduction

From 2005 to 2014, on average, lightning resulted in 30 fatalities (Holle 2016) in the United States (U.S.). A previous study has shown that from 1959 to 1994, 19,814 cases of property-damage from lightning were reported in the U.S., and the annual mean lightning damage from 1992 to1994 was ~32 million dollars (Curran, Holle, and López 2000). Improving lightning forecasts could help mitigate these threats to life and property.

In a thunderstorm, collisions between ice crystals and graupel particles in the presence of supercooled liquid water transfer positive charge to the particle that is growing the fastest (Saunders et al. 2006, Williams, Zhang, and Rydock 1991). Charge regions then form through differential sedimentation of the ice and graupel in a strong updraft, and discharge in the form of lightning when the electric field reaches the atmospheric breakdown limit. Both the updrafts of a thunderstorm and aerosols in the boundary layer can contribute to changes in the hydrometeor microphysics and hence the magnitude of lightning activity (Mansell and Ziegler 2013, Williams et al. 2002). An adequately strong updraft is necessary for the rapid electrification of a convective cell, presumably because of the promoted particle growth and ice-graupel collisions in the presence of supercooled water, as somewhat evidenced by the enhanced radar measured

---

[*]Part of this section is reprinted with permission from "Is the awareness of the aerosol state useful in predicting enhanced lightning for lightning-producing storms over northern Alabama?" by Tong Ren, Anita D Rapp, Shaima L Nasiri, John R Mecikalski, and Jason Apke, 2018. *Journal of Applied Meteorology and Climatology*, 1663-1681, © Copyright [27 July 2018] by American Meteorology Society.

precipitation and non-precipitation ice mass fluxes (Deierling et al. 2008). With typically higher convective available potential energy (CAPE) upon initiation, the updrafts of continental deep convection are generally stronger than oceanic deep convection (Liu, Zipser, and Nesbitt 2007), which may account for the observation that more lightning events occur over continents than over oceans (e.g. Cecil, Buechler, and Blakeslee 2014, Christian et al. 2003, Zipser 1994). More recent studies suggest that increases in updraft volume rather than maximum updraft speed is the primary contributor to rapid increases in total lightning flash rate on an individual storm basis (Deierling and Petersen 2008, Schultz et al. 2017), although updraft volume and speed are related.

A number of studies have also hypothesized relationships between aerosols ingested into convection and the total lightning. Aerosols can suppress the rainfall during the warm rain phase of deep convection by reducing the droplet size which limits collision and coalescence (e.g. Albrecht 1989, Feingold et al. 2003), and the resultant increased number of particles may be lifted above the freezing level (e.g. Andreae et al. 2004, Khain, Rosenfeld, and Pokrovsky 2005, van den Heever et al. 2006). Consequently, like the effects of a strong updraft, increased supercooled water may reinforce the growth of ice particles, increasing the effectiveness of the non-inductive charging process (Williams et al. 2002). Many observational studies have reported increased lightning activity with increased aerosol ingestion (Albrecht, Morales, and Silva Dias 2011; Altaratz et al. 2010; Altaratz et al. 2014; Orville et al. 2001; Proestakis, Kazadzis, Lagouvardos, Kotroni, Amiridis, et al. 2016; Proestakis, Kazadzis, Lagouvardos, Kotroni, and Kazantzidis 2016; Stolz, Rutledge, and Pierce 2015; Stolz et al. 2017; Storer, Heever, and L'Ecuyer 2014; Wang et al. 2011; Yuan et al. 2011; Yuan et al. 2012). A twelve-year record of flash density over the Houston, Texas area shows a high frequency of summer lightning activity

over the urban and downstream areas of Houston as compared to nearby oceanic regions, which may be in part due to the increased air pollutants from urbanization (Orville et al. 2001) and the petroleum refinery capacity (Steiger et al. 2002). Naccarato et al. (2003) suggested that both urban heat island and aerosol effects contribute to the increased cloud-to-ground (CG) lightning flashes over three large metropolitan areas in Southeastern Brazil. Stolz et al. (2015) suggest that increased lightning rate densities are associated with high normalized CAPE values in combination with high cloud condensation nuclei (CCN) concentrations over the tropics. Stolz et al. (2017) show that total lightning density increases with increasing normalized CAPE, increasing CCN concentration, decreasing warm cloud depth, increasing vertical wind shear, and decreasing relative humidity. Positive correlations between aerosol loading and lightning flashes were found at inter-annual timescales over the West Pacific Ocean (Yuan et al. 2011), the Pearl River Delta megacity area in China (Wang et al. 2011), and the major urban areas in South Korea (Kar, Liou, and Ha 2009). Increased aerosol particles from the exhaust of ships are coincident with enhanced lightning strike rate density over the shipping lanes in the eastern Indian Ocean and the South China Sea (Thornton et al. 2017). However, such positive correlations are not present everywhere (Altaratz et al. 2010; Coquillat et al. 2013; Williams et al. 2002). For example, it appears that the impact of pollutants on lightning activity may be more significant downwind of Paris, France than over the surrounding areas (Coquillat et al. 2013). van den Heever and Cotton (2007) suggested that the development of storms downwind of St. Louis, Missouri is determined by the urban-force convergence rather than the presence of increased aerosols concentrations.

This aerosol-lightning relationship has also been explored during the pre-monsoon season over the Amazon (Williams et al. 2002). Though thunderstorms tend to occur during periods of

relatively higher aerosol concentration in the Amazonian wet season (Albrecht et al. 2011), the radiative forcing of smoke aerosols during the dry season may stabilize the lower troposphere and thus inhibit deep convection and cloud electrification (Altaratz et al. 2010). Rodriguez, da Rocha, and Bombardi (2010) suggested no significant aerosol effect on the development of thunderstorms in austral summer over São Paulo, Brazil. Tan et al. (2016) show a negative correlation between monthly mean AOD and lightning flash density over Nanjing, China. The coupling between microphysics and dynamics has been surveyed by Altaratz et al. (2014) in the context of convection invigoration by aerosols. Previous studies have shown that whether aerosols enhance or suppress convection is dependent on meteorological conditions (e.g., Albrecht, Morales, and Silva Dias 2011; Fan et al. 2009; Storer, Heever, and L'Ecuyer 2014; Storer, van den Heever, and Stephens 2010). Fan et al. (2009) suggest that in the presence of weak wind shear, increased aerosols invigorate isolated deep convection, and the invigoration maximizes as CCN concentration reaches 500 cm^{-3} or higher in their model simulations. In the presence of strong wind shear, increased aerosols may suppress isolated deep convection (Fan et al. 2009). The suppression is even stronger in a more humid environment with a higher CAPE (Fan et al. 2009). Aerosols can modulate the storm response to different forcings, where the storm response to forcings is also affected by available CAPE (Storer, van den Heever, and Stephens 2010). Hence, the aerosol impact on lightning may vary at different locations and times. Parameterizations have been suggested for modeling lightning (e.g. Mansell and Ziegler 2013; Mansell, Ziegler, and Bruning 2010), where the meteorological conditions can be controlled to study the aerosol effects on lightning features (e.g. Wang et al. 2011). Although numerous studies have focused on the linkage between aerosols and lightning, whether aerosol observations are helpful for lightning prediction remains unclear.

Numerous observational studies have compared lightning to radar characteristics of storms (Bringi et al. 1997; Byers and Braham 1949; Carey and Rutledge 1996; Carey and Rutledge 2000; Dye et al. 1986; Goodman et al. 1988; Larsen and Stansbury 1974; Marshall and Radhakant 1978; Schultz, Petersen, and Carey 2011; Schultz et al. 2017; Williams, Weber, and Orville 1989). An exponential growth (or the maximum growth rate) of precipitation ice volume often peaks prior to the peak occurrence of lightning flash rate (FR), with as much as a 20 minute time lag (Carey and Rutledge 1996; Goodman et al. 1988), and this feature has been used for lightning forecasts (Mosier et al. 2011; Vincent et al. 2004) and severe weather warnings (Gatlin and Goodman 2010; Schultz, Petersen, and Carey 2011; Schultz et al. 2017). A radar-measured 40-dBZ intensity echo at the –10˚C isotherm was found as the best indicator of CG lightning with a mean lead time of 14.7 minutes over central North Carolina (Vincent et al. 2004). A tradeoff between lead-time and false alarm rate can be readily made by tuning the radar echo threshold (Vincent et al. 2004). Vertically-integrated ice, a new radar-derived product, has been developed for improving lightning nowcasts over Houston, Texas (Mosier et al. 2011). Simulations from a cloud-resolving model have been used for forecasting lightning threat, but the accuracy of this method is restricted by the model incapability of predicting the instantaneous locations of a storm (McCaul Jr et al. 2009). In addition, synoptic map analyses—such as the forecast 18- and 30-hour sea level pressure fields—are useful for analyzing the distribution of thunderstorms and thus lightning over an area (Reap 1994). Moreover, regional geostationary satellite and radar observations in advance of first-flash lightning have been documented (Harris et al. 2010; Mecikalski et al. 2013).

Although various techniques have been used for forecasting lightning formation, to the best of our knowledge, none of these techniques has included satellite aerosol retrievals in

prediction. The objective of this study is to examine if satellite aerosol retrievals are useful for prediction of enhanced lightning in lightning-producing storms. The objective is achieved by the following: (1) examine if the aerosol products currently available can be used for potential lightning inferences, in terms of FRs, and (2) determine how useful the aerosol state in statistical inference models is compared to the forecast of other meteorological variables in the context of enhanced lightning FR inferences.

2.2. Data and Methodology

2.2.1. Lightning flashes

This study focuses on the northern Alabama region of the U. S. where lightning data have been collected and archived by the North Alabama Lightning Mapping Array (NALMA) since 2002 (Goodman et al. 2005; Koshak et al. 2004). Total (intra-cloud and cloud-to-ground) lightning flashes are derived (McCaul Jr et al. 2005) from the NALMA very-high-frequency (VHF) source data for each June-July-August (JJA) time-period when lightning is most active (e.g. Albrecht et al. 2016; Christian et al. 2003). The detection efficiency of the NALMA is a function of distance and azimuthal angle (Chmielewski and Bruning 2016). Figure 2 shows the distributions of the mean FR during 14:00–17:00 Local Standard Time (LST) in JJA from 2002–2014 over northern Alabama. The LST is 6 hours behind the Coordinated Universal Time (UTC), i.e. LST = UTC – 06:00. Because the location uncertainty of the VHF sources increases with distance (Thomas et al. 2004), we show only the flashes that occurred within a circle centered at the LMA network with a radius of 150 km, where the detection efficiency is greater than 90% (Chmielewski and Bruning 2016).

Only lightning events that are detected by at least 6 stations are archived by LMAs (Rison et al. 1999). The FR distributions shown in Figure 2(a-d) were filtered using different

thresholds of station numbers. In agreement with the recent study of Chmielewski and Bruning (2016), the NALMA detection efficiency is dependent upon the azimuthal angle and distance (Figure 2). Because the following analyses are based on the lightning statistics of individual storm samples averaged over the circle centered at the NALMA with a radius of 150 km, the bias in detected flashes that results from the detection efficiency variation does not affect the results. Use of an increased station number threshold may remedy the azimuthal variability of detected lightning flashes, but also could reduce the number of identified flash events, and thus a tradeoff must be made.

We selected the flashes that were detected by at least 7 stations for reducing the difference between the detection efficiencies of the NALMA at the center and edge of the study area. As shown in Figure 2(b), although the azimuthal variability is not completely removed, an adequate number of flash events is retained for statistical analysis. However, Figure 2(c-d) show that if only the strongest flash events are used, then no flashes are identified in parts of the circular area. Specifying such stringent criteria would preclude the analysis of storms with lower FRs.

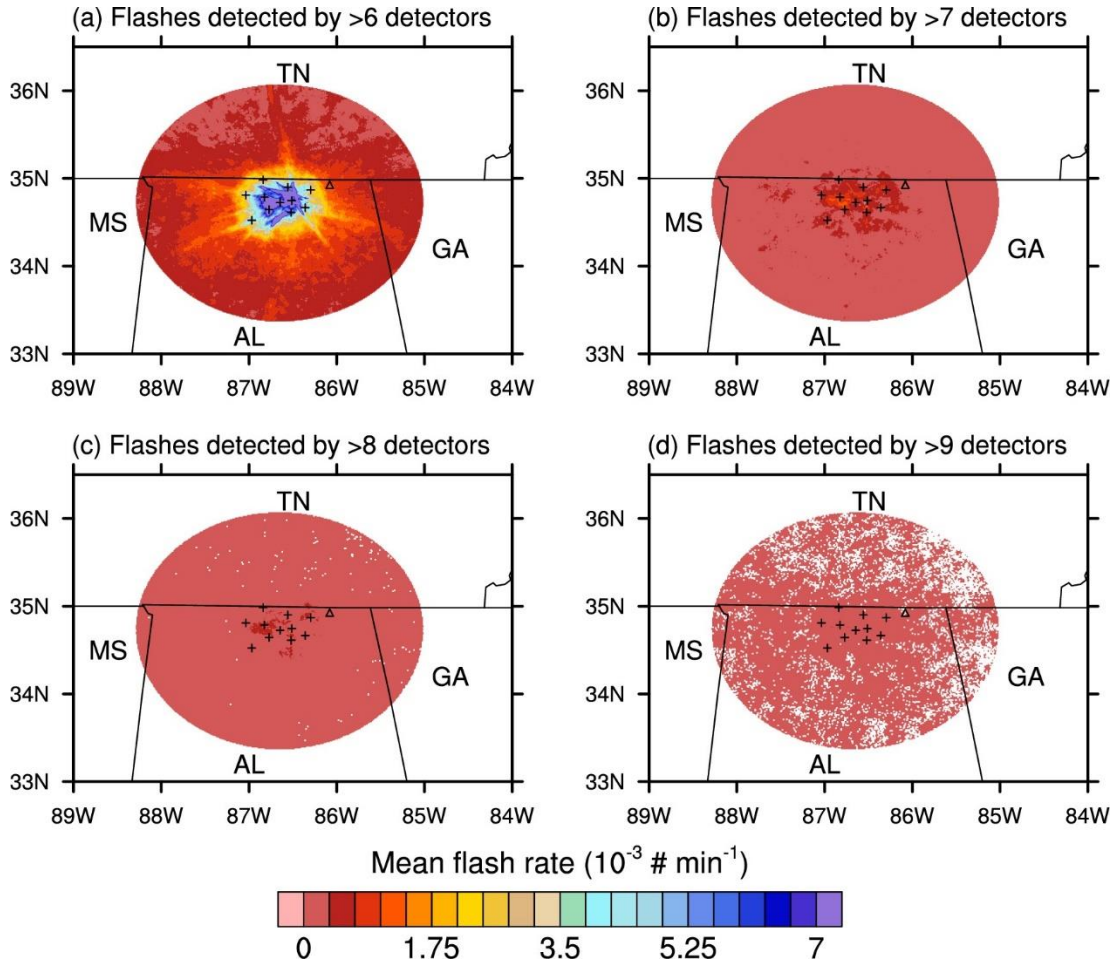

Figure 2. Distributions of the mean flash rate (10^{-3} # min^{-1}) during 14:00–17:00 LST in JJA from 2002–2014 over northern Alabama. The flashes that were included in the mean flash rate were detected by at least 6, 7, 8, and 9 stations in panels (a), (b), (c), and (d), respectively. For example, the flash events in (a) are detected by 6 or more stations, while the flash events in (b) were detected by 7 or more stations. AL, GA, MS, and TN are short for Alabama, Georgia, Mississippi, and Tennessee, respectively. The + symbols show the detector locations of the NALMA. The triangle is the location of the NEXRAD KHTX site.

2.2.2. Satellite and ground-based aerosol retrievals

Aerosol conditions in terms of AOD can be retrieved globally from satellite observations. Currently, the Multi-angle Imaging Spectroradiometer (MISR), the Moderate-resolution Imaging Spectroradiometer (MODIS), and the Ozone Monitoring Instrument (OMI) on-board the Aqua and Terra satellites have more than 10 years of aerosol retrievals, which can be used to study the

potential of applying satellite aerosol retrievals for lightning prediction. Unlike MODIS and MISR, OMI is not designed for aerosol retrievals. OMI aerosol products contain AOD at satellite channel wavelengths 354 nm, 388 nm, and 500 nm, among which the 500 nm AOD is derived by extrapolation and hence is of a lower accuracy (Livingston et al., 2009). The swath of aerosols retrievals from MISR (Martonchik and Diner 1992; Martonchik et al. 1998) is 360 km wide, while the swath of MODIS aerosol retrievals (Levy et al. 2007a,b) is 2,330 km wide. Depending on the latitude, MODIS and MISR have global coverage of 1-2 days and 2-9 days, respectively (e.g. Liu et al. 2007b). In other words, during a period such as a week during summer, MODIS aerosol retrievals are available more frequently than MISR aerosol retrievals, and hence MODIS provides more samples than MISR for studying the usefulness of aerosol retrievals in statistical models of lightning inferences.

The presence of aerosols over the dark surface scatters more incident solar radiation back to the space. The MODIS aerosol retrieval algorithm makes use of the observations from two visible (0.47 μm and 0.66 μm) and one near-infrared (2.12 μm) channels to detect aerosol signals, where empirical relationships between the surface reflectance at 2.12 μm and the ones at the two visible bands are assumed (Levy, Remer, and Dubovik 2007; Levy et al. 2007). AOD is a column-averaged quantity. Theoretically, all the layers of aerosol particles in the vertical atmospheric column contribute to the backscattered solar radiation received by the sensor. In the atmosphere, often most aerosol particles are within the planetary boundary layer (PBL) and the aerosol concentration decreases exponentially with height above the PBL (e.g. He et al. 2008). MODIS AOD retrievals can characterize the aerosol loading within the PBL but cannot resolve their vertical distribution. Moreover, MODIS AOD retrievals only apply to clear sky conditions. AOD cannot be retrieved from the MODIS measurements if there is a cloud. Both the 3-km

spatial resolution Collection 6 Terra and Aqua MODIS L2_04 aerosol retrievals (Levy et al. 2013) are used for this study.

In the daytime, the Terra satellite passes northern Alabama around noon, and the Aqua satellite passes northern Alabama in the early afternoon. If the storms occur a long period after the satellite overpass, then the MODIS AOD retrievals may not represent the aerosol conditions when the storms occur, because aerosol properties change over time (Liu et al. 2011; Smirnov et al. 2002). Fortunately, lightning flash rate generally peaks in the late afternoon over continents (Blakeslee et al. 2014; Williams and Heckman 1993). Over North America, the annual flash rate peaks at 1500 LST (Blakeslee et al. 2014), a few hours later than the Terra and Aqua overpass times. Figure 3 shows the averaged diurnal variation of the logarithm base 10 of FR ($\log_{10}$(FR)) for JJAs from 2002 to 2014 over northern Alabama. As shown in Figure 3, $\log_{10}$(FR) peaks around 14:00–17:00 LST, in agreement with previous studies (Blakeslee et al. 2014; Williams and Heckman 1993). The diurnal variation of $\log_{10}$(FR) suggests that most lightning events occur a few hours after the satellite overpass times. Therefore, this study focuses on the most active lightning period 14:00–17:00 LST right after the Aqua satellite overpass time.

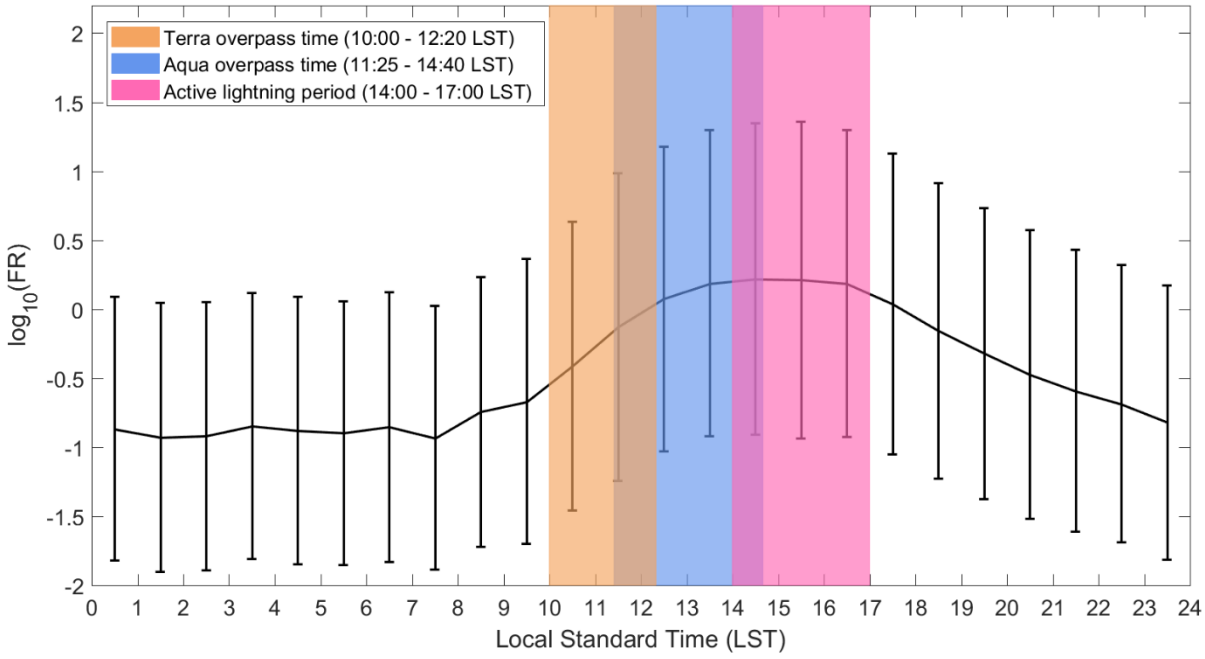

Figure 3. Mean diurnal variation of the logarithm (base 10) of flash rate in JJA from 2002 to 2014 over northern Alabama. The error bars show the standard deviations. The brown-shaded area shows the range of the Terra satellite overpass times, and the blue-shaded area shows the range of the Aqua satellite overpass times.
.

It has been reported that the uncertainty of MODIS AOD retrievals over land is about ± 0.05 ± 0.20×AOD with a root mean square error (RMSE) less than 0.1 (Chu et al. 2002). To assess whether the MODIS AOD errors are small enough to be useful for this study, the MODIS AOD retrievals in 2008 and 2009 are compared with the AErosol RObotic NETwork (AERONET; Holben et al. 1998) Level 2.0 AOD data from the University of Alabama in Huntsville (UAH) site (34˚43′30″ N, 86˚38′42″ W), which are cloud-screened and quality-assured. AERONET is a network of Sun photometers, which point directly at the sun. AOD can be retrieved from the Sun photometer measurement of sunlight attenuation along the atmospheric

path if it is clear of clouds. Ichoku et al. (2002) suggested that a 50 x 50 km^2 air mass captured by MODIS over a Sun photometer site will be sampled by the Sun photometer during 1 hour, and the correlations decrease as the area increases (Kovacs 2006). We compare the averaged MODIS aerosol retrievals over a circle centered at the UAH site with a radius of 50 km with the AERONET AODs averaged 30 min before and after the satellite overpass time. The AOD retrievals are available only in 2008 and 2009 at the UAH site of AERONET. The result of this comparison is discussed in Section 2.3.1.

2.2.3. Meteorological variables

As apparent in Section 2.2.1, correlations between aerosols and lightning, if present, do not necessarily reveal a causal relationship between them. Such correlations could also be related to associations between aerosols and the meteorological conditions that dominate or regulate convection and lightning. In other words, forecasts of the meteorological variables related to such conditions—including updraft strength (Zipser and Lutz 1994), organization of convection (Krehbiel et al. 2000; MacGorman and Rust 1998), and synoptic weather environment (Jacobson and Krider 1976)—may be more useful than satellite aerosol retrievals in terms of lightning prediction. Therefore, in addition to the correlation analysis of aerosols and lightning, correlation analyses were performed of meteorological forecasts and lightning. The following meteorological variables were analyzed: forecasts of CAPE that are a measure of the maximum speed of the updraft in the absence of background shear (Emanuel 1994); the vertical wind shear that plays an important role in convection organization (Robe and Emanuel 2001; Rotunno, Klemp, and Weisman 1988; Weisman and Klemp 1982); and the prevailing wind direction at 850 hPa that indicates the synoptic-scale air mass in the southeastern U.S. summer precipitation regime (Li, Li, and Kushnir 2012). The vertical wind shear between 850 and 200 hPa is adopted

here, for it is one of the noteworthy synoptic features of the warm season heavy rainfall over the interior southeastern U.S. (Konrad 1997).

Global CAPE fields are derived from the European Centre for Medium-Range Weather Forecasts (ECMWF) ERA-Interim forecast (Dee et al. 2011). We call the derived CAPE fields CAPE forecast hereinafter. The CAPE forecast is initialized twice a day at 00:00 and 12:00 UTC. We use the 9–hour CAPE forecast field that is initialized at 12:00 UTC (06:00 LST) so that the CAPE forecast is at 21:00 UTC (15:00 LST), which falls within the active lightning period—14:00–17:00 LST. The horizontal resolution of the CAPE forecast is 0.75°. Because the ERA-Interim 6-hourly normal wind field data and forecasts are not freely available at 15:00 LST, 3-hourly 1.25° wind field reanalysis data were used from the Modern Era Retrospective Reanalysis (MERRA) (Rienecker et al. 2011) to calculate the wind shear and wind direction at 15:00 LST. The MERRA wind shear data highly agree with the observations at nearest weather stations at 06:00 LST (not shown), suggesting the uncertainty introduced by using different sets of forecast/reanalysis data is small.

2.2.4. Analysis steps

The probability distribution of the flash rate (FR; # min^{-1}) during the active lightning period over the study area in Figure 2 is highly skewed, so a logarithmic transformation (base 10) is applied for a distribution close to normal. The distribution is presented in the results section (Section 2.3.2). The domain-averaged Terra and Aqua AOD retrievals are then matched with later afternoon lightning events during 14:00–17:00 LST in the 13 summers from 2002–2014 for studying the statistical relationship between AOD and the logarithm of flash rate, $\log_{10}$(FR). Only satellite overpasses with at least 20 MODIS AOD retrievals are kept so that the average AOD is adequately representative over our study area. In addition, MODIS cannot

discern between some thin clouds and aerosols, and the thin clouds are wrongly regarded as aerosols for optical depth retrievals. In other words, some cloudy pixels that show large optical depths are misinterpreted by MODIS as clear sky pixels with heavy pollution. Therefore, the mean AODs that exceed 1.0 are discarded to remove the potential false heavy pollution cases, although it should be noted that this criterion may also remove some real heavy pollution cases (Van Donkelaar et al. 2011) and cannot remove all the false cases. The cloud influence can be avoided by making use of chemistry models (Stolz, Rutledge, and Pierce 2015; Stolz et al. 2017; Storer, Heever, and L'Ecuyer 2014) to estimate AOD (or CCN concentration). Andreae (2009) suggests a power law relation between AOD at 500 nm and CCN concentration (# cm^{-3}) at a supersaturation of 0.4%, where $AOD = 0.0027 \cdot CCN^{0.640}$. This empirical relation is adopted here to estimate CCN concentration using MODIS AOD retrievals. Because CCN rather than aerosols are the main players in the cloud microphysics that impact the lightning activity (Williams et al. 2002), the results of the analyses in this study are shown in both AOD and CCN scales. In addition, as previously mentioned, whether aerosols invigorate or suppress deep convection is dependent on meteorological conditions (e.g., Fan et al. 2009; Storer, van den Heever, and Stephens 2010) and hence the usefulness of aerosol information for lightning prediction may vary with environments. The domain-averaged CAPE forecast, wind shear, and wind direction data are matched with afternoon lightning for studying the statistical relationships between these variables and $\log_{10}$(FR). The cases are further separated into prescribed CAPE forecast and wind shear categories, and then AOD is correlated with $\log_{10}$(FR) for each category. The results of the correlation analyses are presented in Sections 2.3.2 and 2.3.3.

Because the majority of lightning flashes occur over the deep convective area (DCA; e.g., Holle et al. 1994; Vincent et al. 2004), an association between AOD and increased FR could be

due to an enhancement in deep convective area in conditions also favorable for high AOD. The Level 3 composite radar reflectivity data from the Hytop, Alabama (34.927 N, 86.080 W) KHTX Next Generation Weather Radar System (NEXRAD) as marked in Figure 2 are used to define the DCA. The fraction of DCA (F_{DCA}) is estimated by calculating the fraction of the study area where the composite radar reflectivity is greater than a threshold (30, 35, and 40 dBZ). The DCA defined as such includes not only the area of the updraft cores but also the area of heavy stratiform precipitation that meets the reflectivity threshold. It is merely a rough estimation of the storm area where lightning is likely to occur, which is similar with the Larsen area (Carey and Rutledge 2000; Larsen and Stansbury 1974). The mean F_{DCA} is calculated by averaging the corresponding values for all the radar scans during the active lightning period. To determine how the FR changes with the DCA, the FR/DCA is calculated by normalizing the FR during radar scans by the DCA. All lightning flashes over the study region within 4 min after the time of the radar scan are counted. The mean FR/DCA is calculated by averaging the corresponding values for all scans during the active lightning period. The domain-averaged AOD is then correlated with the logarithm (base 10) of the mean fraction of DCA and the logarithm (base 10) of the mean areal FR. The results of the correlation analyses are presented in Section 2.3.5.

In addition, in some cases, the detected VHF sources do not look like lightning discharges. These detected sources are often sparsely distributed over the study area where no high composite radar reflectivity area (i.e. DCA) is present. In the correlation analyses of this study, only those cases when a DCA is detected by the radar during the active lightning period are kept. The composite radar reflectivity threshold of 30 dBZ is chosen to filter the storm-related lightning cases. Table 1 documents the sources of all the data used in this study. A flow chart of analysis steps is shown in Figure 4. The following results section starts with the

comparison between MODIS and AERONET AOD retrievals, followed by the correlation analyses of AOD and lightning flashes in different meteorological conditions. Then, the probability of enhanced lightning conditioned on AOD and CAPE forecast is presented. Caveats about the causality of the correlations are discussed last.

Table 1. Data sources.

Variables	Sources
Lightning flash	NALMA
AOD	MODIS (Terra and Aqua) Level 2 Collection 6
	AERONET (UAH) Level 2.0
CAPE forecast	ECMWF ERA-Interim
Wind shear	MERRA
Composite radar reflectivity	NEXRAD (KHTX) Level 3

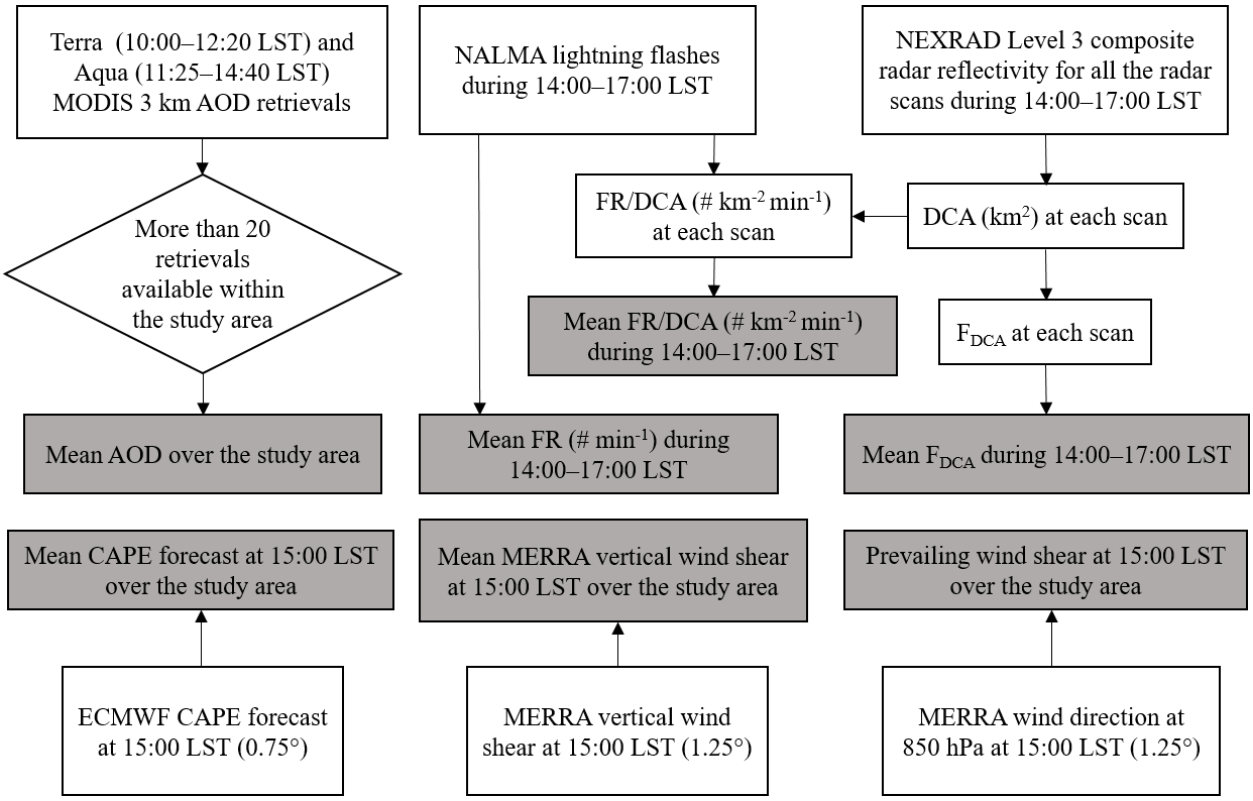

Figure 4. Flowchart of analysis steps

2.3. Results

2.3.1. Validations of MODIS AOD retrievals

Satellite AOD retrievals are representative of the aerosol conditions when storms occur only if the change of aerosol particle concentration between the time of the satellite observation and active lightning period is small. The afternoon active lightning period is about 2–4 hours later than the satellite overpass time. Figure 5 shows mean diurnal variation of AOD at 550 nm in JJA from 2008 to 2009 at the UAH site of AERONET. At each time, the error bar shows the standard error, which is defined as the ratio of the associated standard deviation to square root of sample number. As observed by the ground-based Sun photometer, on average, the daytime variation of AOD over northern Alabama is small with an amplitude of about 0.03. AOD is

maximum during 10:00 to 11:00, which corresponds to the Terra overpass period. AERONET AOD is at its minimum from 14:00 to 15:00 LST, which corresponds to the end of the Aqua overpass and beginning of the active lightning period. Therefore, Aqua aerosol retrievals are probably more representative of the aerosol state during the active lightning period. The diurnal variation of aerosol particle (or CCN) concentration is largely affected by local and regional weather conditions, including the type of air mass, wind direction, and the formation and dissipation of cumulus clouds upwind of the measuring site (e.g. Jin, Shepherd, and King 2005; Radke and Hobbs 1969; Shen et al. 2011). Increases in CCN concentration often stem from new particle formations (Sihto et al. 2011). The diurnal variation of AOD shown in Figure 5 resembles those previously reported at Midway Island and Tahiti (Smirnov et al. 2002).

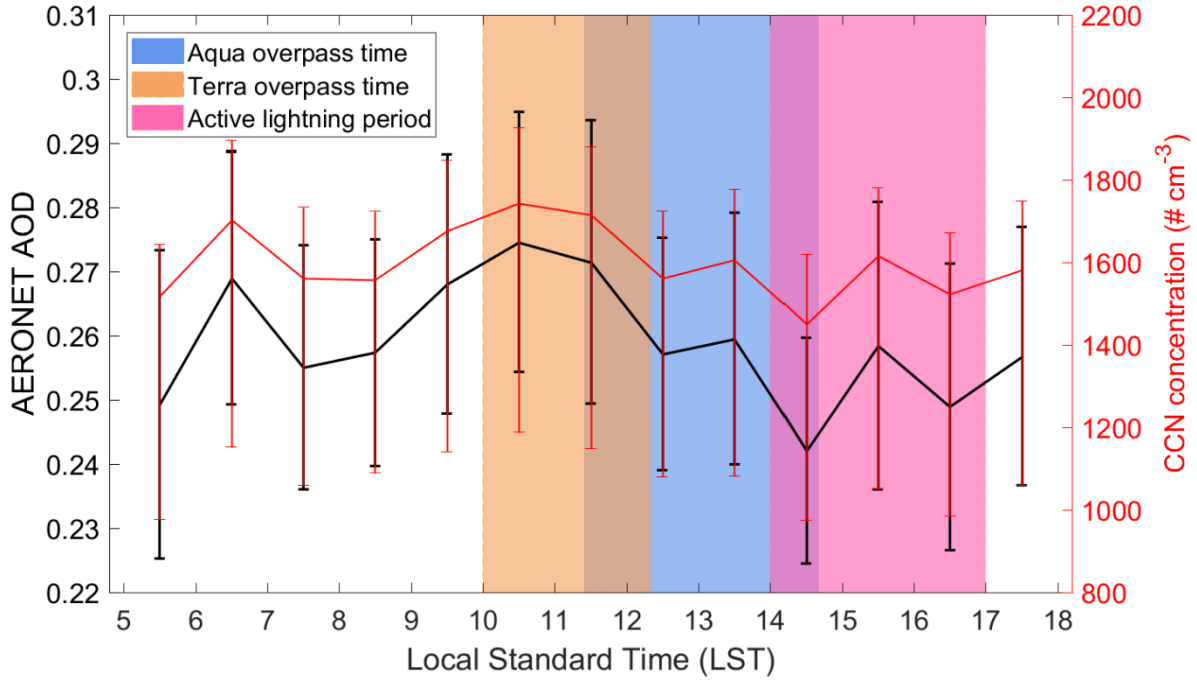

Figure 5. Mean diurnal variation of AOD at 550 nm (black curve; left Y-axis) and associated CCN concentration estimation (Andreae 2009; red curve; right Y-axis) in JJA from 2008 to 2009 at the UAH site of AERONET. The error bars show the standard errors. The brown, blue, and pink shaded areas correspond to the Terra overpass time interval, the Aqua overpass time interval, and the active lightning period (14:00 to 17:00 LST), respectively.

In addition, the uncertainties of the MODIS AOD retrievals need to be small enough so that significant differences in aerosol loadings can be distinguished. Thus, the MODIS AOD retrievals are compared with those at the UAH AERONET site. As shown in Figure 6, the proportions of samples that fall within the error estimates are 64.3% and 46.3% for the Terra and Aqua MODIS retrievals, respectively. The RMSEs of the two are 0.145 and 0.132, respectively, greater than the previously reported 0.1 (Chu et al. 2002). It appears that the MODIS AOD retrievals are larger than those from AERONET. However, as shown in Figure 6, the “low” and

"high" aerosol loading cases can be distinguished in the AOD retrievals, suggesting the possibility of applying the retrievals for lightning predictions.

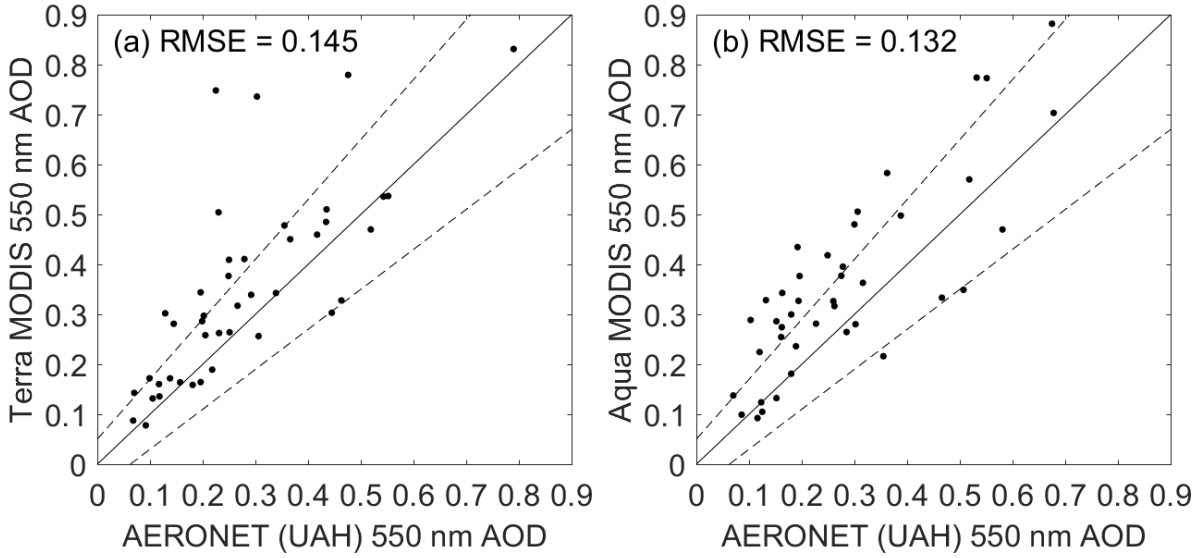

Figure 6. Scatterplots of MODIS and AERONET AOD retrievals at 550 nm in the JJAs from 2008 to 2009. The left and right panels are for Terra and Aqua MODIS, respectively. In each panel, the two dashed lines mark the previously reported MODIS AOD uncertainties ± 0.05 ± 0.20×AOD (Chu et al. 2002). Each MODIS AOD is the average over a circle centered at the UAH site with a radius of 50 km. Each AERONET AOD is the average 0.5 hour before and after the satellite overpass time.

2.3.2. Statistical relationships

Figure 7 shows the probability distributions of FR and $\log_{10}$(FR) during 14:00–17:00 LST in the JJAs from 2002–2014 over northern Alabama. The FR during the active lightning period has a strong variation, ranging 7 orders of magnitude. The probability distribution of FR is highly skewed. Many cases have low FRs and a few cases have extraordinarily high FRs. After the logarithmic transformation, the distribution of FR has a more normal distribution. The mean (M) and standard deviation (σ) of $\log_{10}$(FR) are 0.31 and 1.07, respectively. Figure 8 shows the

scatterplots of $\log_{10}$(FR) and MODIS AOD retrievals. It appears that both Terra and Aqua MODIS AOD retrievals are only weakly correlated with $\log_{10}$(FR) with correlation coefficients of 0.127 and 0.122, respectively. The apparent weak association between AOD and $\log_{10}$(FR) is not necessarily indicative of a causal relationship. Presumably, it is contributed in part by the aerosol invigoration of convection as suggested by previous studies (e.g. Williams et al. 2002). However, because precipitation scavenging is a highly efficient removal mechanism of water-soluble aerosol particles (Atlas and Giam 1988; Hales and Dana 1979), we speculate that the concentration of air pollution may gradually increase in consecutive non-rainy days and produce a high value right before being washed out. Moreover, the polluted environment might tend to be associated with particular meteorological conditions that occasionally lead to enhanced lightning. These hypothetical linkages could also lead to the weak positive correlation between AOD and $\log_{10}$(FR). Some of the noise in the relationship can be smoothed out if the data are binned into discrete intervals (Stolz et al. 2017), but the strength of the positive correlation depends on the number of bins selected (not shown).

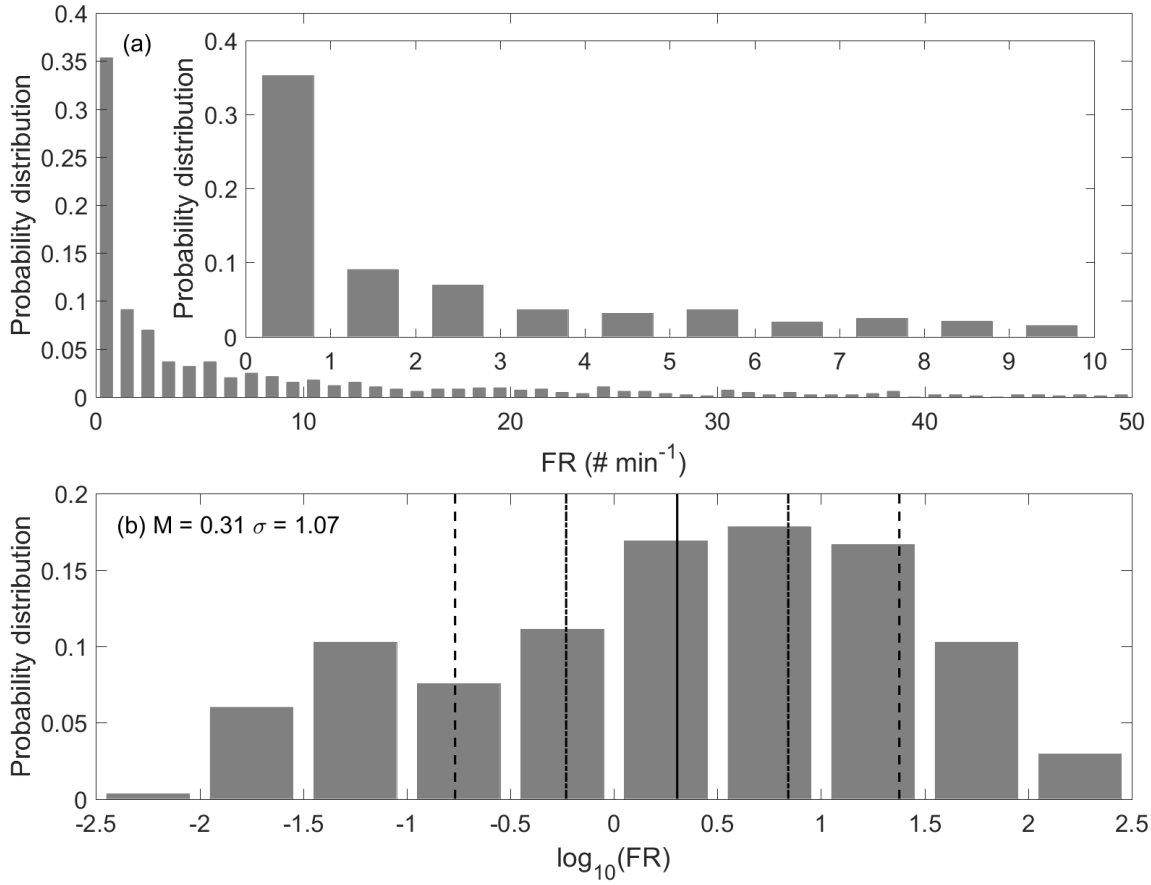

Figure 7. The probability distributions of flash rate in # min^{-1} (a) and the logarithm of flash rate (b) during 14:00-17:00 LST in the JJAs from 2002 to 2014 over northern Alabama. The inset of the upper panel is a close-up of the samples with a flash rate less than 10 # min^{-1}. M and σ are the mean and standard deviation of the logarithm of flash rate, respectively. The solid back line denotes the mean; the two dashed lines denote M ± σ, respectively; and the two dot-dashed lines denote M ± σ/2, respectively.

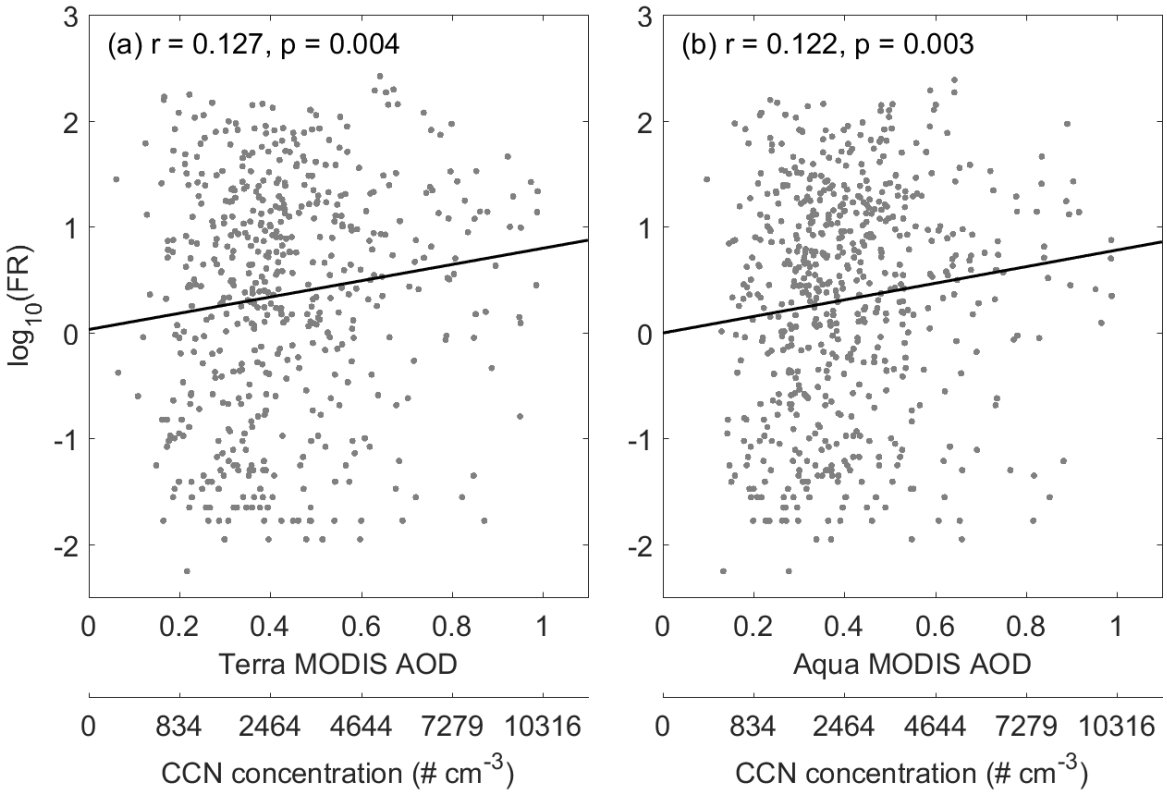

Figure 8. Scatterplots of the logarithm of flash rate and the mean MODIS AOD with associated CCN scale using Andreae (2009). The left and right panels are for Terra and Aqua, respectively. In each panel, the solid line is the linear regression. r is the correlation coefficient and p is the p-value of the *t* test.

2.3.3. Correlations in different meteorological conditions

Previous studies (e.g. Rodriguez, da Rocha, and Bombardi 2010; Williams et al. 2002) have suggested that meteorological conditions may be more important than aerosols in regulating convection and lightning. Figures 9(a) and 9(b) show the scatterplots of the $\log_{10}$(FR) and the square root of CAPE ($CAPE^{1/2}$) forecast and the $\log_{10}$(FR) and the wind shear, respectively. The $CAPE^{1/2}$, an indicator of the maximum updraft without background shear, has a moderate correlation with the $\log_{10}$(FR), stronger than those between the MODIS AOD and the $\log_{10}$(FR). The correlation coefficient is 0.530. These results agree with the previous studies (e.g. Williams

et al. 2002; Zipser and Lutz 1994), which underscores the remarkable role the strong updraft plays in determining the lightning FR.

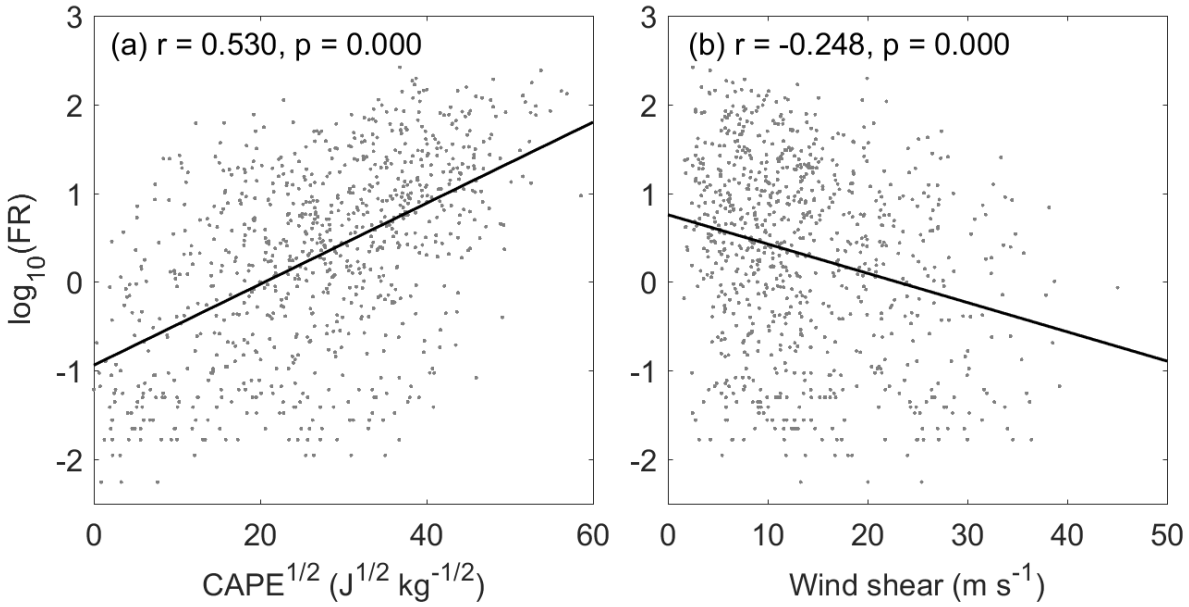

Figure 9. Scatterplot of the logarithm of flash rate and the square root of CAPE forecast (a), and scatterplot of the logarithm of flash rate and the wind shear (b). In each panel, the solid line is the linear regression. r is the correlation coefficient and p is the p-value of the *t* test.

Increasing the vertical wind shear above the boundary layer generally leads to stronger organized convection (Robe and Emanuel 2001) and hence more flashes. By contrast, the wind shear shows a weak negative correlation with $\log_{10}$(FR) with a correlation coefficient of -0.248. The negative correlation between the wind shear and $\log_{10}$(FR) in this study may be explained by the negative association between the wind shear and the CAPE (not shown). In the summer when solar heating and CAPE tend to be strongest, the upper jet stream is often located north of Alabama, leading to decreased deep-layer vertical wind shear, yet adequate instability for thunderstorms that could still have a high FR. In the mesoscale convective complex, the deep-

layer vertical wind shear can be weakened as convection intensifies via the vertical momentum transport (Wu and Yanai 1994).

The correlations between the MODIS AOD retrievals and $\log_{10}$(FR) are weak (Figure 8). However, as previously mentioned, whether aerosols enhance or suppress convection is dependent upon CAPE and wind shear (Fan et al. 2009; Storer, van den Heever, and Stephens 2010). Therefore, the correlation between aerosols and FR, and hence the usefulness of the MODIS AOD retrievals in predicting lightning, may vary with meteorological conditions. Figure 10 shows the correlation coefficients between the mean MODIS AOD and the $\log_{10}$(FR) in different wind shear and CAPE forecast groups. The strongest correlation between the MODIS AOD and the $\log_{10}$(FR) is present when wind shear is weak (Figure 10), in agreement with Fan et al. (2009). The correlation appears to be strongest and most significant if the forecast CAPE is low and the wind shear is weak. As a result, the MODIS AOD-based enhanced lightning tendency information might be more useful in terms of forecast metrics, if a weak wind shear and/or low CAPE environment is forecast. However, the forecasts of variables CAPE and wind shear still have stronger correlations with lightning FR (Figure 9).

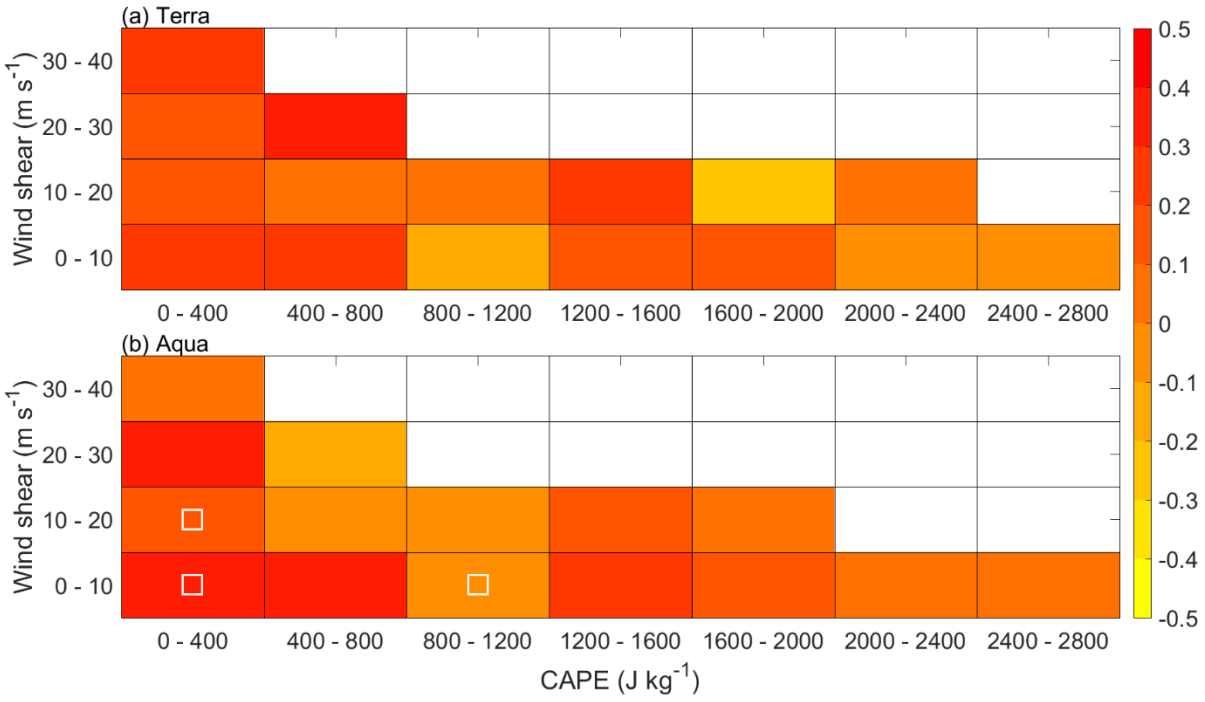

Figure 10. Correlation coefficients between the MODIS AOD and the $\log_{10}$(FR) in different wind shear and CAPE forecast categories. The upper and lower panels are for the Terra and Aqua cases, respectively. White squares denote the correlations that pass the *t* test at a significance level of 0.05.

Figures 11(a) and 11(b) show the boxplot of $\log_{10}$(FR) in different wind direction regimes and the corresponding sample proportions, respectively. The prevailing wind observations are grouped into one of the eight directions, north (N), northeast (NE), east (E), southeast (SE), south (S), southwest (SW), west (W), and northwest (NW), over the study area using the MERRA 850 hPa wind data. It appears that $\log_{10}$(FR) is somewhat dependent upon prevailing wind directions. A large portion of lightning cases are associated with days with prevailing westerly winds (Figure 11), and such lightning events appear to be stronger than those associated with easterlies in terms of the median of $\log_{10}$(FR) (Figure 11), suggesting that wind directions may be indicative of air mass and intensification of convection. The storms with relatively higher FRs

over the study area from the west may be associated with baroclinicity, or cases of baroclinic Rossby-type short waves, while the storms with relatively low FRs from the east may be local thermally-driven thunderstorms. A comparison of Figures 8, 9, and 11 suggests that aerosols are less important than thermodynamics in shaping the FR in a convective system. Forecasts of other meteorological variables that are more closely linked to the intensification of convection, such as $CAPE^{1/2}$, are without doubt more useful than satellite AOD retrievals in lightning inferences.

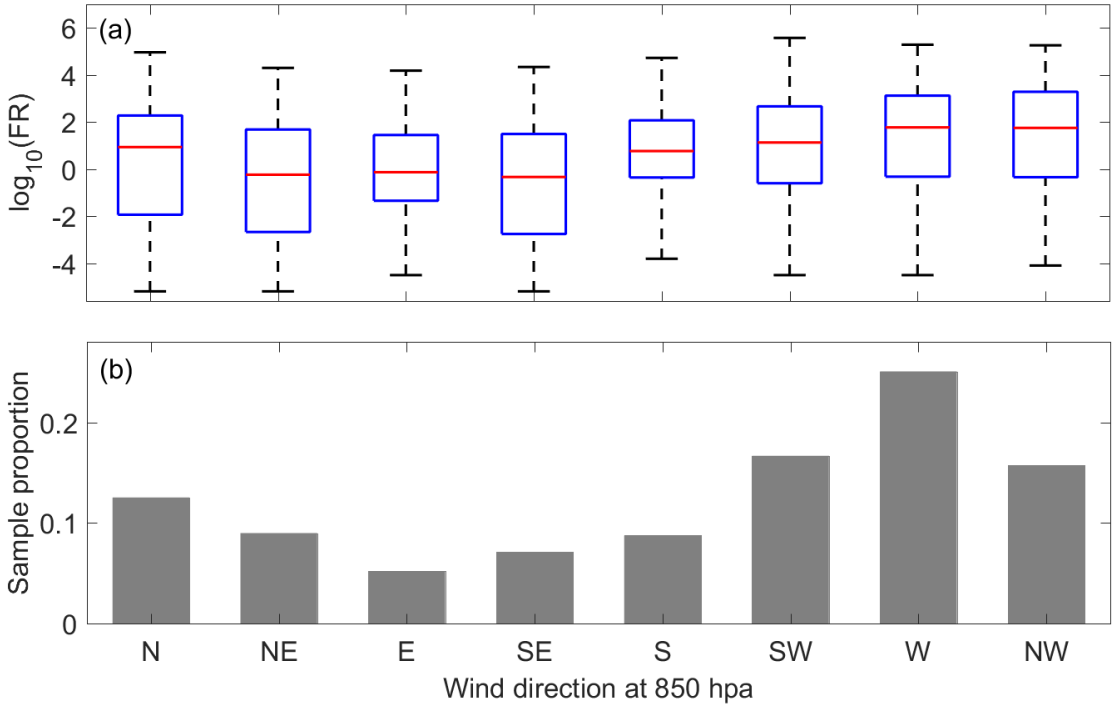

Figure 11. Boxplot of the logarithm of flash rate in different wind direction regimes (upper panel), and the corresponding sample proportions (lower panel). On each blue box in the upper panel, the central red line is the median, and the bottom and top edges of the box are the 25th and 75th percentiles, respectively. The whiskers extend to the most extreme data points excluding the outliers.

Figure 12 shows the correlation coefficients between AOD and $\log_{10}$(FR) in the 8 wind direction regimes. The correlation is stronger and more significant when northerlies prevail than when southerlies prevail over the study area, suggesting that aerosols might have a greater impact on the FRs for the thunderstorms that move from north to south than those that move from south to north. Over northern Alabama, northerly winds tend to bring with them more polluted continental air masses that have resided over the U.S. for several days at least, with aerosol source regions in the Midwest, Ohio Valley, and northeastern U.S. In contrast, southerly winds are associated with more pristine air masses from the Gulf of Mexico, although smoke pollution scenarios occasionally happen when central American biomass burning is active (Saide et al. 2015). These results support, in the presence of northerly winds, the increased correlation between aerosols and lightning flashes contributed by the impacts of land-based aerosols on increased lightning FRs.

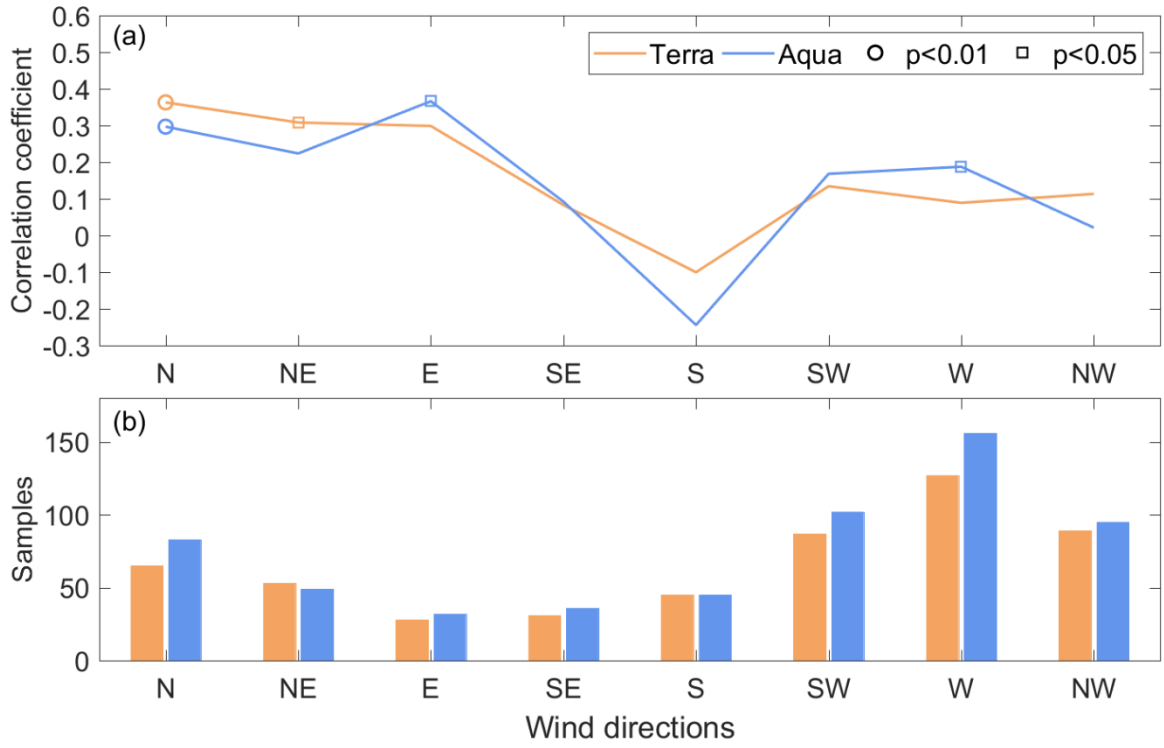

Figure 12. Correlation coefficients between AOD and $\log_{10}$(FR) in the 8 wind direction regimes (a), and the corresponding samples (b). The correlations that pass the *t* test with significance levels of 0.01 and 0.05 are marked by circles and squares, respectively.

2.3.4. Conditional probability of enhanced lightning

In spite of the weak correlations between the MODIS AOD retrievals and $\log_{10}$(FR), such AOD retrievals may be useful in inferences of lightning activity in combination with the forecasts of other meteorological variables. Here, we use the MODIS AOD retrievals and the forecasts of $CAPE^{1/2}$ for an illustration. A half standard deviation (σ) above the mean (M) is used as a threshold to separate the enhanced lightning ($\log_{10}(FR) > M + \sigma/2$) from the less active lightning cases ($\log_{10}(FR) < M - \sigma/2$), and then the conditional probability of enhanced lightning events is discussed. The subjective choice of the $M \pm \sigma/2$ thresholds has also been adopted by previous meteorological and climatological studies, such as the classification of the El Niño

Southern Oscillation (ENSO) events (Phillips, Cane, and Rosenzweig 1998; Ropelewski and Halpert 1996).

First, if the AOD is the only available predictor of enhanced lightning, an AOD threshold (AOD_0) is selected to maximize the conditional probability of enhanced lightning given that $AOD > AOD_0$ occurs, i.e. maximizing $Prob(\log_{10}(FR) > M + \sigma/2 \mid AOD > AOD_0)$. Figure 13 shows the conditions when the maximum probabilities of enhanced lightning conditioned on the MODIS AOD-based inference are reached. This probability maximizes when $AOD_0 = 0.40$ using the Terra MODIS AOD retrievals, and it maximizes when $AOD_0 = 0.44$ using the Aqua MODIS AOD retrievals. Such an enhanced lightning inference minimizes the false alarm ratio (FAR), since $FAR = 1 - Prob(\log_{10}(FR) > M + \sigma/2 \mid AOD > AOD_0)$. As shown in Figure 13, the FAR of an enhanced lightning inference decreases from 178/268 (66.4%) when the Terra $AOD \leq 0.40$ to 138/257 (53.7%) when the Terra $AOD > 0.40$; it decreases from 258/380 (67.9%) when the Aqua $AOD \leq 0.44$ to 122/218 (56.0%) when the Aqua $AOD > 0.44$. Hence, if the AOD is the only accessible variable for enhanced lightning prediction, then at best only about half of such inferences will be correct.

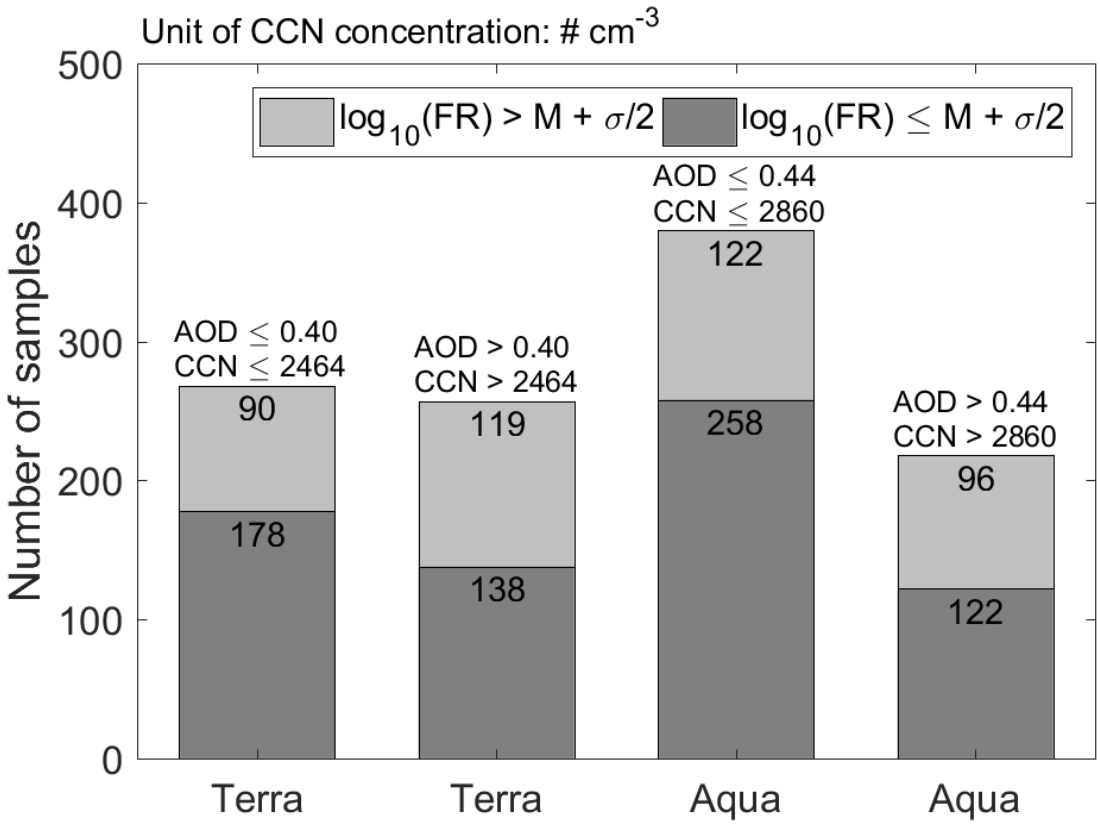

Figure 13. Conditions when the maximum conditional probabilities of enhanced lightning are reached given that AOD > AOD_0 (or CCN > CCN_0; Andreae 2009), Prob($\log_{10}$(FR) > M + σ/2 | AOD > AOD_0)$|_{max}$. The left and right panels are for the Terra MODIS and the Aqua MODIS, respectively.

If the CAPE forecast is also available, the two variables can be used together for enhanced lightning inference. In a similar way, the AOD and CAPE forecast thresholds are selected to maximize the conditional probability of enhanced lightning given that both AOD > AOD_0 and $CAPE^{1/2}$ > $CAPE_0^{1/2}$ occur. Figure 13 shows the occurrence probability of enhanced lightning conditioned on using both the CAPE forecasts and the MODIS AOD retrievals, Prob($\log_{10}$(FR) > M + σ/2 | AOD > AOD_0, $CAPE^{1/2}$ > $CAPE_0^{1/2}$), i.e. the likeliness of a successful inference of an enhanced lightning event for any pair of arbitrarily selected AOD_0 and

$CAPE_0$. The higher the threshold of the predictor (AOD_0 or $CAPE_0^{1/2}$) is, the lower the FAR is. Notwithstanding the secondary role aerosols play in shaping lightning activity compared to the CAPE (Figures 8 and 9), an enhanced lightning predictor that includes AOD can have a lower FAR than that based only on $CAPE^{1/2}$, when a relatively low $CAPE^{1/2}$ is forecast (Figure 14). It should be noted that the samples included in the conditional probability analyses (Figures 13 and 14) are all the cases where lightning flashes were detected by the NALMA; the cases with no detected lightning flashes are not included.

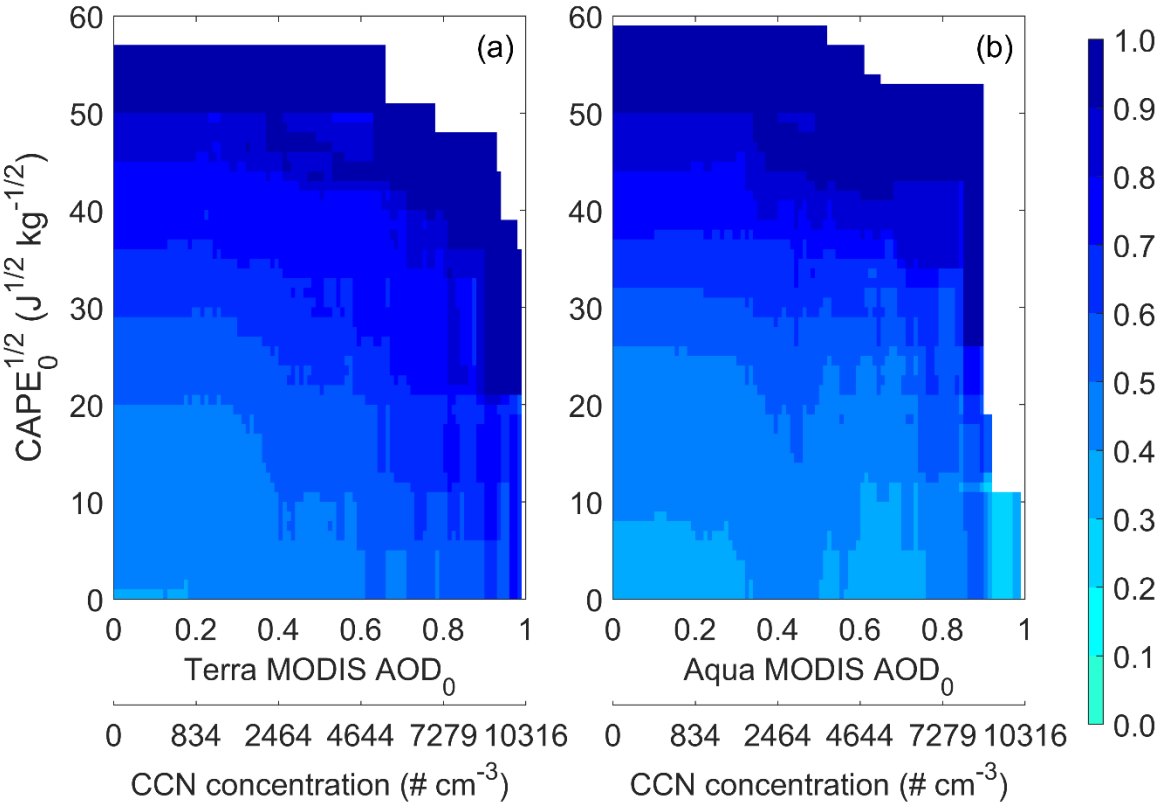

Figure 14. The occurrence probability of enhanced lightning conditioned on the inference using both the square roots of CAPE forecasts and the AOD retrievals from the Terra MODIS (left) or the Aqua MODIS (right) with associated CCN scales using Andreae (2009), Prob($\log_{10}$(FR) > M + σ/2 | AOD > AOD_0, $CAPE^{1/2}$ > $CAPE_0^{1/2}$).

As shown in Figure 14, enhanced lightning will always happen if the forecast $CAPE^{1/2}$ is greater than 50 $J^{1/2}$ $kg^{-1/2}$ for lightning-producing storms. In such a situation, the conditional probability of enhanced lightning is not affected if the aerosol state is known. However, if weaker CAPE is predicted, then the awareness of aerosol state may increase the conditional probability of enhanced lightning. When the Terra AOD is greater than 0.90, enhanced lightning will most likely occur if the $CAPE^{1/2}$ forecast is greater than 22 $J^{1/2}$ $kg^{-1/2}$; when the Aqua AOD is greater than 0.85, enhanced lightning will most likely occur if the $CAPE^{1/2}$ forecast is greater than 29 $J^{1/2}$ $kg^{-1/2}$ (Figure 14). The results suggest that a polluted environment seems more favorable for enhanced lightning than a clean environment, if the CAPE forecast is not large. The results shown in Figure 14 resemble the one in the shallow warm cloud depth (between 2.0 and 3.5 km) regime over continents reported by Stolz et al. (2015) using CCN concentration and normalized CAPE.

2.3.5. Deep convective area and flash rate per unit deep convective area

The association between a polluted environment and increased FR may result from the linkage between aerosols and the area covered by deep convection or the linkage between aerosols and the number of flashes per storm area. The aerosol-lightning enhancement may be caused by enhanced updraft strength of convective cores or more widespread storm area, of which the underlying mechanisms may not be the same. Table 2 documents the correlation coefficients between AOD and $\log_{10}(F_{DCA})$ and the correlation coefficients between AOD and $\log_{10}$(FR/DCA). AOD and $\log_{10}(F_{DCA})$ show weak correlations, which are not sensitive to the radar reflectivity thresholds used to define the DCA (Table 2). The correlation coefficient between the Aqua MODIS AOD and the $\log_{10}(F_{DCA})$ is slightly higher than that between of the Terra MODIS AOD. The correlations are greater than their AOD and $\log_{10}$(FR) counterparts

(Figure 8 and Table 2). This suggests that the areal coverage of deep convection also increases with an increase in AOD, however whether this is linked to aerosol state or other coincident meteorological conditions is unknown. In fact, the thermodynamic quantity CAPE and the aerosol AOD are not independent variables. The square root of CAPE forecast has correlation coefficients of 0.326 and 0.277 with Terra and Aqua MODIS AOD retrievals, respectively (not shown).

Table 2. Correlation coefficients between AOD and $\log_{10}(F_{DCA})$ and correlation coefficients between AOD and $\log_{10}$(FR/DCA). Asterisks specify significance levels: * indicates *t* test statistics at a significance level of 0.05; ** indicates *t* test statistics at a significance level of 0.01.

DCA definition	Terra MODIS AOD		Aqua MODIS AOD	
	vs. $\log_{10}(F_{DCA})$	vs. $\log_{10}$(FR/DCA)	vs. $\log_{10}(F_{DCA})$	vs. $\log_{10}$(FR/DCA)
≥30 dBZ	0.200**	-0.106*	0.216**	-0.122**
≥35 dBZ	0.168**	-0.105*	0.186**	-0.112**
≥40 dBZ	0.177**	-0.097*	0.183**	-0.113**

On the contrary, AOD and $\log_{10}$(FR/DCA) show weak negative correlations, which are also not sensitive to the definitions of DCA (Table 2). As a consequence, not only are polluted environments associated with an increased DCA, but also are associated with a decreased FR per storm area. However, we have not analyzed the storm characteristics that comprised this distribution. The positive dependence between AOD and $\log_{10}(F_{DCA})$ supports previous modeling studies, which suggest that clouds arising in a polluted environment produce stronger downdrafts

and gust fronts, and stronger secondary convection (Khain et al. 2005; Lee and Feingold 2010). We speculate that the aerosol enhancement of lightning, if present, may be associated with enhanced convergence in the boundary layer and secondary convection.

2.4. Discussion and Conclusions

Among currently available satellite aerosol retrievals, MODIS aerosol retrievals were explored here for their utility in improving lightning nowcasts. The long-term mean lightning activity peaks in the late afternoon over northern Alabama, consistent with worldwide activity (Blakeslee et al. 2014; Williams and Heckman 1993), including the three major components of the global electrical circuit—Africa, South America and the Maritime Continent (Williams and Satori 2004). In the daytime, the Terra and Aqua satellites pass the area near noon and in the early afternoon local time, respectively, about 2–4 hours earlier than the peak lightning activity period. In addition, the AERONET ground-based Sun photometer measurements show that the difference between the mean aerosol loadings near the satellite overpass time and the active lightning period is less than 3%. Moreover, the uncertainties of MODIS AOD retrievals are low (RMSE < 0.15). Hence, Terra and Aqua MODIS AOD retrievals may be close to the aerosol loading state during the active lightning period, and thus have the potential for improving lightning predictions.

The lightning FR and MODIS AOD retrievals show weak positive correlations, smaller than those between FR and the forecasts of meteorological variables that are crucial to the intensification of convection. Consequently, MODIS AOD retrievals are less useful than such meteorological forecasts in lightning prediction. Correlations between FR and AOD retrievals become stronger and more significant if a weak wind shear and/or a low CAPE environment are forecasted. They are stronger and more significant when northerly winds prevail than when

southerly winds prevail. For the storms where a CAPE forecast is available, an enhanced lightning predictor that includes AOD may have a lower FAR than that based only on CAPE forecast. When an adequately strong CAPE is forecasted, enhanced lightning will always occur irrespective of the aerosol state. However, when relatively weaker CAPE is forecasted, enhanced lightning is more likely to occur in a polluted environment than in a clean environment.

The correlation between aerosols and FR does not necessarily suggest that aerosols impact deep convection. The association between aerosols and the DCA may contribute to the correlations. However, it does not appear that increased AOD is associated with increased flashes per storm area. Our findings show a weak negative correlation between aerosols and the flashes per storm area. We speculate that the aerosol enhancement of lightning, if present, may be associated with enhanced convergence in the boundary layer and secondary convection (Khain, Rosenfeld, and Pokrovsky 2005; Lee and Feingold 2010). Stronger correlations are present between aerosols and flashes (or DCAs) in particular meteorological conditions such as weak vertical wind shear and prevailing northerly winds. The results suggest that knowledge of aerosols may improve lightning forecasts with aerosol sensitive microphysics schemes in the context of lightning rate parameterizations (e.g. Fierro et al. 2013).

If the aerosol microphysics effect (Williams et al. 2002) is the main link between aerosols and lightning activity, then the correlations between aerosol and lightning flash rate would be stronger if CCN were the measured quantity rather than AOD. The MODIS aerosol algorithm has been adapted to the Visible Infrared Imaging Radiometer Suite (VIIRS) instrument on board the Suomi National Polar-orbiting Partnership (S-NPP) satellite, which was launched more recently in October 2011 (Jackson et al. 2013). The VIIRS aerosol retrievals may be used as part

of a real-time lightning prediction component in a similar way after the Terra and Aqua satellites are retired.

This study focuses on the diurnally most active lightning period, 2–4 hours later than the Terra and Aqua overpass times. However, lightning also occurs at other times. Whether or not satellite aerosol retrievals are capable of improving the prediction of lightning that occurs after a longer period—such as the nighttime or the next morning—remains unknown. The Geostationary Operational Environmental Satellite R (*GOES-R*) series will provide AOD retrievals 12 times per hour over the contiguous United States (CONUS) during the daytime using Advanced Baseline Imager (ABI) observations. GOES-R (GOES–16 and beyond) aerosol retrievals may have greater potential than MODIS for improving the predictions of lightning outside the most active lightning period. The aerosol invigoration of convection sometimes occurs in the downwind area from the aerosol source (e.g. Fan et al. 2015; Wang et al. 2014). The usefulness of the information about aerosol upwind of deep convection and the types of aerosols (Proestakis, Kazadzis, Lagouvardos, Kotroni, Amiridis, et al. 2016) in improving lightning forecast has not been discussed in this study and may be important in regions with large anthropogenic aerosol variability.

2.5. References

Albrecht, Bruce A. 1989. "Aerosols, cloud microphysics, and fractional cloudiness." *Science* no. 245 (4923):1227-1230. doi: 10.1126/science.245.4923.1227.

Albrecht, Rachel I, Steven J Goodman, Dennis E Buechler, Richard J Blakeslee, and Hugh J Christian. 2016. "Where are the lightning hotspots on Earth?" *Bulletin of the American Meteorological Society* no. 97 (11):2051-2068. doi: 10.1175/BAMS-D-14-00193.2.

Albrecht, Rachel I, Carlos A Morales, and Maria AF Silva Dias. 2011. "Electrification of precipitating systems over the Amazon: Physical processes of thunderstorm development." *Journal of Geophysical Research: Atmospheres* no. 116 (D8). doi: 10.1029/2010JD014756.

Altaratz, O, I Koren, LA Remer, and E Hirsch. 2014. "Cloud invigoration by aerosols—Coupling between microphysics and dynamics." *Atmospheric Research* no. 140:38-60. doi: 10.1016/j.atmosres.2014.01.009.

Altaratz, Orit, Ilan Koren, Yoav Yair, and Colin Price. 2010. "Lightning response to smoke from Amazonian fires." *Geophysical Research Letters* no. 37:L07801. doi: 10.1029/2010gl042679.

Andreae, M. O., D. Rosenfeld, P. Artaxo, A. A. Costa, G. P. Frank, K. M. Longo, and M. A. F. Silva-Dias. 2004. "Smoking rain clouds over the Amazon." *Science* no. 303 (5662):1337-1342. doi: 10.1126/science.1092779.

Andreae, Meinrat O. 2009. "Correlation between cloud condensation nuclei concentration and aerosol optical thickness in remote and polluted regions." *Atmospheric Chemistry and Physics* no. 9 (2):543-556. doi: 10.5194/acp-9-543-2009.

Atlas, E, and CS Giam. 1988. "Ambient concentration and precipitation scavenging of atmospheric organic pollutants." *Water, Air, & Soil Pollution* no. 38 (1):19-36. doi: 10.1007/BF00279583.

Blakeslee, Richard J, Douglas M Mach, Monte G Bateman, and Jeffrey C Bailey. 2014. "Seasonal variations in the lightning diurnal cycle and implications for the global electric circuit." *Atmospheric Research* no. 135:228-243. doi: 10.1016/j.atmosres.2012.09.023.

Bringi, VN, K Knupp, A Detwiler, L Liu, IJ Caylor, and RA Black. 1997. "Evolution of a Florida thunderstorm during the Convection and Precipitation/Electrification Experiment: The case of 9 August 1991." *Monthly Weather Review* no. 125 (9):2131-2160. doi: 10.1175/1520-0493(1997)125<2131:EOAFTD>2.0.CO;2.

Byers, Horace Robert, and Roscoe R Braham. 1949. *The thunderstorm: report of the Thunderstorm Project*: US Government Printing Office.

Carey, Lawrence D, and Steven A Rutledge. 2000. "The relationship between precipitation and lightning in tropical island convection: A C-band polarimetric radar study." *Monthly Weather Review* no. 128 (8):2687-2710. doi: 10.1175/1520-0493(2000)128<2687:TRBPAL>2.0.CO;2.

Carey, LD, and SA Rutledge. 1996. "A multiparameter radar case study of the microphysical and kinematic evolution of a lightning producing storm." *Meteorology and Atmospheric Physics* no. 59 (1-2):33-64. doi: 10.1007/BF01032000.

Cecil, Daniel J, Dennis E Buechler, and Richard J Blakeslee. 2014. "Gridded lightning climatology from TRMM-LIS and OTD: Dataset description." *Atmospheric Research* no. 135:404-414.

Chmielewski, Vanna C, and Eric C Bruning. 2016. "Lightning Mapping Array flash detection performance with variable receiver thresholds." *Journal of Geophysical Research: Atmospheres* no. 121 (14):8600-8614. doi: 10.1002/2016JD025159.

Christian, H. J., R. J. Blakeslee, D. J. Boccippio, W. L. Boeck, D. E. Buechler, K. T. Driscoll, S. J. Goodman, J. M. Hall, W. J. Koshak, D. M. Mach, and M. F. Stewart. 2003. "Global frequency and distribution of lightning as observed from space by the Optical Transient

Detector." *Journal of Geophysical Research-Atmospheres* no. 108 (D1). doi: 10.1029/2002jd002347.

Chu, DA, YJ Kaufman, C Ichoku, LA Remer, D Tanré, and BN Holben. 2002. "Validation of MODIS aerosol optical depth retrieval over land." *Geophysical Research Letters* no. 29 (12):1617. doi: 10.1029/2001GL013205,.

Coquillat, Sylvain, Marie-Pierre Boussaton, Magalie Buguet, Dominique Lambert, Jean-Francois Ribaud, and Andy Berthelot. 2013. "Lightning ground flash patterns over Paris area between 1992 and 2003: Influence of pollution?" *Atmospheric Research* no. 122:77-92. doi: 10.1016/j.atmosres.2012.10.032.

Curran, E Brian, Ronald L Holle, and Raúl E López. 2000. "Lightning casualties and damages in the United States from 1959 to 1994." *Journal of Climate* no. 13 (19):3448-3464. doi: 10.1175/1520-0442(2000)013<3448:LCADIT>2.0.CO;2.

Dee, DP, SM Uppala, AJ Simmons, P Berrisford, P Poli, S Kobayashi, U Andrae, MA Balmaseda, G Balsamo, and P Bauer. 2011. "The ERA-Interim reanalysis: Configuration and performance of the data assimilation system." *Quarterly Journal of the Royal Meteorological Society* no. 137 (656):553-597. doi: 10.1002/qj.828.

Deierling, Wiebke, and Walter A Petersen. 2008. "Total lightning activity as an indicator of updraft characteristics." *Journal of Geophysical Research: Atmospheres* no. 113 (D16). doi: 10.1029/2007JD009598.

Deierling, Wiebke, Walter A Petersen, John Latham, Scott Ellis, and Hugh J Christian. 2008. "The relationship between lightning activity and ice fluxes in thunderstorms." *Journal of Geophysical Research: Atmospheres* no. 113 (D15). doi: 10.1029/2007JD009700.

Dye, JE, JJ Jones, WP Winn, TA Cerni, B Gardiner, D Lamb, RL Pitter, J Hallett, and CPR Saunders. 1986. "Early electrification and precipitation development in a small, isolated Montana cumulonimbus." *Journal of Geophysical Research: Atmospheres* no. 91 (D1):1231-1247. doi: 10.1029/JD091iD01p01231.

Emanuel, Kerry A. 1994. *Atmospheric convection*. New York: Oxford University Press.

Fan, Jiwen, Daniel Rosenfeld, Yan Yang, Chun Zhao, L Ruby Leung, and Zhanqing Li. 2015. "Substantial contribution of anthropogenic air pollution to catastrophic floods in Southwest China." *Geophysical Research Letters* no. 42 (14):6066-6075. doi: 10.1002/2015GL064479.

Fan, Jiwen, Tianle Yuan, Jennifer M Comstock, Steven Ghan, Alexander Khain, L Ruby Leung, Zhanqing Li, Vanderlei J Martins, and Mikhail Ovchinnikov. 2009. "Dominant role by vertical wind shear in regulating aerosol effects on deep convective clouds." *Journal of Geophysical Research: Atmospheres* no. 114 (D22):D22206. doi: 10.1029/2009JD012352.

Feingold, Graham, Wynn L. Eberhard, Dana E. Veron, and Michael Previdi. 2003. "First measurements of the Twomey indirect effect using ground-based remote sensors." *Geophysical Research Letters* no. 30 (6):1287. doi: 10.1029/2002gl016633.

Fierro, Alexandre O, Edward R Mansell, Donald R MacGorman, and Conrad L Ziegler. 2013. "The implementation of an explicit charging and discharge lightning scheme within the WRF-ARW model: Benchmark simulations of a continental squall line, a tropical cyclone, and a winter storm." *Monthly Weather Review* no. 141 (7):2390-2415. doi: 10.1175/MWR-D-12-00278.1.

Gatlin, Patrick N, and Steven J Goodman. 2010. "A total lightning trending algorithm to identify severe thunderstorms." *Journal of Atmospheric and Oceanic Technology* no. 27 (1):3-22. doi: 10.1175/2009JTECHA1286.1.

Goodman, SJ, R Blakeslee, H Christian, W Koshak, J Bailey, J Hall, E McCaul, D Buechler, C Darden, and J Burks. 2005. "The North Alabama lightning mapping array: Recent severe storm observations and future prospects." *Atmospheric Research* no. 76 (1):423-437. doi: 10.1016/j.atmosres.2004.11.035.

Goodman, Steven J, Dennis E Buechler, Patrick D Wright, and W David Rust. 1988. "Lightning and precipitation history of a microburst-producing storm." *Geophysical Research Letters* no. 15 (11):1185-1188. doi: 10.1029/GL015i011p01185.

Hales, Jeremy M, and M Terry Dana. 1979. "Precipitation scavenging of urban pollutants by convective storm systems." *Journal of Applied Meteorology* no. 18 (3):294-316. doi: 10.1175/1520-0450(1979)018<0294:PSOUPB>2.0.CO;2.

Harris, Ryan J, John R Mecikalski, Wayne M MacKenzie Jr, Philip A Durkee, and Kurt E Nielsen. 2010. "The definition of GOES infrared lightning initiation interest fields." *Journal of Applied Meteorology and Climatology* no. 49 (12):2527-2543. doi: 10.1175/2010JAMC2575.1.

He, Qianshan, Chengcai Li, Jietai Mao, Alexis Kai-Hon Lau, and D. A. Chu. 2008. "Analysis of aerosol vertical distribution and variability in Hong Kong." *Journal of Geophysical Research* no. 113 (D14):D14211. doi: 10.1029/2008jd009778.

Holben, B. N., T. F. Eck, I. Slutsker, D. Tanré, J. P. Buis, k A. Setzer, E. Vermote, J. A. Reagan, Y. J. Kaufman, T. Nakajima, F. Lavenu, I. Jankowiak, and A. Smirnov. 1998. "AERONET — A federated instrument network and data archive for aerosol

characterization." *Remote Sensing of Environment* no. 66:1-16. doi: 10.1016/S0034-4257(98)00031-5.

Holle, Ronald L. 2016. "A summary of recent national-scale lightning fatality studies." *Weather, Climate, and Society* no. 8 (1):35-42. doi: 10.1175/WCAS-D-15-0032.1.

Holle, Ronald L, Andrew I Watson, Raúl E López, Donald R Macgorman, Robert Ortiz, and William D Otto. 1994. "The life cycle of lightning and severe weather in a 3-4 June 1985 PRE-STORM mesoscale convective system." *Monthly Weather Review* no. 122 (8):1798-1808.

Ichoku, Charles, D Allen Chu, Shana Mattoo, Yoram J Kaufman, Lorraine A Remer, Didier Tanré, Ilya Slutsker, and Brent N Holben. 2002. "A spatio-temporal approach for global validation and analysis of MODIS aerosol products." *Geophysical Research Letters* no. 29 (12):MOD1-1-MOD1-4. doi: 10.1029/2001GL013206.

Jackson, John M, Hongqing Liu, Istvan Laszlo, Shobha Kondragunta, Lorraine A Remer, Jingfeng Huang, and Ho-Chun Huang. 2013. "Suomi-NPP VIIRS aerosol algorithms and data products." *Journal of Geophysical Research: Atmospheres* no. 118 (22). doi: 10.1002/2013JD020449.

Jacobson, Elizabeth A, and E Philip Krider. 1976. "Electrostatic field changes produced by Florida lightning." *Journal of the Atmospheric Sciences* no. 33 (1):103-117. doi: 10.1175/1520-0469(1976)033<0103:EFCPBF>2.0.CO;2.

Jin, Menglin, J Marshall Shepherd, and Michael D King. 2005. "Urban aerosols and their variations with clouds and rainfall: A case study for New York and Houston." *Journal of Geophysical Research: Atmospheres* no. 110 (D10). doi: 10.1029/2004JD005081.

Kar, S. K., Y. A. Liou, and K. J. Ha. 2009. "Aerosol effects on the enhancement of cloud-to-ground lightning over major urban areas of South Korea." *Atmospheric Research* no. 92 (4):80-87. doi: 10.1016/j.atmosres.2008.09.040.

Khain, A, D Rosenfeld, and A Pokrovsky. 2005. "Aerosol impact on the dynamics and microphysics of deep convective clouds." *Quarterly Journal of the Royal Meteorological Society* no. 131 (611):2639-2663. doi: doi: 10.1256/qj.04.62.

Konrad, Charles E. 1997. "Synoptic-scale features associated with warm season heavy rainfall over the interior southeastern United States." *Weather and Forecasting* no. 12 (3):557-571. doi: 10.1175/1520-0434(1997)012<0557:SSFAWW>2.0.CO;2.

Koshak, WJ, RJ Solakiewicz, RJ Blakeslee, SJ Goodman, HJ Christian, JM Hall, JC Bailey, EP Krider, MG Bateman, and DJ Boccippio. 2004. "North Alabama Lightning Mapping Array (LMA): VHF source retrieval algorithm and error analyses." *Journal of Atmospheric and Oceanic Technology* no. 21 (4):543-558. doi: 10.1175/1520-0426(2004)021<0543:NALMAL>2.0.CO;2.

Kovacs, Thomas. 2006. "Comparing MODIS and AERONET aerosol optical depth at varying separation distances to assess ground-based validation strategies for spaceborne lidar." *Journal of Geophysical Research: Atmospheres* no. 111 (D24). doi: 10.1029/2006JD007349.

Krehbiel, Paul R, Ronald J Thomas, William Rison, Timothy Hamlin, Jeremiah Harlin, and Michael Davis. 2000. "GPS-based mapping system reveals lightning inside storms." *Eos, Transactions American Geophysical Union* no. 81 (3):21-25. doi: 10.1029/00EO00014.

Larsen, HR, and EJ Stansbury. 1974. "Association of lightning flashes with precipitation cores extending to height 7 km." *Journal of Atmospheric and Terrestrial Physics* no. 36 (9):1547IN231549-15481553. doi: 0021-9169(74)90232-3.

Lee, Seoung-Soo, and Graham Feingold. 2010. "Precipitating cloud-system response to aerosol perturbations." *Geophysical Research Letters* no. 37 (23). doi: 10.1029/2010GL045596.

Levy, Robert C, Lorraine A Remer, and Oleg Dubovik. 2007. "Global aerosol optical properties and application to Moderate Resolution Imaging Spectroradiometer aerosol retrieval over land." *Journal of Geophysical Research: Atmospheres* no. 112 (D13). doi: 10.1029/2006JD007815.

Levy, Robert C, Lorraine A Remer, Shana Mattoo, Eric F Vermote, and Yoram J Kaufman. 2007. "Second-generation operational algorithm: Retrieval of aerosol properties over land from inversion of Moderate Resolution Imaging Spectroradiometer spectral reflectance." *Journal of Geophysical Research: Atmospheres* no. 112 (D13). doi: 10.1029/2006JD007811.

Levy, Robert C., S. Mattoo, L. A. Munchak, L. A. Remer, A. M. Sayer, F. Patadia, and N. C. Hsu. 2013. "The Collection 6 MODIS aerosol products over land and ocean." *Atmospheric Measurement Techniques* no. 6 (11):2989-3034. doi: 10.5194/amt-6-2989-2013.

Li, L. F., W. H. Li, and Y. Kushnir. 2012. "Variation of the North Atlantic subtropical high western ridge and its implication to Southeastern US summer precipitation." *Climate Dynamics* no. 39 (6):1401-1412. doi: 10.1007/s00382-011-1214-y.

Liu, C. T., E. J. Zipser, and S. W. Nesbitt. 2007. "Global distribution of tropical deep convection: Different perspectives from TRMM infrared and radar data." *Journal of Climate* no. 20 (3):489-503. doi: 10.1175/jcli4023.1.

Liu, PF, CS Zhao, T Göbel, E Hallbauer, A Nowak, L Ran, WY Xu, ZZ Deng, N Ma, and K Mildenberger. 2011. "Hygroscopic properties of aerosol particles at high relative humidity and their diurnal variations in the North China Plain." *Atmospheric Chemistry and Physics* no. 11 (7):3479-3494. doi: 10.5194/acp-11-3479-2011.

Liu, Yang, Meredith Franklin, Ralph Kahn, and Petros Koutrakis. 2007. "Using aerosol optical thickness to predict ground-level PM 2.5 concentrations in the St. Louis area: a comparison between MISR and MODIS." *Remote Sensing of Environment* no. 107 (1):33-44. doi: 10.1016/j.rse.2006.05.022.

Livingston, JM, J Redemann, PB Russell, O Torres, B Veihelmann, P Veefkind, R Braak, A Smirnov, L Remer, and RW Bergstrom. 2009. "Comparison of aerosol optical depths from the Ozone Monitoring Instrument (OMI) on Aura with results from airborne sunphotometry, other space and ground measurements during MILAGRO/INTEX-B." *Atmospheric Chemistry and Physics* no. 9 (18):6743-6765.

MacGorman, Donald. R , and W. David Rust. 1998. *The electrical nature of storms*. New York: Oxford University Press.

Mansell, Edward R, and Conrad L Ziegler. 2013. "Aerosol effects on simulated storm electrification and precipitation in a two-moment bulk microphysics model." *Journal of the Atmospheric Sciences* no. 70 (7):2032-2050. doi: 10.1175/JAS-D-12-0264.1.

Mansell, Edward R, Conrad L Ziegler, and Eric C Bruning. 2010. "Simulated electrification of a small thunderstorm with two-moment bulk microphysics." *Journal of the Atmospheric Sciences* no. 67 (1):171-194.

Marshall, JS, and S Radhakant. 1978. "Radar precipitation maps as lightning indicators." *Journal of Applied Meteorology* no. 17 (2):206-212. doi: 10.1175/1520-0450(1978)017<0206:RPMALI>2.0.CO;2.

Martonchik, John V, and David J Diner. 1992. "Retrieval of aerosol optical properties from multi-angle satellite imagery." *Geoscience and Remote Sensing, IEEE Transactions on* no. 30 (2):223-230.

Martonchik, John V, David J Diner, Ralph A Kahn, Thomas P Ackerman, Michel M Verstraete, Bernard Pinty, and Howard R Gordon. 1998. "Techniques for the retrieval of aerosol properties over land and ocean using multiangle imaging." *Geoscience and Remote Sensing, IEEE Transactions on* no. 36 (4):1212-1227.

McCaul Jr, Eugene W, J Bailey, J Hall, SJ Goodman, RJ Blakeslee, and DE Buechler. 2005. A flash clustering algorithm for North Alabama Lightning Mapping Array data. Paper read at Preprints, Conf. on Meteorological Applications of Lightning data.

McCaul Jr, Eugene W, Steven J Goodman, Katherine M LaCasse, and Daniel J Cecil. 2009. "Forecasting lightning threat using cloud-resolving model simulations." *Weather and Forecasting* no. 24 (3):709-729. doi: 10.1175/2008WAF2222152.1.

Mecikalski, John R, Xuanli Li, Lawrence D Carey, Eugene W McCaul Jr, and Timothy A Coleman. 2013. "Regional comparison of GOES cloud-top properties and radar characteristics in advance of first-flash lightning initiation." *Monthly Weather Review* no. 141 (1):55-74. doi: 10.1175/mwr-d-12-00120.1.

Mosier, R. M., C. Schumacher, R. E. Orville, and L. D. Carey. 2011. "Radar nowcasting of cloud-to-ground lightning over Houston, Texas." *Weather and Forecasting* no. 26 (2):199-212. doi: 10.1175/2010waf2222431.1.

Naccarato, KP, O Pinto, and IRCA Pinto. 2003. "Evidence of thermal and aerosol effects on the cloud-to-ground lightning density and polarity over large urban areas of Southeastern Brazil." *Geophysical Research Letters* no. 30 (13). doi: 10.1029/2003GL017496.

Orville, R. E., G. Huffines, J. Nielsen-Gammon, R. Y. Zhang, B. Ely, S. Steiger, S. Phillips, S. Allen, and W. Read. 2001. "Enhancement of cloud-to-ground lightning over Houston, Texas." *Geophysical Research Letters* no. 28 (13):2597-2600. doi: 10.1029/2001gl012990.

Phillips, JG, MA Cane, and C Rosenzweig. 1998. "ENSO, seasonal rainfall patterns and simulated maize yield variability in Zimbabwe." *Agricultural and Forest Meteorology* no. 90 (1):39-50. doi: 10.1016/S0168-1923(97)00095-6.

Proestakis, E, S Kazadzis, K Lagouvardos, V Kotroni, V Amiridis, E Marinou, C Price, and A Kazantzidis. 2016. "Aerosols and lightning activity: The effect of vertical profile and aerosol type." *Atmospheric Research* no. 182:243-255. doi: 10.1016/j.atmosres.2016.07.031.

Proestakis, E, S Kazadzis, K Lagouvardos, V Kotroni, and A Kazantzidis. 2016. "Lightning activity and aerosols in the Mediterranean region." *Atmospheric Research* no. 170:66-75. doi: 10.1016/j.atmosres.2015.11.010.

Radke, LF, and PV Hobbs. 1969. "Measurement of cloud condensation nuclei, light scattering coefficient, sodium-containing particles, and Aitken nuclei in the Olympic Mountains of

Washington." *Journal of the Atmospheric Sciences* no. 26 (2):281-288. doi: 10.1175/1520-0469(1969)026<0281:MOCCNL>2.0.CO;2.

Reap, Ronald M. 1994. "Analysis and prediction of lightning strike distributions associated with synoptic map types over Florida." *Monthly Weather Review* no. 122 (8):1698-1715. doi: 10.1175/1520-0493(1994)122<1698:AAPOLS>2.0.CO;2.

Rienecker, Michele M, Max J Suarez, Ronald Gelaro, Ricardo Todling, Julio Bacmeister, Emily Liu, Michael G Bosilovich, Siegfried D Schubert, Lawrence Takacs, and Gi-Kong Kim. 2011. "MERRA: NASA's modern-era retrospective analysis for research and applications." *Journal of Climate* no. 24 (14):3624-3648. doi: 10.1175/JCLI-D-11-00015.1.

Rison, W, RJ Thomas, PR Krehbiel, T Hamlin, and J Harlin. 1999. "A GPS-based three-dimensional lightning mapping system: Initial observations in central New Mexico." *Geophysical Research Letters* no. 26 (23):3573-3576. doi: 10.1029/1999GL010856.

Robe, Françoise R, and Kerry A Emanuel. 2001. "The effect of vertical wind shear on radiative-convective equilibrium states." *Journal of the Atmospheric Sciences* no. 58 (11):1427-1445. doi: 10.1175/1520-0469(2001)058<1427:TEOVWS>2.0.CO;2.

Rodriguez, Carlos A Morales, Rosmeri P da Rocha, and Rodrigo Bombardi. 2010. "On the development of summer thunderstorms in the city of São Paulo: Mean meteorological characteristics and pollution effect." *Atmospheric Research* no. 96 (2):477-488. doi: 10.1016/j.atmosres.2010.02.007.

Ropelewski, Chester F, and Michael S Halpert. 1996. "Quantifying southern oscillation-precipitation relationships." *Journal of Climate* no. 9 (5):1043-1059. doi: 10.1175/1520-0442(1996)009<1043:QSOPR>2.0.CO;2.

Rotunno, Richard, Joseph B Klemp, and Morris L Weisman. 1988. "A theory for strong, long-lived squall lines." *Journal of the Atmospheric Sciences* no. 45 (3):463-485. doi: 10.1175/1520-0469(1988)045<0463:ATFSLL>2.0.CO;2.

Saide, PE, SN Spak, RB Pierce, JA Otkin, TK Schaack, AK Heidinger, AM Silva, M Kacenelenbogen, J Redemann, and GR Carmichael. 2015. "Central American biomass burning smoke can increase tornado severity in the US." *Geophysical Research Letters* no. 42 (3):956-965. doi: 10.1002/2014GL062826.

Saunders, CPR, H Bax-Norman, C Emersic, EE Avila, and NE Castellano. 2006. "Laboratory studies of the effect of cloud conditions on graupel/crystal charge transfer in thunderstorm electrification." *Quarterly Journal of the Royal Meteorological Society* no. 132 (621):2653-2673. doi: 10.1256/qj.05.218.

Schultz, Christopher J, Lawrence D Carey, Elise V Schultz, and Richard J Blakeslee. 2017. "Kinematic and microphysical significance of lightning jumps versus nonjump increases in total flash rate." *Weather and Forecasting* no. 32 (1):275-288. doi: 10.1175/WAF-D-15-0175.1.

Schultz, Christopher J, Walter A Petersen, and Lawrence D Carey. 2011. "Lightning and severe weather: A comparison between total and cloud-to-ground lightning trends." *Weather and Forecasting* no. 26 (5):744-755. doi: 10.1175/WAF-D-10-05026.1.

Shen, XJ, JY Sun, YM Zhang, B Wehner, A Nowak, T Tuch, XC Zhang, TT Wang, HG Zhou, and XL Zhang. 2011. "First long-term study of particle number size distributions and new particle formation events of regional aerosol in the North China Plain." *Atmospheric Chemistry and Physics* no. 11 (4):1565-1580. doi: 10.5194/acp-11-1565-2011.

Sihto, S-L, J Mikkilä, J Vanhanen, M Ehn, L Liao, K Lehtipalo, PP Aalto, J Duplissy, T Petäjä, and V-M Kerminen. 2011. "Seasonal variation of CCN concentrations and aerosol activation properties in boreal forest." *Atmospheric Chemistry and Physics* no. 11 (24):13269-13285. doi: 10.5194/acp-11-13269-2011.

Smirnov, A, BN Holben, TF Eck, I Slutsker, B Chatenet, and RT Pinker. 2002. "Diurnal variability of aerosol optical depth observed at AERONET (Aerosol Robotic Network) sites." *Geophysical Research Letters* no. 29 (23). doi: 10.1029/2002GL016305.

Steiger, S. M., R. E. Orville, and G. Huffines. 2002. "Cloud-to-ground lightning characteristics over Houston, Texas: 1989-2000." *Journal of Geophysical Research-Atmospheres* no. 107 (D11). doi: 10.1029/2001jd001142.

Stolz, Douglas C, Steven A Rutledge, and Jeffrey R Pierce. 2015. "Simultaneous influences of thermodynamics and aerosols on deep convection and lightning in the tropics." *Journal of Geophysical Research: Atmospheres* no. 120 (12):6207-6231. doi: 10.1002/2014JD023033.

Stolz, Douglas C, Steven A Rutledge, Jeffrey R Pierce, and Susan C Heever. 2017. "A global lightning parameterization based on statistical relationships among environmental factors, aerosols, and convective clouds in the TRMM climatology." *Journal of Geophysical Research: Atmospheres* no. 122:7461–7492. doi: 10.1002/2016JD026220.

Storer, Rachel L, Susan C Van Den Heever, and Graeme L Stephens. 2010. "Modeling aerosol impacts on convective storms in different environments." *Journal of the Atmospheric Sciences* no. 67 (12):3904-3915. doi: 10.1175/2010JAS3363.1.

Storer, RL, SC Heever, and TS L'Ecuyer. 2014. "Observations of aerosol-induced convective invigoration in the tropical east Atlantic." *Journal of Geophysical Research: Atmospheres* no. 119 (7):3963-3975. doi: 10.1002/2013JD020272.

Tan, YB, L Peng, Z Shi, and HR Chen. 2016. "Lightning flash density in relation to aerosol over Nanjing (China)." *Atmospheric Research* no. 174:1-8. doi: 10.1016/j.atmosres.2016.01.009.

Thomas, Ronald J, Paul R Krehbiel, William Rison, Steven J Hunyady, William P Winn, Timothy Hamlin, and Jeremiah Harlin. 2004. "Accuracy of the lightning mapping array." *Journal of Geophysical Research: Atmospheres* no. 109 (D14):D14207. doi: 10.1029/2004JD004549.

Thornton, Joel A, Katrina S Virts, Robert H Holzworth, and Todd P Mitchell. 2017. "Lightning enhancement over major oceanic shipping lanes." *Geophysical Research Letters* no. 44:9102-9111. doi: 10.1002/2017GL074982.

van den Heever, Susan C, Gustavo G Carrió, William R Cotton, Paul J DeMott, and Anthony J Prenni. 2006. "Impacts of nucleating aerosol on Florida storms. Part I: Mesoscale simulations." *Journal of the Atmospheric Sciences* no. 63 (7):1752-1775. doi: 10.1175/JAS3713.1.

van den Heever, Susan C, and William R Cotton. 2007. "Urban aerosol impacts on downwind convective storms." *Journal of Applied Meteorology and Climatology* no. 46 (6):828-850. doi: 10.1175/JAM2492.1.

Van Donkelaar, Aaron, Randall V Martin, Robert C Levy, Arlindo M da Silva, Michal Krzyzanowski, Natalia E Chubarova, Eugenia Semutnikova, and Aaron J Cohen. 2011. "Satellite-based estimates of ground-level fine particulate matter during extreme events:

A case study of the Moscow fires in 2010." *Atmospheric Environment* no. 45 (34):6225-6232. doi: 10.1016/j.atmosenv.2011.07.068.

Vincent, Brandon R, Lawrence D Carey, Douglas Schneider, Kermit Keeter, and Rod Gonski. 2004. "Using WSR–88D reflectivity data for the prediction of cloud–to–ground lightning: A central North Carolina study." *National Weather Association Digest* no. 27:35-44.

Wang, Y., Q. Wan, W. Meng, F. Liao, H. Tan, and R. Zhang. 2011. "Long-term impacts of aerosols on precipitation and lightning over the Pearl River Delta megacity area in China." *Atmospheric Chemistry and Physics* no. 11 (23):12421-12436. doi: 10.5194/acp-11-12421-2011.

Wang, Yuan, Minghuai Wang, Renyi Zhang, Steven J Ghan, Yun Lin, Jiaxi Hu, Bowen Pan, Misti Levy, Jonathan H Jiang, and Mario J Molina. 2014. "Assessing the effects of anthropogenic aerosols on Pacific storm track using a multiscale global climate model." *Proceedings of the National Academy of Sciences* no. 111 (19):6894-6899.

Weisman, Morris L, and Joseph B Klemp. 1982. "The dependence of numerically simulated convective storms on vertical wind shear and buoyancy." *Monthly Weather Review* no. 110 (6):504-520. doi: 10.1175/1520-0493(1982)110<0504:TDONSC>2.0.CO;2.

Williams, E. R., and G. Satori. 2004. "Lightning, thermodynamic and hydrological comparison of the two tropical continental chimneys." *Journal of Atmospheric and Solar-Terrestrial Physics* no. 66 (13-14):1213-1231. doi: 10.1016/j.jastp.2004.05.015.

Williams, E. R., R. Zhang, and J. Rydock. 1991. "Mixed-phase microphysics and cloud electrification." *Journal of the Atmospheric Sciences* no. 48 (19):2195-2203. doi: 10.1175/1520-0469(1991)048<2195:mpmace>2.0.co;2.

Williams, E., D. Rosenfeld, N. Madden, J. Gerlach, N. Gears, L. Atkinson, N. Dunnemann, G. Frostrom, M. Antonio, B. Biazon, R. Camargo, H. Franca, A. Gomes, M. Lima, R. Machado, S. Manhaes, L. Nachtigall, H. Piva, W. Quintiliano, L. Machado, P. Artaxo, G. Roberts, N. Renno, R. Blakeslee, J. Bailey, D. Boccippio, A. Betts, D. Wolff, B. Roy, J. Halverson, T. Rickenbach, J. Fuentes, and E. Avelino. 2002. "Contrasting convective regimes over the Amazon: Implications for cloud electrification." *Journal of Geophysical Research: Atmospheres* no. 107 (D20):8082. doi: 10.1029/2001jd000380.

Williams, ER, and SJ Heckman. 1993. "The local diurnal variation of cloud electrification and the global diurnal variation of negative charge on the Earth." *Journal of Geophysical Research: Atmospheres* no. 98 (D3):5221-5234. doi: 10.1029/92JD02642.

Williams, ER, ME Weber, and RE Orville. 1989. "The relationship between lightning type and convective state of thunderclouds." *Journal of Geophysics Research* no. 94:13213-13220. doi: 10.1029/JD094iD11p13213.

Wu, Xiaoqing, and Michio Yanai. 1994. "Effects of vertical wind shear on the cumulus transport of momentum: Observations and parameterization." *Journal of the atmospheric sciences* no. 51 (12):1640-1660. doi: 10.1175/1520-0469(1994)051<1640:EOVWSO>2.0.CO;2.

Yuan, T. L., L. A. Remer, H. S. Bian, J. R. Ziemke, R. Albrecht, K. E. Pickering, L. Oreopoulos, S. J. Goodman, H. B. Yu, and D. J. Allen. 2012. "Aerosol indirect effect on tropospheric ozone via lightning." *Journal of Geophysical Research-Atmospheres* no. 117:D18213. doi: 10.1029/2012jd017723.

Yuan, Tianle, Lorraine A Remer, Kenneth E Pickering, and Hongbin Yu. 2011. "Observational evidence of aerosol enhancement of lightning activity and convective invigoration." *Geophysical Research Letters* no. 38 (4):L04701. doi: 10.1029/2010GL046052.

Zipser, Edward J. 1994. "Deep cumulonimbus cloud systems in the tropics with and without lightning." *Monthly Weather Review* no. 122 (8):1837-1851. doi: 10.1175/1520-0493(1994)122<1837:DCCSIT>2.0.CO;2.

Zipser, Edward J, and Kurt R Lutz. 1994. "The vertical profile of radar reflectivity of convective cells: A strong indicator of storm intensity and lightning probability?" *Monthly Weather Review* no. 122 (8):1751-1759. doi: 10.1175/1520-0493(1994)122<1751:TVPORR>2.0.CO;2.

3. LIGHTNING AND ASSOCIATED CONVECTION FEATURES IN THE PRESENCE OF ABSORBING AEROSOLS OVER NORTHERN ALABAMA

3.1. Introduction

Lightning plays an important role in the Earth-atmosphere system and is one of the major causes of fire ignitions in wooded areas (e.g. Flannigan and Wotton 1991; Rorig and Ferguson 1999). Lightning-produced nitrogen oxides (LNO_x) can be transported by deep convection to the upper troposphere (UT) where their lifetimes are prolonged (Jaeglé 2007). Increased LNO_x can lead to increased ozone production in UT, which may in turn warm the climate (Yuan et al. 2012). Siu et al. (2015) shows that almost all the nitric oxide (NO) in the uppermost outflow layer is generated by lightning.

In a thunderstorm, collisions among ice particles in the presence of supercooled liquid water make the particles charged (Saunders et al. 2006; Takahashi 1978). Differential sedimentation of graupel and small ice crystals in an updraft then results in charge regions. An adequately large volume of a strong updraft is necessary for cloud charge separation and lightning (Deierling and Petersen 2008; Deierling et al. 2008; Schultz et al. 2017; Zipser 1994). It has been suggested that aerosols may enhance lightning via invigoration of deep convection (Albrecht, Morales, and Silva Dias 2011; Altaratz et al. 2010; Altaratz et al. 2014; Proestakis, Kazadzis, Lagouvardos, Kotroni, Amiridis, et al. 2016; Proestakis, Kazadzis, Lagouvardos, Kotroni, and Kazantzidis 2016; Stolz, Rutledge, and Pierce 2015; Stolz et al. 2017; Wang et al. 2011; Williams et al. 2002; Yuan et al. 2011). Increased aerosol particles lead to increased cloud condensation nuclei (CCN; Albrecht 1989), resulting a distribution of liquid cloud droplets with higher number concentrations and lower mean diameters, which lowers the efficiency of

collision and coalescence (Albrecht 1989; Feingold et al. 2003) during the warm precipitation phase of a storm. As a consequence, cloud droplets that would have fallen to the surface may be later lifted above the freezing level as the convective system further develops, invigorating convection through release of latent heat (Andreae et al. 2004; Jenkins, Pratt, and Heymsfield 2008; Khain, Rosenfeld, and Pokrovsky 2005; Rosenfeld et al. 2008; Storer, Heever, and L'Ecuyer 2014; van den Heever et al. 2006).

In addition, increased aerosol particles also generally bring more ice nuclei (IN) whose role in the microphysical processes of mixed-phase clouds is important but less well understood (Seinfeld et al. 2016). The cloud glaciation temperature is dependent upon the ice-nucleating ability of aerosols (Hoose and Möhler 2012; Murray et al. 2012; Roberts and Hallett 1968). Heterogeneous ice nucleation occurs at warmer temperatures in the presence of effective IN, such as mineral dusts, biological species, and soot (Cziczo et al. 2004; DeMott, Cziczo, et al. 2003; DeMott, Sassen, et al. 2003; Levi and Rosenfeld 1996; McCluskey et al. 2014; Richardson et al. 2007; Schaefer 1949; Wilson et al. 2015). Model studies have suggested that increased IN concentration facilitates heterogeneous freezing and may result in increased ice concentrations (Li, Xue, and Yang 2013). Satellite observations have shown that dust aerosols favor ice particle formation within an altocumulus cloud that has warmer base and top temperatures (Sassen et al. 2003). In the same study, Sassen et al. (2003) also suggest that deep convection may be affected by high loading episodes of African dust. If clouds glaciate at a warmer temperature in a thunderstorm, then there may be more supercooled water lifted above the lower glaciation level and more latent heat released, invigorating the convection. It has been found that increased total lightning density is associated with decreased warm cloud depth, which is the distance between the lifted condensation level and the freezing level (Stolz, Rutledge, and Pierce 2015; Stolz et al.

2017). Hence, it may be speculated that the aerosol-lightning-enhancement is due in part to adding not only more CCN, but also more IN. Hereinafter, we call this potential impact of aerosols on lightning the CCN/IN-mechanism, since both enhanced CCN and/or enhanced IN can lead to more supercooled water above the freezing level and invigorated convection through latent heat release, and ultimately enhanced non-inductive charge separation.

Aerosol-lightning-enhancements are difficult to examine using observational data. Lightning activity was not significantly different between pristine and polluted environmental conditions in the pre-monsoon regime over the Amazon (Williams et al. 2002). Although thunderstorms occur more frequently in the relatively polluted environment during the Amazonian wet season (Albrecht, Morales, and Silva Dias 2011), lightning flash rate did not increase with satellite aerosol optical depth (AOD) retrievals during the Amazonian dry season, when the loading of smoke aerosols is high (AOD > 0.3) (Altaratz et al. 2010). Presumably, the high loading of smoke aerosols stabilizes the lower troposphere and suppresses the deep convective clouds (Altaratz et al. 2010). Rodriguez, da Rocha, and Bombardi (2010) suggest no significant aerosol enhancement of lightning in austral summer over São Paulo, Brazil. Moreover, the influence of aerosols on lightning activity is present only in the lee side of Paris, France (Coquillat et al. 2013). Perhaps, the CCN/IN-mechanism applies in some particular meteorological conditions and/or aerosols can enhance lightning through not only their microphysical effects.

Among all types of aerosols, absorbing aerosols—such as black carbon and mineral dust—can absorb solar radiation (Huang et al. 2009; Li et al. 2010). Interestingly, a number of previously reported aerosol-lightning-enhancement and aerosol-convection-invigoration studies are in the presence of absorbing aerosols, although less-absorbing aerosols have also been

reported to enhance lightning via invigorating deep convection (Yuan et al. 2011). Ingested Saharan dust aerosols appeared to invigorate the deep convection of the rain bands of a tropical storm (Jenkins, Pratt, and Heymsfield 2008). In the Intertropical Convergence Zone (ITCZ) over the Atlantic where Saharan dust and African biomass burning aerosols are carried by the prevailing easterlies, AOD correlated positively with cloud fraction and negatively with cloud top pressure (Koren et al. 2005); such correlations did not appear to result from meteorological conditions or retrieval artifacts (Koren, Feingold, and Remer 2010). AOD and lightning flash rate (FR) show a coincident trend in the presence of the low loading of smoke aerosols (AOD < 0.2) over the Amazon region in the dry season (Altaratz et al. 2010). Smoke aerosols have been observed by the space-borne lidar more frequently in lightning-active cases than non-lightning-active ones over the broader Mediterranean area (Proestakis, Kazadzis, Lagouvardos, Kotroni, and Kazantzidis 2016b). Enhanced lightning flash rate density has been observed over the main shipping lanes in the eastern Indian Ocean and the South China Sea, where increased absorbing aerosols from exhaust of ships are present (Thornton et al. 2017).

Absorbing aerosols cool the surface and heat the atmosphere, stabilizing the lower troposphere and suppression of convection with an increased convection inhibition (CIN; Wang et al. 2013); and the convective available potential energy (CAPE) is gradually accumulated (Wang et al. 2013). Once the CIN is overcome, more intense convection can develop (Wang et al. 2013). This may also be a mechanism for aerosols to enhance lightning. Hereinafter, we call this hypothetical mechanism the CAPE-mechanism. In addition, absorbing aerosols suppress turbulence in the planetary boundary layer (PBL) (Ding et al. 2016; Dong et al. 2017; Li et al. 2017; Wilcox et al. 2016). The suppression of PBL turbulent mixing may enhance low-level wind shear, favorable for tornado occurrence in an already severe weather conducive

environment (Saide et al. 2015). Saide et al. (2015) also suggest the potential impact of absorbing aerosols on non-tornadic thunderstorms through enhanced low level shear, and hence lightning activity may be linked to absorbing aerosols through this mechanism, which we call the PBL-mechanism hereinafter. Therefore, in addition to the CCN/IN-mechanism, the CAPE- and PBL-mechanisms may also contribute to enhanced lightning in the presence of absorbing aerosols. However, to the best of our knowledge, how absorbing aerosols differ from non-absorbing aerosols in correlations with lightning FR remains unclear.

We hypothesize that aerosols may enhance lightning through not only the microphysical effects as described in the CCN/IN-mechanism but also the radiative effects as described in the CAPE- and PBL-mechanisms. If the CAPE mechanism applies, then AOD and CAPE will show an increased correlation in the presence of absorbing aerosols. If the PBL mechanism applies, then AOD and the planetary boundary layer height (PBLH) will show a decreased (or more negative) correlation. The objectives of this study are to examine (1) the comparative associations of lightning with absorbing and non-absorbing aerosols; (2) the aerosol situations, meteorological conditions, and ground-based radar reflectivity statistics in association with lightning variability to shed light on which of the previously mentioned three mechanisms may work in the studied storms.

3.2. Data and Methodology

This study focuses on northern Alabama where long-term lightning data that dates back to 2002 are available from the North Alabama Lightning Mapping Array (NALMA) (Carey and Stough 2016; Goodman et al. 2005; Koshak et al. 2004). Lightning is most active in summer (June-July-August; JJA) over northern Alabama (Albrecht et al. 2016; Christian et al. 2003), and hence we focus on storm cases in the JJAs from 2002 to 2015. Because the location uncertainty

of the detected lightning source increases with distance (Chmielewski and Bruning 2016; Thomas et al. 2004), the study area is restricted to a circle centered at the NALMA network with a radius of 150 km (Figure 15), where the detection efficiency of the NALMA is above 90% (Chmielewski and Bruning 2016). The LMA locates the lightning sources by measuring how fast the impulsive very high frequency (VHF) radiation travels from the source to each of the stations, and archives lightning sources detected by at least 6 stations (Rison et al. 1999). In this study, the lightning flashes detected by 7 stations or more are used to further ensure the accuracy of flash locations, although a portion of the weak lightning signals are missed by this stricter criterion.

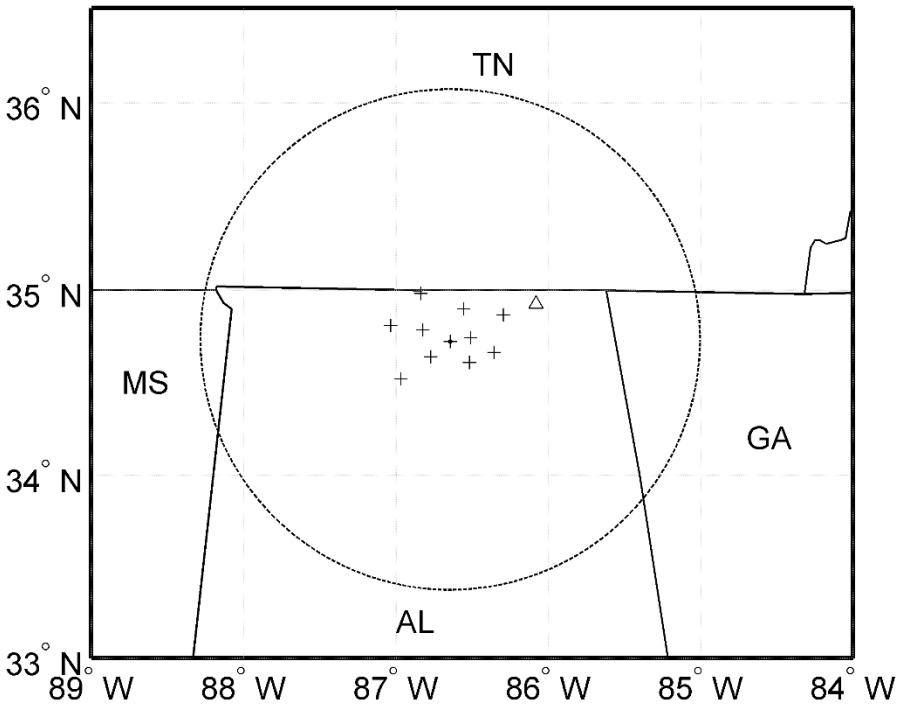

Figure 15. A map of the study area. The dashed circle is centered at the NALMA network with a radius of 150 km. AL, GA, MS, and TN are short for Alabama, Georgia, Mississippi, and Tennessee, respectively. The pluses are the detector locations of the NALMA. There were 10 NALMA stations before 2008, 11 in 2008, and 14 after 2008. The pluses in each panel mark the locations of the 11 NALMA stations through 2008. Not shown are three stations, one in Tennessee and two in Georgia, built after 2008. The triangle is the location of the KHTX site.

The overall aerosol loading is characterized using AOD retrievals (Levy, Remer, and Dubovik 2007; Levy et al. 2007) that also date back to 2002 from the Moderate-resolution Imaging Spectroradiometer (MODIS) on the Aqua satellite, which overpasses the study area in the early afternoon every day. MODIS AOD retrievals have been widely used in numerous meteorological and environmental studies (e.g. Niu and Li 2012; Van Donkelaar, Martin, and

Park 2006). Absorbing aerosols are more capable of absorbing solar radiation than non-absorbing aerosols. Satellite observations of ultraviolet (UV) radiation have been used to retrieve absorbing aerosols (Herman et al. 1999). Aerosol Index (AI) retrievals that date back to 2005 from the Ozone Monitoring Instrument (OMI) (Levelt et al. 2006) are used to discriminate between absorbing and non-absorbing aerosols. The OMI is carried by the Aura satellite that also overpasses the study area in the early afternoon. The OMI AI retrieval algorithm is inherited from the Total Ozone Mapping Spectrometer (TOMS) (Herman et al. 1997), and the AI is derived from the backscattered radiance measurements at two wavelengths, 331 and 360 nm. The AI retrievals are available in both clear-sky and cloudy conditions (Hsu, Herman, and Tsay 2003; Hsu et al. 1999; Torres et al. 2007; Yu et al. 2012) and have been frequently used in studies related to absorbing aerosols (e.g. Chiapello and Moulin 2002; Wilcox 2010).

Figure 16 shows the long-term mean diurnal variation of the logarithm base 10 of flash rate, $\log_{10}$(FR), over the study area in the JJAs from 2002 to 2015. The logarithmic transformation makes FR a more normal distribution. The lightning activity peaks in the late afternoon, in agreement with previous studies (Blakeslee et al. 2014; Chronis and Koshak 2016; Williams and Heckman 1993), shortly after the Aura and Aqua overpasses. The mean AOD is derived by averaging the available MODIS Collection 6 Level 2 AOD retrievals at a spatial resolution of 3 km (Levy and Hsu 2015; Levy et al. 2013) within the study area. At least 20 available retrievals are needed to ensure the sample mean is adequately representative of the mean AOD over the study area (i.e. spatial representativeness). In addition, often thin and small clouds are not discerned by MODIS and are misinterpreted as clear sky conditions with heavy pollution (Altaratz et al. 2014). Therefore, only cases with mean AOD less than 1.0 are kept to remove possible false heavy pollution cases, although it should be noted that this criterion may

also exclude some real heavy pollution cases (Van Donkelaar et al. 2011) and cannot remove the false cases completely. The mean AI is derived in the same way by averaging available AI retrievals within the study area using Version 003 of the OMI Level 2 OMTO3 data (Bhartia 2005). The spatial resolution of AI retrievals is 13 x 24 km, coarser than that of AOD retrievals. At least 10 available retrievals are needed to ensure spatial representativeness. Kim et al. (2007) used an AI threshold (AI_0) of 0.7 to partition the absorbing and non-absorbing aerosols during the Atmospheric Brown Cloud—East Asian Regional Experiment campaign. Their AI_0 is adopted in this study. In each case, aerosols are considered absorbing if the mean AI > 0.7, and they are considered non-absorbing if the mean AI ≤ 0.7. The probability distribution of AI appears to have multiple modes over Northern Alabama, and the subjectively selected AI_0 acts as a rough cutoff of the least absorbing mode (Figure 17).

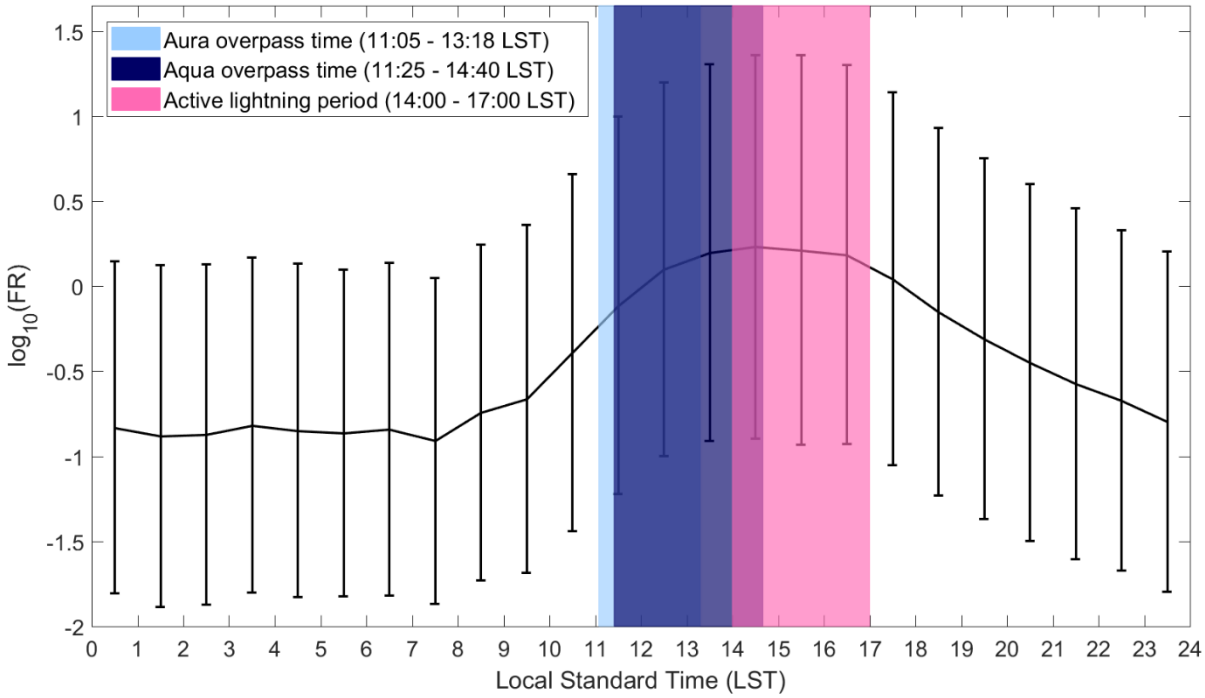

Figure 16. Long-term mean diurnal cycle of the logarithm of flash count, $\log_{10}$(FR), over northern Alabama in the JJAs from 2002 to 2015. The error bars show the standard deviations of $\log_{10}$(FR). The Aura satellite overpass time, the Aqua satellite overpass time, and the active lightning period are light blue-, dark blue-, and pink-shaded, respectively.

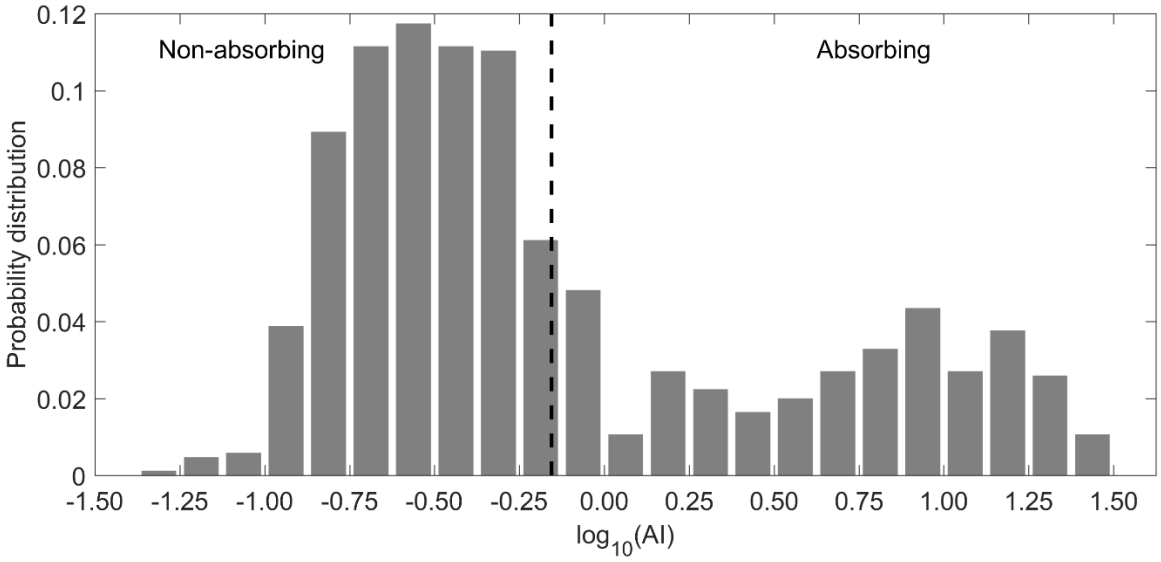

Figure 17. Probability distribution of the logarithm of mean AI, $\log_{10}$(AI), over northern Alabama in the JJAs from 2005 to 2015. The dashed line marks the selected AI threshold (AI_0 = 0.7) that separates the absorbing and non-absorbing aerosols. The logarithmic transformation (base 10) makes each of the AI mode a more normal distribution.

Convection invigoration, the consequence of the potential aerosol impacts on deep convection and lightning, occurs when the enhanced conditional instability is released (e.g. Fan et al. 2008). The consequence of the impact of detected aerosol situation on deep convection lags the aerosol detection time. Therefore, this study focuses on describing the lightning features during 14:00–17:00 Local Standard Time (LST) right after the satellite overpasses. The lightning flashes are counted over the study area during this active lightning period (180 min) to characterize the lightning activity of individual storms. Lightning FR in a given area is contributed by the lightning-producing deep convective area (LPDCA) and the flash rate per unit LPDCA (FR/LPDCA). Radar observations have been frequently used in identifying the lightning-producing storms (Bringi et al. 1997; Byers and Braham 1949; Carey and Rutledge 1996; Carey and Rutledge 2000; Dye et al. 1986; Goodman et al. 1988; Larsen and Stansbury

1974; MacGorman and Rust 1998; Marshall and Radhakant 1978; Schultz, Petersen, and Carey 2011; Schultz et al. 2017; Williams, Weber, and Orville 1989). The Level 3 composite radar reflectivity data from the Hytop, Alabama (34.927 N, 86.080 W) KHTX WSR-88D are used in this study to estimate the LPDCA (Carey and Rutledge 2000; Larsen and Stansbury 1974). Every contiguous storm area where lightning flashes are present is considered a LPDCA if the composite radar reflectivity of each grid box in this area is greater than or equal to a threshold (30, 35, and 40 dBZ).

To examine if absorbing aerosols may have a greater impact on lightning and convection than non-absorbing aerosols, the mean AOD is first correlated with FR for cases in the presence of absorbing and non-absorbing aerosols, respectively; then it is correlated with the mean fraction of the LPDCA (F_{LPDCA}) over the study area and the mean FR/LPDCA during the active lightning period, respectively. The mean F_{LPDCA} is obtained by averaging the fractions for all the radar scans during the active lightning period. The FR/LPDCA is obtained by normalizing the FR during each radar scan by the detected LPDCA. The flashes over the study region within 4 minutes after the time of the scan are counted. The mean FR/LPDCA is then derived by averaging the normalized rates for all the scans during the active lightning period.

In addition to the aerosol loading, the lightning and associated convection features (LPDCA and FR/LPDCA) are related to meteorological conditions. Lightning FR is regulated by both AOD and CAPE (Proestakis, Kazadzis, Lagouvardos, Kotroni, Amiridis, et al. 2016; Williams et al. 2002). The microphysics and dynamics are coupled in the context of aerosol invigoration of convection (Altaratz et al. 2014). Aerosol microphysical effects are sensitive to meteorological conditions (e.g., Albrecht, Morales, and Silva Dias 2011; Fan et al. 2009; Storer, van den Heever, and L'Ecuyer 2014; Storer, van den Heever, and Stephens 2010; Zhao et al.

2018). Whether aerosols invigorate or suppress deep convection is dependent upon the vertical wind shear (VWS) (Fan et al. 2009), which shapes the structure of convection (Malkus 1949) and is one of the prominent synoptic features (Konrad 1997). To compare the relative importance of aerosols and meteorological conditions in potential regulations of lightning and associated convection, FR, F_{LPDCA}, and FR/LPDCA are correlated with CAPE and VWS, respectively. The horizontal winds at 850 and 200 hPa are used to calculate the VWS (Konrad 1997). Moreover, as described in the PBL-mechanism, the turbulent mixing in the PBL is related to low-level convergence, secondary convection, and possibly lightning. To diagnose the unstable boundary layer characteristics in the storms, FR, F_{LPDCA}, and FR/LPDCA are also correlated with the planetary boundary layer height.

The CAPE, VWS, and PBLH data are taken from the Modern-Era Retrospective analysis for Research and Applications, Version 2 (MERRA-2), which assimilates the atmospheric aerosols with their radiative effects included in the atmospheric fields (Randles et al. 2016). The 3-hourly instantaneous MERRA-2 Assimilated Meteorological Fields on model levels (GMAO 2015b) are used to calculate the CAPE at 15:00 LST (21:00 UTC) that falls within the active lightning period. The gridded CAPE values are then averaged over the study area. The wind fields at 14:30, 15:30, and 16:30 LST (20:30, 21:30, and 22:30 UTC) from the 1-hourly time-averaged MERRA-2 Single-Level Diagnostics (GMAO 2015d) are averaged to obtain the mean VWS between 850 and 200 hPa during the active lightning period. Then, the gridded time-averaged VWS values are averaged over the study area. The PBLHs at 14:30, 15:30, and 16:30 LST (20:30, 21:30, and 22:30 UTC) from the 1-hourly time-averaged MERRA-2 Surface Flux Diagnostics (GMAO 2015c) are averaged to obtain the mean PBLH during the active lightning period. Then, the gridded time-averaged PBLH values are averaged over the entire study area. In

numerical models, the PBLH is generally determined by examining where the bulk Richard number (Ri_b) exceeds a prescribed threshold (Zhang et al. 2014). The suppression of turbulent mixing by a capping inversion above the unstable boundary layer makes Ri_b exceed the threshold at a lower level, resulting in a reduced PBLH.

If the CAPE-mechanism applies, then AOD and CAPE should show an increased positive correlation in the presence of absorbing aerosols, although the reverse is not true. Similarly, if the PBL-mechanism applies in the presence of absorbing aerosols, then AOD and PBLH will show a negative correlation, although the reverse is not true either. The necessary condition of the CAPE-mechanism is examined by correlating the AOD retrievals with the instantaneous MERRA-2 $CAPE^{1/2}$ within the active lightning period (15:00 LST) and before (12:00 LST) for all the storm cases and the cases in the presence of absorbing aerosols, respectively. The necessary condition of the PBL-mechanism is examined by correlating the AOD retrievals with the mean MERRA-2 PBLHs during 14:00–17:00 LST and during 12:00–14:00 LST, respectively. The mean PBLH during 12:00–14:00 LST is obtained by averaging the 1-hourly time-averaged PBLHs at 12:30 and 13:30 LST (18:30 and 19:30 UTC).

Last, a polluted case and a clean case are selected to illustrate the aerosol, convection, and meteorological situations in more detail with additional datasets, including (1) the vertical cross sections of radar reflectivity (Z) and differential reflectivity (Z_{DR}) from the KHTX WSR-88D Level 2 data; (2) vertical profiles of temperature (T), dew point temperature (Td), and horizontal wind at 12:00 LST from the 3-hourly instantaneous MERRA-2 Assimilated Meteorological Fields on pressure level (GMAO 2015a); and (3) the aerosol type retrievals from the Version 3.30 Level 2 vertical feature mask products (CALIPSO Science Team 2015; Vaughan et al. 2009) from the Cloud-Aerosol Lidar with Orthogonal Polarization (CALIOP), the

lidar instrument on the CALIPSO (Cloud-Aerosol Lidar and Infrared Pathfinder Satellite Observations) satellite (Omar et al. 2009). Six pre-defined aerosol types are identified based primarily on CALIOP volume depolarization ratio measurements and associated extinction-to-backscatter ratios (lidar ratios) (Omar et al. 2009). Previous studies have suggested that whether absorbing aerosols suppress or enhance the strength of capping inversion (Yu, Liu, and Dickinson 2002) and convection (Koch and Del Genio 2010) is related to the vertical distribution of aerosol particles. The altitudes of the absorbing aerosol layers present in the selected cases are shown using the CALIPO aerosol type retrievals. The sources of all the data used in this study are documented in Table 3. The following results section starts with the correlation analysis of AOD and FR in presence of non-absorbing and absorbing aerosols, followed by correlation analyses related to storm area and FR per storm. Then, the correlations between AOD and CAPE and between AOD and PBLH are presented. Last, a comparative study of a clean case and a polluted case is shown.

Table 3. Data sources.

Variables	Sources
Lightning flash	NALMA
AOD	Aqua MODIS Level 2 Collection 6 (3 km)
AI	Version 003 OMI Level 2 OMTO3
CAPE and freezing level	MERRA-2 Assimilated Meteorological Fields (model level)
VWS	MERRA-2 Single-Level Diagnostics
PBLH	MERRA-2 Surface Flux Diagnostics
Vertical profiles of T, Td, and wind	MERRA-2 Assimilated Meteorological Fields (pressure level)
Vertical profiles of aerosol types	Version 3.30 CALIOP Level 2 vertical feature mask
Composite radar reflectivity	WSR-88D (KHTX) Level 2 and 3
Z and Z_{DR}	WSR-88D (KHTX) Level 2

3.3. Results

3.3.1. Absorbing aerosols vs. non-absorbing aerosols

A total of 592 storm-related lightning cases are found over northern Alabama in the summers during 2002–2015 when Aqua MODIS AOD retrievals are available. There are 173 cases during 2005–2015 dominated by absorbing aerosols based on an AI_0 of 0.7. Irrespective of the aerosol absorbance, the overall correlation coefficient between the mean AOD and $\log_{10}$(FR) for all the 592 cases is 0.107, smaller than that (0.246) for the 173 absorbing aerosol cases (Figure 18) and

that (0.141) for the 252 non-absorbing aerosol cases (Table 4). First, the positive correlation between AOD and $\log_{10}$(FR) does not necessarily suggest that aerosols have an impact on lightning. The positive correlation between AOD and $\log_{10}$(FR) may be contributed by some meteorological condition that is conductive to more intense storms and favorable for more aerosols. Even if aerosols can enhance lightning, the weak correlation suggests that the enhancement is not strong. In other words, aerosols are without doubt secondary in regulating the lightning FR, at least over northern Alabama.

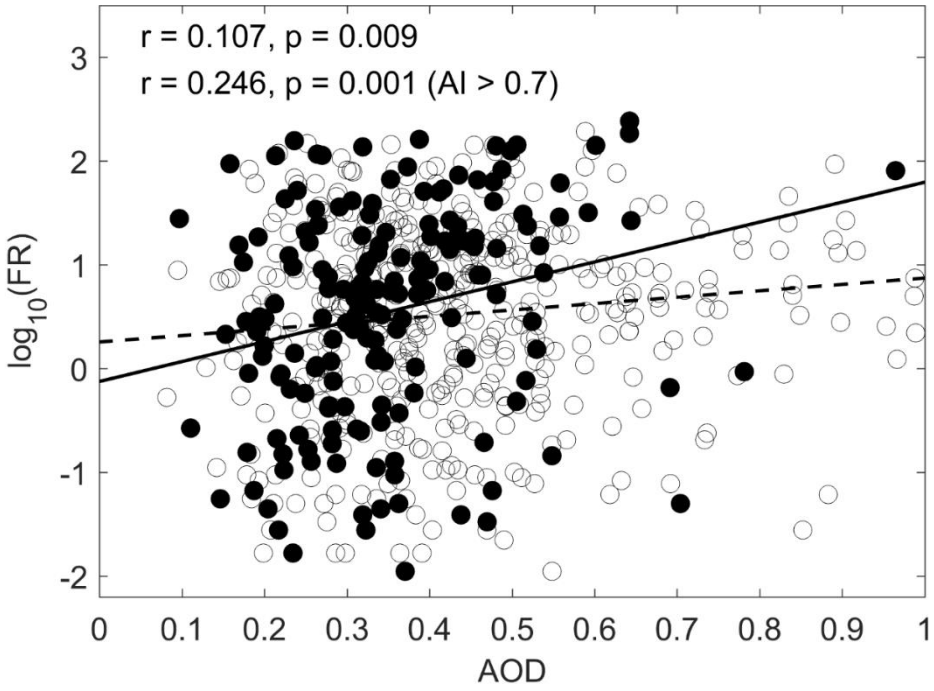

Figure 18. Scatterplot of $\log_{10}$(FR) vs. the domain-averaged AOD during the JJAs from 2002 to 2015. Among the cases from 2005 to 2015, those mean AIs greater than 0.7 are marked by dots. The dashed line is the linear regression of $\log_{10}$(FR) on AOD for all the cases (circles and dots); the upper r and p are the corresponding correlation coefficient and p-value, respectively. The solid line is the linear regression of $\log_{10}$(FR) on AOD for all the cases from 2005 to 2015 where AIs are greater than 0.7 (dots); the lower r and p are the corresponding correlation coefficient and p-value, respectively. The Aqua MODS AOD retrievals date back to 2002; the OMI AI retrievals date back to 2005.

The increased correlation coefficient between AOD and $\log_{10}$(FR) in the presence of absorbing aerosols may suggest that if aerosols can enhance lightning, the enhancement becomes stronger if the aerosols are more absorbing. However, the increased correlation may also result from some meteorological condition that is conductive to more intensified storms and brings more absorbing aerosols. The increased correlation between the optical depth of absorbing aerosols and lightning FR is not sensitive to the selected AI_0 that separates absorbing and non-absorbing aerosols. Table 4 documents correlation coefficients between AOD and $\log_{10}$(FR) for absorbing and non-absorbing aerosols using different AI thresholds. The correlation coefficient between the optical depth of absorbing aerosols and lightning FR is consistently stronger than that between the optical depth of non-absorbing aerosols and lightning FR, regardless of the selected AI_0. As the selected AI_0 becomes increasingly smaller or larger than 0.7, the correlation coefficient between absorbing aerosols and FR and that between of non-absorbing are getting closer, AI thresholds ranging from 0.2 to 1.9 with an increment of 0.1 are tested, and the results are the same (not shown).

Table 4. Correlation coefficients between AOD and $\log_{10}$(FR) for absorbing (r_a, $AI > AI_0$) and non-absorbing aerosols (r_{na}, $AI \leq AI_0$) using Different AI Thresholds (AI_0). Asterisks specify significance levels: * indicates *t* test statistics at a significance level of 0.05; ** indicates *t* test statistics at a significance level of 0.01.

AI_0	0.4	0.5	0.6	0.7	0.8	0.9	1.0
r_a	0.180**	0.235**	0.234**	0.246**	0.222**	0.238**	0.238**
r_{na}	0.151*	0.135*	0.135*	0.141*	0.157*	0.150*	0.146*

3.3.2. Correlations with storm area and flash rate per storm

Increased lightning FR can be contributed by increased LPDCA or increased FR/LPDCA. Both aerosols and meteorological conditions correlate with the two parameters. Table 5 documents the correlation coefficients among the variables, where the LPDCA is defined using a composite radar reflectivity threshold of 30 dBZ. The correlation coefficients are also calculated with the LPDCA defined using the 35 and 40 dBZ thresholds, and the results are close and lead to the same conclusions (not shown). The logarithmic transformation (base 10) makes the mean F_{LPDCA} and the mean FR/LPDCA more normal distributions. We take the square roots of CAPE and VWS to make the distributions more normal. The square root of CAPE is correlated to convective cloud updraft strength (Emanuel 1994). Table 6 is same as Table 5 except for the cases in presence of absorbing aerosols.

Table 5. Correlation coefficients among the variables for all the cases. Asterisks specify significance levels: ** indicates *t* test statistics at a significance level of 0.01.

	AOD	$CAPE^{1/2}$	PBLH	$VWS^{1/2}$
$\log_{10}(FR)$	0.107**	0.467**	-0.192**	-0.224**
$\log_{10}(F_{LPDCA})$	0.168**	0.297**	-0.400**	-0.092**
$\log_{10}(FR/LPDCA)$	-0.127**	0.378**	0.185**	-0.260**

Table 6. Correlation coefficients among the variables for all the cases in the presence of absorbing aerosols. Asterisks specify significance levels: * indicates *t* test statistics at a significance level of 0.05; ** indicates *t* test statistics at a significance level of 0.01.

	AOD	$CAPE^{1/2}$	PBLH	$VWS^{1/2}$
$\log_{10}(FR)$	0.246**	0.472**	-0.206**	-0.317**
$\log_{10}(F_{LPDCA})$	0.265**	0.290**	-0.449**	-0.168*
$\log_{10}(FR/LPDCA)$	0.078	0.389**	0.242	-0.300**

Overall, $CAPE^{1/2}$ shows the strongest positive correlation with FR, and it correlates better with $\log_{10}(FR/LPDCA)$ than with $\log_{10}(F_{LPDCA})$, suggesting that both the area of a convective system and the flash rate per unit storm area within the system are related to CAPE. However, the positive correlation between AOD and $\log_{10}(FR)$ appears to be primarily contributed by the association between the aerosol loading and the storm area rather than any association between the aerosol loading and the flash rate per unit storm area. The results may suggest that even if aerosols can enhance lightning by invigorating deep convection, the invigoration may not act the same as that by an increase of CAPE, at least over northern Alabama. In agreement with the previous studies that have suggested the importance of updraft in determining FR (Deierling and Petersen 2008; Deierling et al. 2008; Schultz et al. 2017; Zipser 1994), the results in Tables 5 and 6 also show that CAPE plays a more important role in regulating the flash rate per unit storm area. However, aerosols do not appear to have a significant influence on the flash rate per unit storm area. As documented in Table 5, AOD even shows a weak negative correlation with FR/LPDCA. Therefore, if the CCN/IN-mechanism applies, it may be not only ideally regarded as an individual deep convective cell invigoration but also an "invigoration" through enhanced low-

level convergence and secondary convection (Khain, Rosenfeld, and Pokrovsky 2005; Lee and Feingold 2010). Moreover, the distinctive "invigoration" of deep convection by aerosols and CAPE, if present, cannot be reconciled solely by the CAPE-mechanism, because if adding more absorbing aerosols only resulted in increased CAPE, then both the storm area and the flash rate per unit storm area would have increased.

As documented in Table 6, in the presence of absorbing aerosols, the decreased correlation between $CAPE^{1/2}$ and $\log_{10}(F_{LPDCA})$ is close to the increased correlation between AOD and $\log_{10}(F_{LPDCA})$. The FR per unit storm area appears to be still primarily regulated by CAPE. It does not seem that the elevated correlation between the loading of absorbing aerosols and the storm area can be readily explained using the convection invigoration as described in the CCN/IN-mechanism. To the best of our knowledge, none of the previous studies have suggested absorbing aerosols are more efficient CCN than non-absorbing aerosols. As efficient IN, mineral dust aerosols that are absorbing aerosols may potentially influence storms (Sassen et al. 2003), however increased IN cannot be straightforwardly linked to increased storm area due to the limited knowledge of mixed clouds. Moreover, it is not evident that the identified absorbing aerosols in this study necessarily consist of efficient ice-nucleating particles. Therefore, we hypothesize that the increased correlation between AOD and $\log_{10}(F_{LPDCA})$ in the presence of absorbing may be due in part to the interaction between absorbing aerosols and turbulent mixing in the PBL, as described in the PBL-mechanism.

Absorbing aerosols absorb the incident solar radiation and prevent it from reaching the surface, cooling the surface and heating the layer above. This helps maintain a capping inversion that can suppress the turbulent mixing in the unstable PBL (Wilcox et al. 2016) and result in a decreased PBLH (Ding et al. 2016; Dong et al. 2017). The suppression of turbulent mixing can

also enhance the low-level wind shear (Saide et al. 2015), which can in turn facilitate the turbulent mixing over the surrounding area and hence potentially trigger deep convection nearby. The interaction of cold pool and enhanced low-level wind shear plays a key role in new cell formation in convective systems (Knupp and Cotton 1982; Rotunno, Klemp, and Weisman 1988; Weisman and Rotunno 2004). Such a mechanism may also link increased absorbing aerosols to increased storm area.

As documented in Tables 5 and 6, reduced PBLH is associated with increased storm area. PBLH shows a weak negative correlation with FR. The correlation appears to be mostly contributed by the negative association between PBLH and LPDCA as a consequence of radiative-convective adjustment. On one hand, the clouds of a storm prevent the sunlight from reaching the surface, weaken the turbulent mixing, and hence reduce the PBLH. On the other hand, as described in the PBL-mechanism, the suppressed turbulent mixing within the lower PBL leads to enhanced low-level wind shear, which may be linked to secondary convection over the surrounding area. In addition, VWS shows relatively weak correlation with FR. Its correlation is more negative with the FR/LPDCA than with the F_{LPDCA}, especially in the presence of absorbing aerosols. The results may suggest that enhanced VWS above the PBL is associated with reduced FR per unit storm area, which may be due to the negative association between VWS and CAPE (not shown). Vertical momentum transport in a mesoscale convective complex tends to reduce the deep-layer VWS as convection intensifies (Wu and Yanai 1994).

Together, the results in Tables 5 and 6 suggest that lightning is more active (in terms of FR) in the presence of absorbing aerosols, and this feature may result from the synthesis of multiple mechanisms, including all the processes described by the CCN/IN-, CAPE- and PBL-

mechanisms. Among the mechanisms, the PBL-mechanism is seemingly the strongest link between absorbing aerosols and increased storm area.

3.3.3. Categorized CAPE

As documented in Tables 5 and 6 and in agreement with previous studies (e.g. Williams et al. 2002), both CAPE and aerosols influence the FR of a storm; and CAPE appears to be more influential, particularly in determining the FR/LPDCA. The potential impacts of aerosols on lightning via the CCN/IN- and PBL- mechanisms may be more detectable, if CAPE is categorized, i.e. minimizing the effect of the CAPE-mechanism. The storm cases are roughly grouped into the low, median, and high $CAPE^{1/2}$ regimes using a half standard deviation below and above the mean of $CAPE^{1/2}$, $\mu_{CAPE} \pm \sigma_{CAPE}/2$. The subjectively selected thresholds have been used in previous analytical studies, including the classification of the El Niño Southern Oscillation (ENSO) phases (Phillips, Cane, and Rosenzweig 1998; Ropelewski and Halpert 1996). Figure 19 shows the scatterplots of $\log_{10}(F_{LPDCA})$ vs. AOD in the low, median, and high $CAPE^{1/2}$ regimes, respectively.

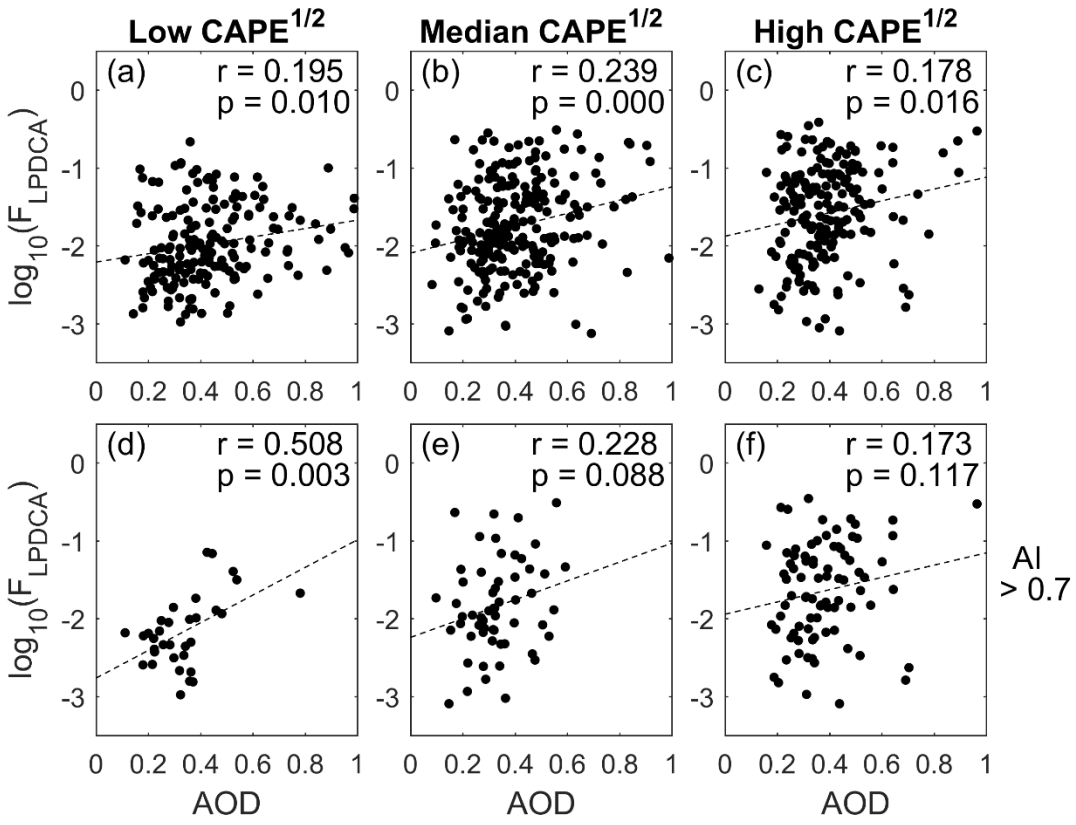

Figure 19. Scatterplots of log10(FLPDCA) vs. AOD in the low, median, and high CAPE1/2 regimes, respectively, which are separated by a half standard deviation (σCAPE) below and above the mean (μCAPE) of the CAPE1/2. μCAPE ± σCAPE/2 = 27.51 ± 9.92/2 J1/2kg-1/2 for all the storm cases (upper panels) and 27.56 ± 10.03/2 J1/2kg-1/2 for all the cases where AI retrievals are available (lower panels). r and p in each panel are the correlation coefficient and the p-value, respectively.

The optical depth of all aerosols and storm area show close positive correlations in all three regimes (Figure 19a-c). The correlation coefficients (0.195, 0.239, and 0.178) are slightly greater than that (0.168) in Table 5 where the $CAPE^{1/2}$ variation is not restricted, suggesting that the apparent aerosol enhancement of the storm area is more pronounced if the variation of CAPE is constrained to a small range. In the presence of absorbing aerosols, the apparently stronger enhancement is present in the low $CAPE^{1/2}$ regime (Figure 19d) with an increased correlation coefficient of 0.508, greater than that (0.195) between the optical depth of all aerosols and the

storm area (Figure 19a) and the counterpart (0.265) in Table 5 where the $CAPE^{1/2}$ is not constrained. As previously mentioned, no prior studies have suggested that the CCN/IN-mechanism works better for more absorbing aerosols; the restriction of the $CAPE^{1/2}$ variation in the correlation analyses reduces the effect of the CAPE-mechanism. Hence, the PBL-mechanism is more likely to explain the increased correlation between the loading of absorbing aerosols and the storm area in the low $CAPE^{1/2}$ regime (Figure 19a and 19d). AOD and $\log_{10}$(FR/LPDCA) do not show any statistically significant correlations except a negative one in the median $CAPE^{1/2}$ regime in the presence of all aerosols, which passes the *t*-test at a 95% confidence interval (not shown). The results suggest that aerosol-lightning-enhancement, if present, is via the enhancement of the LPDCA rather than the FR/LPDCA, at least over Northern Alabama.

3.3.4. The CAPE- and PBL-mechanisms

As previously shown, lightning flashes (FR) and associated convection parameters (F_{LPDCA} and FR/LPDCA) show enhanced correlations with AOD in the presence of absorbing aerosols, leading to speculation that the CAPE- and PBL-mechanisms apply in such storm cases. As shown in Figure 20, AOD is positively correlated with $CAPE^{1/2}$ during the active lightning period (15:00 LST) and before (12:00 LST) for all storm cases. The correlation coefficients double for the cases in the presence of absorbing aerosols (Figure 20). The results suggest that the meteorological conditions conductive to stronger storms may also bring more absorbing aerosols, or the CAPE can be accumulated in the presence of absorbing aerosols as previously described. As shown in Figure 21, AOD and the mean PBLH during the active lightning period show no correlation for all the storm cases but negative correlations for the cases in the presence of absorbing aerosols. The correlation is even more negative, if all the storm cases that have at least one MODIS AOD retrieval within the study area are included (Figure 21b), i.e., relaxing

the spatial representativeness criterion. The optical depth of absorbing aerosols and the mean PBLH also show a negative correlation during 12:00–14:00 LST that falls within the timespan of the Aqua satellite overpass (not shown). While these negative correlations are suggestive, they may be due to some meteorological conditions that reduce the PLBH and lead to increased absorbing aerosol-loading. However, in agreement with previous studies (Ding et al. 2016; Dong et al. 2017), the suppression of turbulent mixing within the PBL by the presence of absorbing aerosols as described in the PBL-mechanism also appears to be plausible.

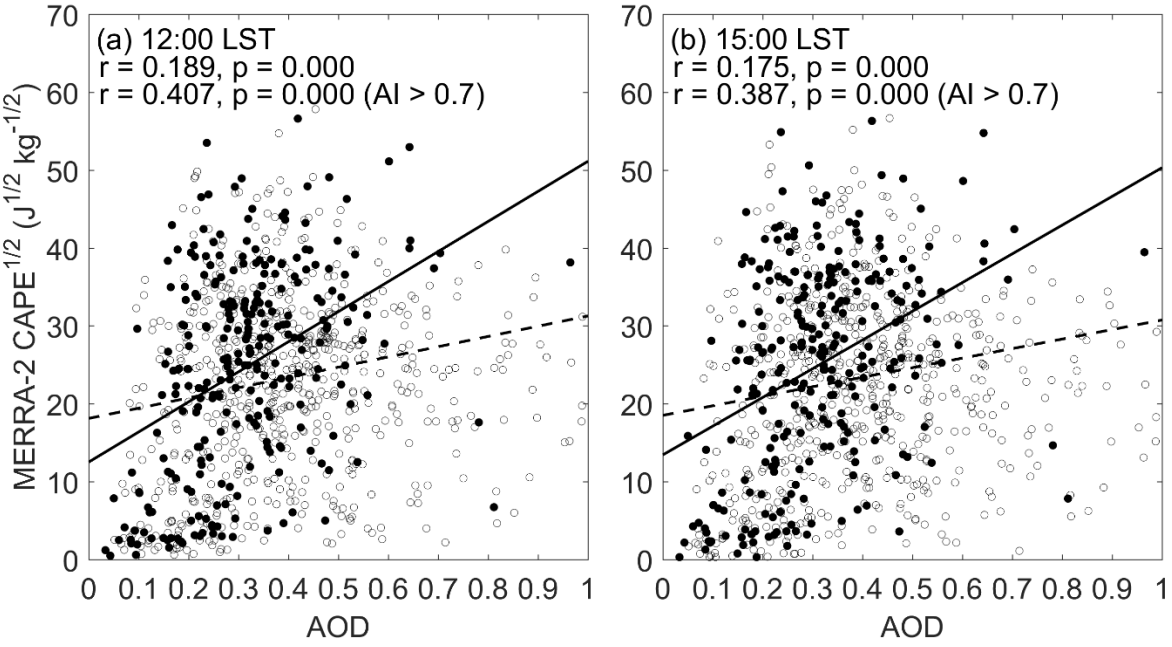

Figure 20. Scatterplots of the MERRA-2 $CAPE^{1/2}$ at 12:00 LST vs. AOD (a) and the MERRA-2 $CAPE^{1/2}$ at 15:00 LST vs. AOD (b) during the JJAs from 2002 to 2015. Among the cases from 2005 to 2015, those AIs greater than 0.7 are marked by dots. In each panel, the dashed line is the linear regression of $CAPE^{1/2}$ on AOD for all the cases (dots and circles) irrespective of their AIs; the upper r and p are the corresponding correlation coefficient and p-value, respectively. The solid line is the linear regression of $CAPE^{1/2}$ on AOD for all the cases from 2005 to 2015 where AIs are greater than 0.7 (dots); the lower r and p are the corresponding correlation coefficient and p-value, respectively. The Aqua MODS AOD retrievals date back to 2002; the OMI AI retrievals date back to 2005.

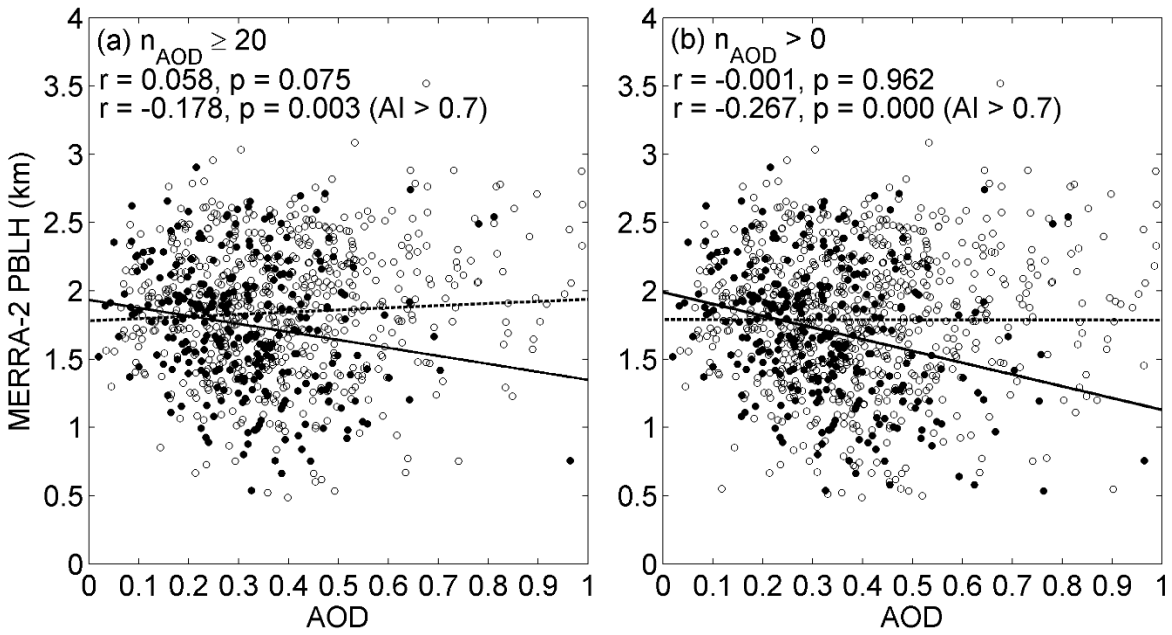

Figure 21. Scatterplots of PBLH vs. AOD for the cases that have at least 20 available AOD retrievals (a) and all the cases (b) during the JJAs from 2002 to 2015. Among the cases from 2005 to 2015, those AIs greater than 0.7 are marked by dots. In each panel, the dashed line is the linear regression of PBLH on AOD for all the cases (dots and circles) irrespective of their AIs; the upper r and p are the corresponding correlation coefficient and p-value, respectively. The solid line is the linear regression of PBLH on AOD for all the cases from 2005 to 2015 where AIs are greater than 0.7 (dots); the lower r and p are the corresponding correlation coefficient and p-value, respectively. n_{AOD} is the number of the available AOD retrievals. The Aqua MODS AOD retrievals date back to 2002; the OMI AI retrievals date back to 2005.

3.3.5. Case studies

3.3.5.1. Selection of two cases

A polluted case and a clean case (Table 7) are subjectively selected to illustrate the lightning and associated convection features in more detail with a focus on the CCN/IN- and PBL- mechanisms using additional observations. Both the cases are taken from the low $CAPE^{1/2}$ regime, where the optical depth of absorbing aerosols correlates best with $\log_{10}(F_{LPDCA})$ (Figure 19). Only those cases that have CALIPSO satellite overpasses and radar polarimetric measurements are considered in the selection for a more detailed analysis.

Table 7. The lightning, aerosol, and meteorological parameters of the selected two cases.

Date	$\log_{10}$ (FR)	$\log_{10}(F_{LPDCA})$ ($\geq$ 30dBZ)	$\log_{10}$(FR/LPDCA) ($\geq$ 30dBZ)	AI	AOD	$CAPE^{1/2}$ ($J^{1/2}$ $kg^{-1/2}$)
18 August, 2012	0.923	-1.501	-2.503	12.5	0.54	12.5
4 August, 2015	0.219	-2.188	-2.444	14.3	0.20	19.2

The AODs of the polluted (18 August 2012) and clean (4 August 2015) cases were 0.54 (95th percentile) and 0.20 (21st percentile), respectively. Although the mean FRs per storm area in the two cases were close, the polluted case showed a larger mean storm area than the clean case (Table 5). As a result, more lightning flashes were detected during the active lightning period in the polluted case than in the clean case (Table 7). The CAPE of the polluted case was smaller than that of the clean case (Table 7), but both were within the low $CAPE^{1/2}$ regime. The large AI (Table 7) in the two cases are suggestive of the presence of absorbing aerosols in both cases, which are also supported by the CALIOP aerosol type retrievals (Figure 22). In the early afternoon (13:10 LST) of 18 August 2012, a smoke layer was detected between 2 and 3 km near the southern boundary of the study area and a polluted dust layer was detected below 2 km near the center of the study area (Figure 22). In the early afternoon (13:04 LST) of 4 August 2015, polluted dust aerosols were detected below 2 km along the track of CALIOP in the eastern part of the study area and between 4 and 5 km near the northeastern boundary.

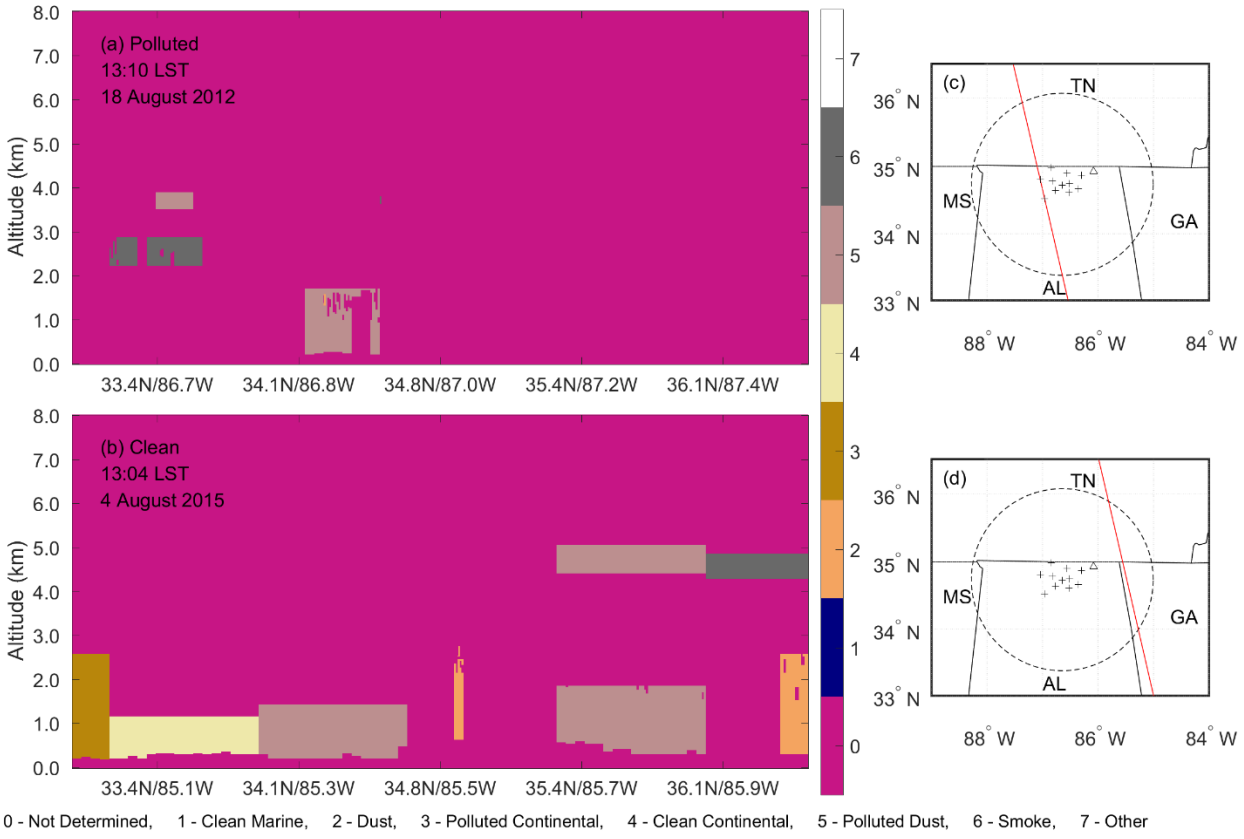

Figure 22. Vertical profiles of aerosol types along the tracks of CALIOP over the study area for the two selected cases, 18 August 2012 (a) and 4 August 2015 (c), respectively. The red lines in panels (c) and (d) mark the ground tracks of CALIOP on the map.

3.3.5.2. The CCN/IN mechanism

In the polluted case, most lightning flashes were produced by a cluster of convective cells that formed in the southern part of the study area (Figure 23a). New cells formed and old cells decayed as this cluster moved eastward. In addition, a strong single cell that occurred close to the southeastern edge of the study area also produced a portion of the flashes (Figure 23a). The convective area extended to Mississippi along a stationary front (Figure 23a). In the clean case, the lightning flashes were contributed by a few single cells; no multi-cell convective system was present. The polluted case shows a maximum FR of 17.00 min^{-1} during the radar scan that started

at 15:03 LST (Figure 23a). The clean case shows a maximum FR of 8.00 min^{-1} during the radar scan that started at 14:45 LST (Figure 23b). The development of individual cells (Figure 23) in the polluted and clean cases is shown by their vertical cross sections of Z (Figure 24) and Z_{DR} (Figure 24) from 5 consecutive radar scans right before their peak FRs.

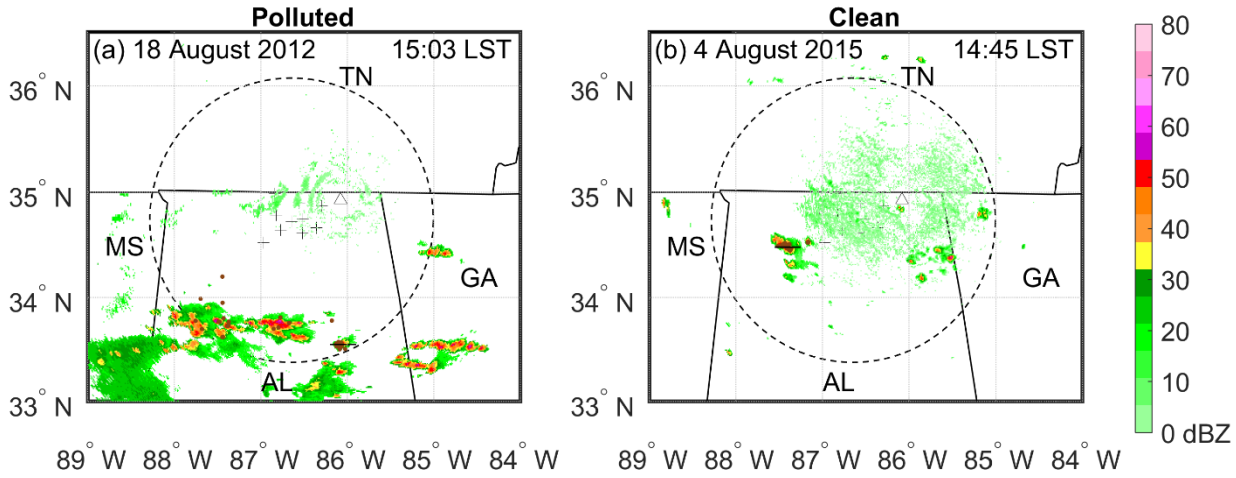

Figure 23. Spatial distributions of composite radar reflectivity when FR peaked during the active lightning period in the polluted (a) and clean (b) cases. In each panel, the horizontal black line across the convective cell marks the location where the vertical cross sections of Z (Figure 24) and ZDR (Figure 25) are shown. AL, GA, MS, and TN are short for Alabama, Georgia, Mississippi, and Tennessee, respectively. The pluses are the detector locations of the NALMA. There were 10 NALMA stations before 2008, 11 in 2008, and 14 after 2008. The pluses in each panel mark the locations of the 11 NALMA stations through 2008. Not shown are three stations, one in Tennessee and two in Georgia, built after 2008. The triangle is the location of the KHTX site.

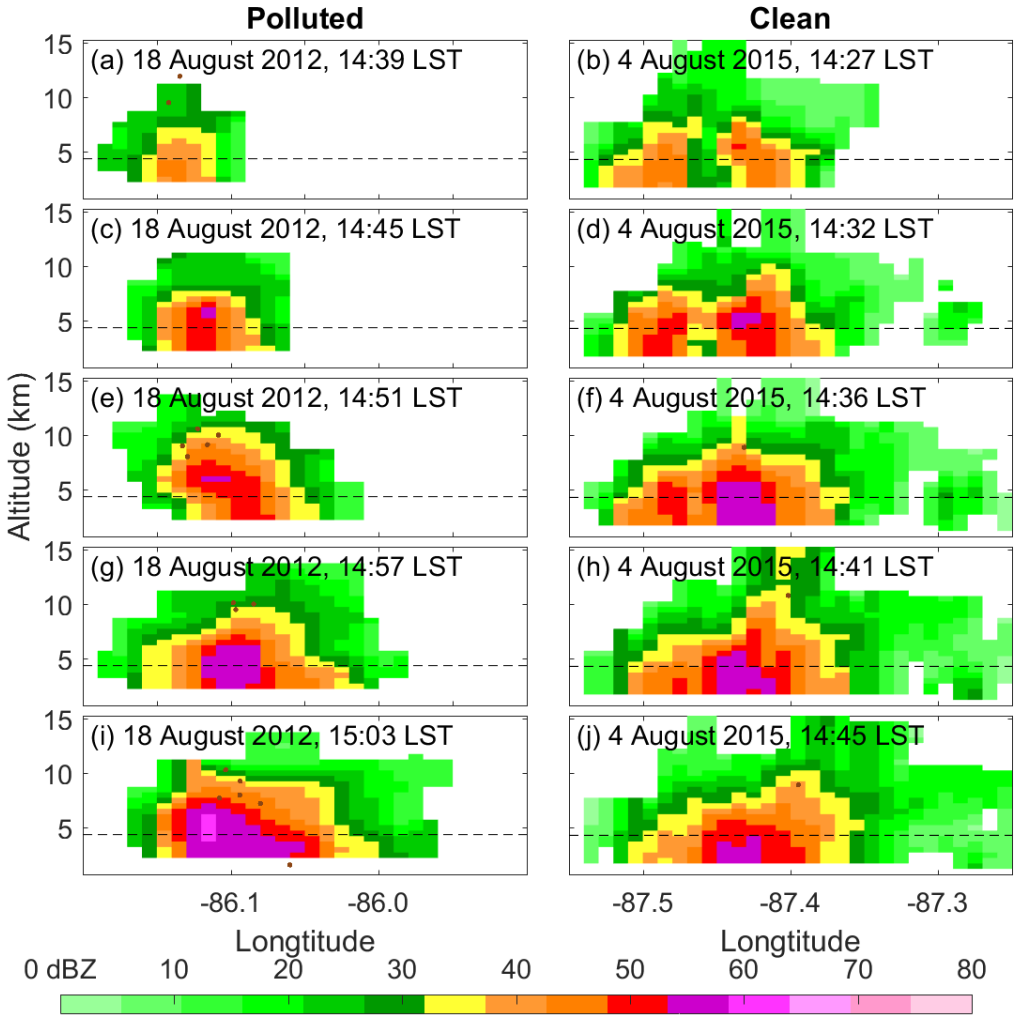

Figure 24. Vertical cross sections of Z (dBZ) at 5 consecutive radar scans for the two selected cases. The left and right panels are for the polluted and clean cases, respectively. In each panel, brown dots are the detected lightning flashes; the dashed black line is the freezing level taken from the MERRA-2.

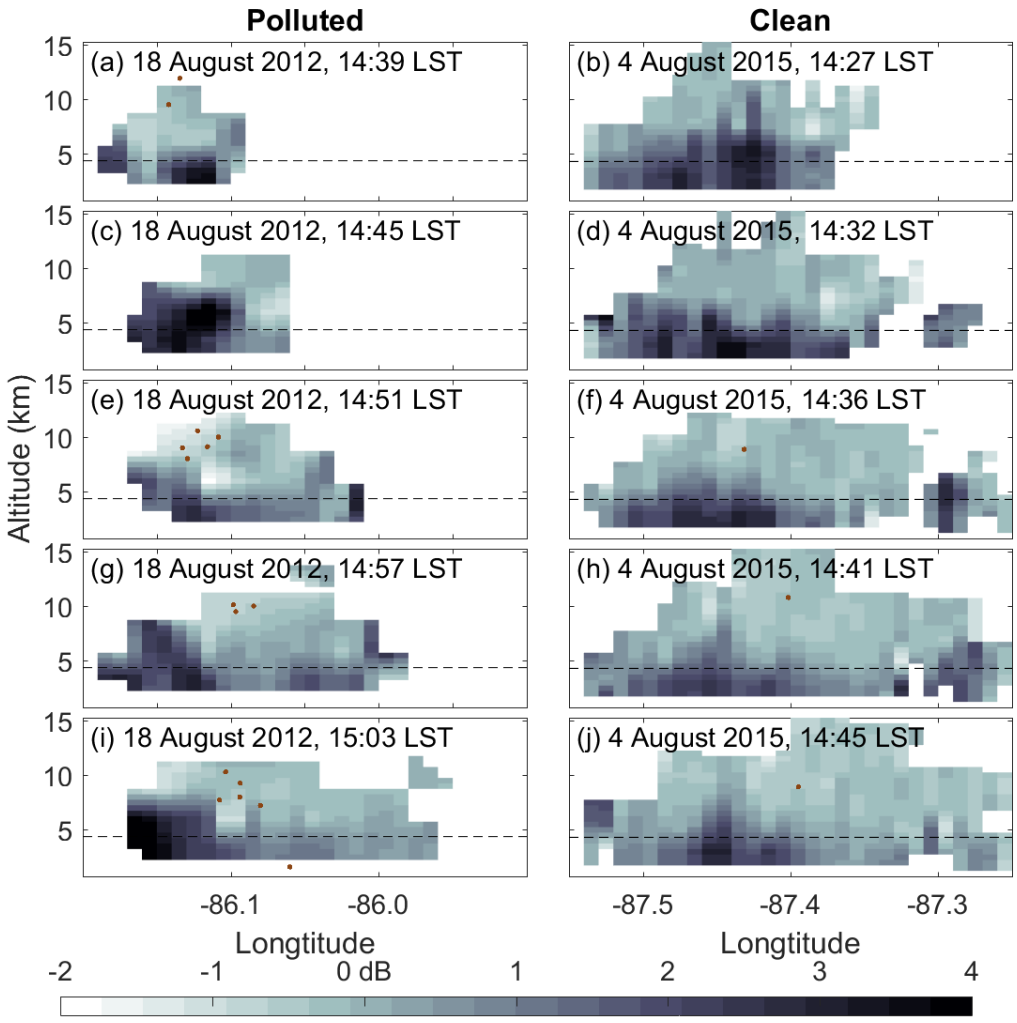

Figure 25. Same as Figure 24 except for Z_{DR} (dB).

The Z maxima above the freezing levels were close in the two cases (Figure 24a-h) before their peak FRs. The Z maximum above the freezing level at the mature stage of the convective cell was greater in the polluted case (Figure 24i) than the counterpart in the clean case (Figure 24j), suggestive of a more invigorated convective cell with more supercooled water lifted above the freezing level in the polluted case (Yuan et al. 2011; Zipser and Lutz 1994). A column of enhanced Z_{DR} around 4.0 was present above the freezing level at 14:45 LST in the polluted

case (Figure 25c), suggesting the presence of increased supercooled water (Bruning et al. 2007; Conway and Zrnić 1993; Herzegh and Jameson 1992; Hubbert et al. 1998; Tuttle et al. 1989) at the growing stage of the convective cell right before the initialization of lightning flashes (Figure 25e). In agreement with a previous study by Bruning et al. (2007), the enhanced Z_{DR} column collapsed right before the initialization of the lightning flashes (Figure 25e), indicative of a cloud-microphysical transition near the lightning initialization locations.

Although increased supercooled water was evidently present above the freezing level in the polluted case based on the single cell comparison, this feature did not necessarily suggest that the CCN/IN mechanism applied to the polluted case. First, we cannot show that the convective cell in the polluted case had an increased number concentration of smaller cloud droplets at the developing stage of convection. The cloud droplet number concentration is dependent upon updraft velocity and aerosol particle number concentration (Ghan et al. 1993; Ghan, Chung, and Penner 2009; Twomey 1959). We did not show the updraft velocities of the two cases, which were difficult to estimate. Moreover, the synoptic-scale environments of the two cases were different. A stationary front was formed in the polluted case from central Texas to central Mississippi at 08:00 LST and last 9 hours until the warm front triumphed over the cold front at 17:00 LST. The occurrence of the thunderstorms during the active lightning period over northern Alabama appeared to be influenced by this stationary front. However, in the clean case, no synoptic-scale weather system was present over the study area or nearby; the occurrence of the thunderstorms appeared to be local thermally-driven. Therefore, in spite of the close CAPEs in the two selected cases, other possible factors that could affect the cloud microphysics might not be ruled out. Recent studies (Rosenfeld et al. 2014; Rosenfeld et al. 2016; Zheng, Rosenfeld, and Li 2015) have suggested a way of estimating CCN concentrations and cloud base updraft

velocities of boundary layer convective clouds simultaneously using satellite observations. Such satellite retrievals, if available, may help disentangle the CCN/IN-mechanism from the influences on deep convection by other factors.

3.3.5.3. The PBL-mechanism

The vertical thermal structures of the two cases were different. A heated layer between 850 and 700 hPa was present at 12:00 LST before the active lightning period in the polluted case, as shown by the reduced lapse rate in this layer (Figure 26). The surface temperature was cooler in the polluted case than in the clean case. The cooling of the surface and heating aloft in the polluted case were potentially contributed by the absorbing aerosol layer between 2 and 3 km (Figure 22a) and/or the passage of a cold front at least 5 hours ago (not shown). The lower level (below 700 hPa) wind shear at 12:00 LST was stronger in the polluted case than in the clean case (Figure 26). The enhanced low-level wind shear in the polluted case was in agreement with the tornado case study where the PBL-mechanism was suggested (Saide et al. 2015). However, the stronger low-level wind shear in the polluted case might also be due to the eastward propagation of the storms that occurred over the study area, not far from a stationary front in Mississippi. Hence, other factors that may lead to enhanced wind shear could not be excluded.

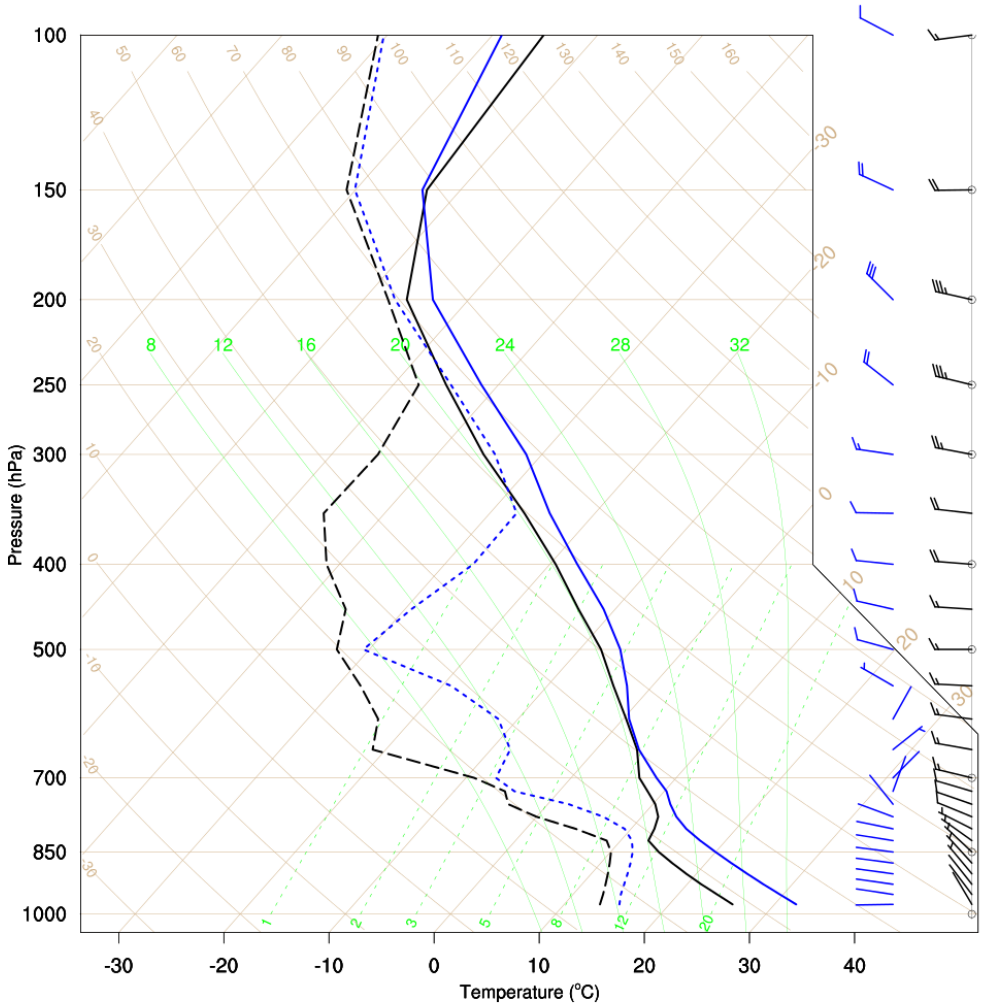

Figure 26. Skew-T log-P diagram at 12:00 LST for the two selected cases. The black solid and dashed curves are the vertical profiles of domain-averaged MERRA-2 temperature and dew point temperature of the polluted case (18 August 2012), respectively. The blue ones are of the clean case (4 August 2015). The black and blue wind barbs are the vertical profiles of domain-averaged MERRA-2 horizontal winds of the polluted and clean cases, respectively.

3.4. Discussion and Conclusions

The lightning FR during the diurnal-peak period (14:00–17:00 LST) over northern Alabama shows a weak correlation with AOD, and it correlates better with the optical depth of absorbing aerosols than that of non-absorbing aerosols. The increased correlation may result

from some meteorological environment that is conductive to enhanced storms and the presence of more absorbing aerosols. It may also be due to a stronger impact on storms by absorbing aerosols, leading to speculation that both the cloud-microphysical (CCN/IN-mechanism) and radiative effects (CAPE- and PBL-mechanisms) of aerosols may contribute to the regulation of storms.

AOD shows a correlation with lightning-producing storm area but no correlation with FR per unit storm area, suggesting that the aerosol invigoration of convection tends to be linked with increased storm area rather than the FR per storm. The correlation between AOD and LPDCA becomes stronger if aerosols are more absorbing and/or storm cases are restricted to the low $CAPE^{1/2}$ regime, suggestive of a stronger regulation of storms in area by absorbing aerosols through the PBL-mechanism. The interactions between absorbing aerosols and boundary layer turbulent mixing as described in the PBL-mechanism is supported by a more negative correlation between AOD and PBLH in the presence of absorbing aerosols. The CAPE-mechanism is also supported by a stronger positive correlation between AOD and CAPE in the presence of absorbing aerosols. The correlation analyses and the features present in the case study suggest that the impacts of aerosols on lightning may result from a synthesis of multiple mechanisms related to both microphysical and radiative effects of aerosols, although other environmental factors other than aerosols cannot be excluded.

In addition, the CAPE- and PBL- mechanisms discussed in the study are the local radiative effects of absorbing aerosols. However, numerous studies have shown that both anthropogenic and natural emissions of absorbing aerosols can interact with meso- and large-scale circulations with resultant redistributions of precipitation (e.g. Jin et al. 2015; Lau et al. 2008; Zhao, Liu, and Leung 2012). Whether the variation of FR over Northern Alabama is

affected by the large-scale impact of absorbing aerosols is not addressed here. Moreover, AOD is a more commonly-used metric for the radiative effects than for the microphysical effects of aerosols (Andreae 2009). Absorbing aerosols—such as dust and smoke particles—are often less hygroscopic (Kim et al. 2006), and hence variations in the optical depth of such absorbing aerosols and the CCN concentration may not be consistent. The correlations between aerosols and FR would be more supportive of the CCN/IN mechanism, if CCN concentration were the measured quantity rather than AOD. Furthermore, the aerosol loading was characterized in a spatially-averaged sense in this study, i.e. averaging the AOD retrievals over the study area. However, aerosol impacts on convection are dependent upon the zones of a storm (Lin et al. 2016). Lin et al. (2016) suggest different responses of shallow cumuli and stratus to increased CCN, if the radiative effect of aerosols is also considered. Whether and how the spatial variability of aerosol loadings may influence a storm remains an area for further research.

3.5. References

Albrecht, Bruce A. 1989. "Aerosols, cloud microphysics, and fractional cloudiness." *Science* no. 245 (4923):1227-1230. doi: 10.1126/science.245.4923.1227.

Albrecht, Rachel I, Steven J Goodman, Dennis E Buechler, Richard J Blakeslee, and Hugh J Christian. 2016. "Where are the lightning hotspots on Earth?" *Bulletin of the American Meteorological Society* no. 97 (11):2051-2068. doi: 10.1175/BAMS-D-14-00193.2.

Albrecht, Rachel I, Carlos A Morales, and Maria AF Silva Dias. 2011. "Electrification of precipitating systems over the Amazon: Physical processes of thunderstorm development." *Journal of Geophysical Research: Atmospheres* no. 116 (D8). doi: 10.1029/2010JD014756.

Altaratz, O, I Koren, LA Remer, and E Hirsch. 2014. "Cloud invigoration by aerosols—Coupling between microphysics and dynamics." *Atmospheric Research* no. 140:38-60. doi: 10.1016/j.atmosres.2014.01.009.

Altaratz, Orit, Ilan Koren, Yoav Yair, and Colin Price. 2010. "Lightning response to smoke from Amazonian fires." *Geophysical Research Letters* no. 37:L07801. doi: 10.1029/2010gl042679.

Andreae, M. O., D. Rosenfeld, P. Artaxo, A. A. Costa, G. P. Frank, K. M. Longo, and M. A. F. Silva-Dias. 2004. "Smoking rain clouds over the Amazon." *Science* no. 303 (5662):1337-1342. doi: 10.1126/science.1092779.

Andreae, Meinrat O. 2009. "Correlation between cloud condensation nuclei concentration and aerosol optical thickness in remote and polluted regions." *Atmospheric Chemistry and Physics* no. 9 (2):543-556. doi: 10.5194/acp-9-543-2009.

Bhartia, Pawan K. 2005. OMI/Aura Ozone (O3) Total Column 1-Orbit L2 Swath 13x24 km V003, Greenbelt, MD, USA, Goddard Earth Sciences Data and Information Services Center (GES DISC), Accessed [Data Access Date] 10.5067/Aura/OMI/DATA2024.

Blakeslee, Richard J, Douglas M Mach, Monte G Bateman, and Jeffrey C Bailey. 2014. "Seasonal variations in the lightning diurnal cycle and implications for the global electric circuit." *Atmospheric Research* no. 135:228-243. doi: 10.1016/j.atmosres.2012.09.023.

Bringi, VN, K Knupp, A Detwiler, L Liu, IJ Caylor, and RA Black. 1997. "Evolution of a Florida thunderstorm during the Convection and Precipitation/Electrification Experiment: The case of 9 August 1991." *Monthly Weather Review* no. 125 (9):2131-2160. doi: 10.1175/1520-0493(1997)125<2131:EOAFTD>2.0.CO;2.

Bruning, Eric C, W David Rust, Terry J Schuur, Donald R MacGorman, Paul R Krehbiel, and William Rison. 2007. "Electrical and polarimetric radar observations of a multicell storm in TELEX." *Monthly Weather Review* no. 135 (7):2525-2544. doi: 10.1175/MWR3421.1.

Byers, Horace Robert, and Roscoe R Braham. 1949. *The thunderstorm: report of the Thunderstorm Project*: US Government Printing Office.

CALIPSO Science Team. 2015. CALIPSO/CALIOP Level 2, Vertical Feature Mask Data, version 3.30, Hampton, VA, USA: NASA Atmospheric Science Data Center (ASDC), Accessed 3 May 2016 at doi: 10.5067/CALIOP/CALIPSO/CAL_LID_L2_VFM-ValStage1-V3-30_L2-003.30.

Carey, L., and S Stough. 2016. North Alabama Lightning Mapping Array (NALMA) Data. Version 1.0. UCAR/NCAR - Earth Observing Laboratory. https://doi.org/10.5065/D6Z899T8. Accessed 07 Sep 2017.

Carey, Lawrence D, and Steven A Rutledge. 2000. "The relationship between precipitation and lightning in tropical island convection: A C-band polarimetric radar study." *Monthly Weather Review* no. 128 (8):2687-2710. doi: 10.1175/1520-0493(2000)128<2687:TRBPAL>2.0.CO;2.

Carey, LD, and SA Rutledge. 1996. "A multiparameter radar case study of the microphysical and kinematic evolution of a lightning producing storm." *Meteorology and Atmospheric Physics* no. 59 (1-2):33-64. doi: 10.1007/BF01032000.

Chiapello, I, and C Moulin. 2002. "TOMS and METEOSAT satellite records of the variability of Saharan dust transport over the Atlantic during the last two decades (1979–1997)." *Geophysical Research Letters* no. 29 (8):1176. doi: 10.1029/2001GL013767.

Chmielewski, Vanna C, and Eric C Bruning. 2016. "Lightning Mapping Array flash detection performance with variable receiver thresholds." *Journal of Geophysical Research: Atmospheres* no. 121 (14):8600-8614. doi: 10.1002/2016JD025159.

Christian, H. J., R. J. Blakeslee, D. J. Boccippio, W. L. Boeck, D. E. Buechler, K. T. Driscoll, S. J. Goodman, J. M. Hall, W. J. Koshak, D. M. Mach, and M. F. Stewart. 2003. "Global frequency and distribution of lightning as observed from space by the Optical Transient Detector." *Journal of Geophysical Research-Atmospheres* no. 108 (D1). doi: 10.1029/2002jd002347.

Chronis, Themistoklis, and William J Koshak. 2016. "Diurnal variation of TRMM/LIS lightning flash radiances." *Bulletin of the American Meteorological Society* (2016). doi: 10.1175/BAMS-D-16-0041.1.

Conway, John W, and Dušan S Zrnić. 1993. "A study of embryo production and hail growth using dual-Doppler and multiparameter radars." *Monthly Weather Review* no. 121 (9):2511-2528. doi: 10.1175/1520-0493(1993)121<2511:ASOEPA>2.0.CO;2.

Coquillat, Sylvain, Marie-Pierre Boussaton, Magalie Buguet, Dominique Lambert, Jean-Francois Ribaud, and Andy Berthelot. 2013. "Lightning ground flash patterns over Paris area between 1992 and 2003: Influence of pollution?" *Atmospheric Research* no. 122:77-92. doi: 10.1016/j.atmosres.2012.10.032.

Cziczo, DJ, DM Murphy, PK Hudson, and DS Thomson. 2004. "Single particle measurements of the chemical composition of cirrus ice residue during CRYSTAL-FACE." *Journal of Geophysical Research: Atmospheres (1984–2012)* no. 109 (D4):D04201. doi: 10.1029/2003JD004032.

Deierling, Wiebke, and Walter A Petersen. 2008. "Total lightning activity as an indicator of updraft characteristics." *Journal of Geophysical Research: Atmospheres* no. 113 (D16). doi: 10.1029/2007JD009598.

Deierling, Wiebke, Walter A Petersen, John Latham, Scott Ellis, and Hugh J Christian. 2008. "The relationship between lightning activity and ice fluxes in thunderstorms." *Journal of Geophysical Research: Atmospheres* no. 113 (D15). doi: 10.1029/2007JD009700.

DeMott, Paul J, Kenneth Sassen, Michael R Poellot, Darrel Baumgardner, David C Rogers, Sarah D Brooks, Anthony J Prenni, and Sonia M Kreidenweis. 2003. "African dust aerosols as atmospheric ice nuclei." *Geophysical Research Letters* no. 30 (14):1732. doi: 10.1029/2003GL017410.

DeMott, PJ, DJ Cziczo, AJ Prenni, DM Murphy, SM Kreidenweis, DS Thomson, R Borys, and DC Rogers. 2003. "Measurements of the concentration and composition of nuclei for cirrus formation." *Proceedings of the National Academy of Sciences* no. 100 (25):14655-14660. doi: 10.1073/pnas.2532677100.

Ding, AJ, X Huang, W Nie, JN Sun, V-M Kerminen, T Petäjä, H Su, YF Cheng, X-Q Yang, and MH Wang. 2016. "Enhanced haze pollution by black carbon in megacities in China." *Geophysical Research Letters* no. 43 (6):2873-2879. doi: 10.1002/2016GL067745.

Dong, Zipeng, Zhanqing Li, Xing Yu, Maureen Cribb, Xingmin Li, and Jin Dai. 2017. "Opposite long-term trends in aerosols between low and high altitudes: a testimony to the aerosol–PBL feedback." *Atmospheric Chemistry and Physics* no. 17 (12):7997-8009. doi: 10.5194/acp-17-7997-2017.

Dye, JE, JJ Jones, WP Winn, TA Cerni, B Gardiner, D Lamb, RL Pitter, J Hallett, and CPR Saunders. 1986. "Early electrification and precipitation development in a small, isolated

Montana cumulonimbus." *Journal of Geophysical Research: Atmospheres* no. 91 (D1):1231-1247. doi: 10.1029/JD091iD01p01231.

Emanuel, Kerry A. 1994. *Atmospheric convection*. New York: Oxford University Press.

Fan, Jiwen, Tianle Yuan, Jennifer M Comstock, Steven Ghan, Alexander Khain, L Ruby Leung, Zhanqing Li, Vanderlei J Martins, and Mikhail Ovchinnikov. 2009. "Dominant role by vertical wind shear in regulating aerosol effects on deep convective clouds." *Journal of Geophysical Research: Atmospheres* no. 114 (D22):D22206. doi: 10.1029/2009JD012352.

Fan, Jiwen, Renyi Zhang, Wei-Kuo Tao, and Karen I Mohr. 2008. "Effects of aerosol optical properties on deep convective clouds and radiative forcing." *Journal of Geophysical Research: Atmospheres* no. 113 (D8). doi: 10.1029/2007JD009257.

Feingold, Graham, Wynn L. Eberhard, Dana E. Veron, and Michael Previdi. 2003. "First measurements of the Twomey indirect effect using ground-based remote sensors." *Geophysical Research Letters* no. 30 (6):1287. doi: 10.1029/2002gl016633.

Flannigan, MD, and BM Wotton. 1991. "Lightning-ignited forest fires in northwestern Ontario." *Canadian Journal of Forest Research* no. 21 (3):277-287. doi: 10.1139/x91-035.

Global Modeling and Assimilation Office (GMAO). 2015a. MERRA-2 inst3_3d_asm_Np: 3d, 3-Hourly,Instantaneous,Pressure-Level,Assimilation,Assimilated Meteorological Fields V5.12.4. Goddard Earth Sciences Data and Information Services Center (GES DISC), accessed 7 August 2017, doi:10.5067/QBZ6MG944HW0.

Global Modeling and Assimilation Office (GMAO). 2015b. MERRA-2 inst3_3d_asm_Nv: 3d, 3-Hourly, Instantaneous, Model-Level, Assimilation, Assimilated Meteorological Fields

V5.12.4. Goddard Earth Sciences Data and Information Services Center (GES DISC), accessed 16 February 2017, doi:10.5067/WWQSXQ8IVFW8.

Global Modeling and Assimilation Office (GMAO). 2015c. MERRA-2 tavg1_2d_flx_Nx: 2d,1-Hourly,Time-Averaged,Single-Level,Assimilation,Surface Flux Diagnostics V5.12.4. Goddard Earth Sciences Data and Information Services Center (GES DISC), accessed 29 November 2016, doi:10.5067/7MCPBJ41Y0K6.

Global Modeling and Assimilation Office (GMAO). 2015d. MERRA-2 tavg1_2d_slv_Nx: 2d,1-Hourly,Time-Averaged,Single-Level,Assimilation,Single-Level Diagnostics V5.12.4. Goddard Earth Sciences Data and Information Services Center (GES DISC), accessed 29 November 2016, doi:10.5067/VJAFPLI1CSIV.

Ghan, Steven J, Catherine C Chung, and Joyce E Penner. 1993. "A parameterization of cloud droplet nucleation part I: single aerosol type." *Atmospheric Research* no. 30 (4):198-221. doi: 10.1016/0169-8095(93)90024-I.

Goodman, SJ, R Blakeslee, H Christian, W Koshak, J Bailey, J Hall, E McCaul, D Buechler, C Darden, and J Burks. 2005. "The North Alabama lightning mapping array: Recent severe storm observations and future prospects." *Atmospheric Research* no. 76 (1):423-437. doi: 10.1016/j.atmosres.2004.11.035.

Goodman, Steven J, Dennis E Buechler, Patrick D Wright, and W David Rust. 1988. "Lightning and precipitation history of a microburst-producing storm." *Geophysical research letters* no. 15 (11):1185-1188. doi: 10.1029/GL015i011p01185.

Herman, JR, N Krotkov, E Celarier, D Larko, and G Labow. 1999. "Distribution of UV radiation at the Earth's surface from TOMS-measured UV-backscattered radiances." *Journal of Geophysical Research* no. 104 (D10):12059-12076. doi: 10.1029/1999JD900062.

Herzegh, Paul H, and Arthur R Jameson. 1992. "Observing precipitation through dual-polarization radar measurements." *Bulletin of the American Meteorological Society* no. 73 (9):1365-1374. doi: 10.1175/1520-0477(1992)073<1365:OPTDPR>2.0.CO;2.

Hoose, C, and O Möhler. 2012. "Heterogeneous ice nucleation on atmospheric aerosols: a review of results from laboratory experiments." *Atmospheric Chemistry and Physics* no. 12 (20):9817. doi: 10.5194/acp-12-9817-2012.

Hsu, N Christina, Jay R Herman, JF Gleason, O Torres, and CJ Seftor. 1999. "Satellite detection of smoke aerosols over a snow/ice surface by TOMS." *Geophysical Research Letters* no. 26 (8):1165-1168. doi: 10.1029/1999GL900155.

Hsu, N Christina, Jay R Herman, and Si-Chee Tsay. 2003. "Radiative impacts from biomass burning in the presence of clouds during boreal spring in southeast Asia." *Geophysical Research Letters* no. 30 (5). doi: 10.1029/2002GL016485.

Huang, J., Q. Fu, J. Su, Q. Tang, P. Minnis, Y. Hu, Y. Yi, and Q. Zhao. 2009. "Taklimakan dust aerosol radiative heating derived from CALIPSO observations using the Fu-Liou radiation model with CERES constraints." *Atmospheric Chemistry and Physics* no. 9:4011-4021. doi: 10.5194/acp-9-4011-2009.

Hubbert, J, VN Bringi, LD Carey, and S Bolen. 1998. "CSU-CHILL polarimetric radar measurements from a severe hail storm in eastern Colorado." *Journal of Applied Meteorology* no. 37 (8):749-775. doi: 10.1175/1520-0450(1998)037<0749:CCPRMF>2.0.CO;2. Jaeglé, Lyatt. 2007. "Pumping up surface air." *Science* no. 315 (5813):772-773. doi: 10.1126/science.1138988.

Jenkins, Gregory S, Aaron S Pratt, and Andrew Heymsfield. 2008. "Possible linkages between Saharan dust and tropical cyclone rain band invigoration in the eastern Atlantic during NAMMA-06." *Geophysical Research Letters* no. 35 (8). doi: 10.1029/2008GL034072.

Jin, Q., J. Wei, Z.-L. Yang, B. Pu, and J. Huang. 2015. "Consistent response of Indian summer monsoon to Middle East dust in observations and simulations." *Atmospheric Chemistry and Physics* no. 1680:7324. doi: 10.5194/acp-15-9897-2015.

Khain, A, D Rosenfeld, and A Pokrovsky. 2005. "Aerosol impact on the dynamics and microphysics of deep convective clouds." *Quarterly Journal of the Royal Meteorological Society* no. 131 (611):2639-2663. doi: doi: 10.1256/qj.04.62.

Kim, Jhoon, Jaehwa Lee, Hee Choon Lee, Akiko Higurashi, Toshihiko Takemura, and Chul Han Song. 2007. "Consistency of the aerosol type classification from satellite remote sensing during the Atmospheric Brown Cloud–East Asia Regional Experiment campaign." *Journal of Geophysical Research: Atmospheres* no. 112 (D22). doi: 10.1029/2006JD008201.

Kim, Jiyoung, Soon-Chang Yoon, Anne Jefferson, and Sang-Woo Kim. 2006. "Aerosol hygroscopic properties during Asian dust, pollution, and biomass burning episodes at Gosan, Korea in April 2001." *Atmospheric Environment* no. 40 (8):1550-1560. doi: 10.1016/j.atmosenv.2005.10.044.

Knupp, Kevin R, and William R Cotton. 1982. "An intense, quasi-steady thunderstorm over mountainous terrain. Part II: Doppler radar observations of the storm morphological structure." *Journal of the Atmospheric Sciences* no. 39 (2):343-358.

Koch, D, and AD Del Genio. 2010. "Black carbon semi-direct effects on cloud cover: review and synthesis." *Atmospheric Chemistry and Physics* no. 10 (16):7685-7696. doi: 10.5194/acp-10-7685-2010.

Konrad, Charles E. 1997. "Synoptic-scale features associated with warm season heavy rainfall over the interior southeastern United States." *Weather and Forecasting* no. 12 (3):557-571. doi: 10.1175/1520-0434(1997)012<0557:SSFAWW>2.0.CO;2.

Koren, Ilan, Graham Feingold, and Lorraine A Remer. 2010. "The invigoration of deep convective clouds over the Atlantic: aerosol effect, meteorology or retrieval artifact?" *Atmospheric Chemistry and Physics* no. 10 (18):8855-8872. doi: 10.5194/acp-10-8855-2010.

Koren, Ilan, Yoram J Kaufman, Daniel Rosenfeld, Lorraine A Remer, and Yinon Rudich. 2005. "Aerosol invigoration and restructuring of Atlantic convective clouds." *Geophysical Research Letters* no. 32 (14). doi: 10.1029/2005GL023187.

Koshak, WJ, RJ Solakiewicz, RJ Blakeslee, SJ Goodman, HJ Christian, JM Hall, JC Bailey, EP Krider, MG Bateman, and DJ Boccippio. 2004. "North Alabama Lightning Mapping Array (LMA): VHF source retrieval algorithm and error analyses." *Journal of Atmospheric and Oceanic Technology* no. 21 (4):543-558. doi: 10.1175/1520-0426(2004)021<0543:NALMAL>2.0.CO;2.

Larsen, HR, and EJ Stansbury. 1974. "Association of lightning flashes with precipitation cores extending to height 7 km." *Journal of Atmospheric and Terrestrial Physics* no. 36 (9):1547IN231549-15481553. doi: 0021-9169(74)90232-3.

Lau, KM, SC Tsay, C Hsu, M Chin, V Ramanathan, GX Wu, Z Li, R Sikka, B Holben, and D Lu. 2008. "The Joint Aerosol–Monsoon Experiment: A new challenge for monsoon

climate research." *Bulletin of the American Meteorological Society* no. 89 (3):369-383. doi: 10.1175/BAMS-89-3-369.

Lee, Seoung-Soo, and Graham Feingold. 2010. "Precipitating cloud-system response to aerosol perturbations." *Geophysical Research Letters* no. 37 (23). doi: 10.1029/2010GL045596.

Levelt, Pieternel F, Gijsbertus HJ van den Oord, Marcel R Dobber, Anssi Malkki, Huib Visser, Johan de Vries, Piet Stammes, Jens OV Lundell, and Heikki Saari. 2006. "The ozone monitoring instrument." *IEEE Transactions on geoscience and remote sensing* no. 44 (5):1093-1101. doi: 10.1109/TGRS.2006.872333.

Levi, Yoav, and Daniel Rosenfeld. 1996. "Ice nuclei, rainwater chemical composition, and static cloud seeding effects in Israel." *Journal of Applied Meteorology* no. 35 (9):1494-1501. doi: 10.1175/1520-0450(1996)035<1494:INRCCA>2.0.CO;2.

Levy, R., and C. Hsu. 2015. MODIS Atmosphere L2 Aerosol Product. NASA MODIS Adaptive Processing System, Goddard Space Flight Center, USA: http://dx.doi.org/10.5067/MODIS/MYD04_L2.006.

Levy, Robert C, Lorraine A Remer, and Oleg Dubovik. 2007. "Global aerosol optical properties and application to Moderate Resolution Imaging Spectroradiometer aerosol retrieval over land." *Journal of Geophysical Research: Atmospheres* no. 112 (D13). doi: 10.1029/2006JD007815.

Levy, Robert C, Lorraine A Remer, Shana Mattoo, Eric F Vermote, and Yoram J Kaufman. 2007. "Second-generation operational algorithm: Retrieval of aerosol properties over land from inversion of Moderate Resolution Imaging Spectroradiometer spectral reflectance." *Journal of Geophysical Research: Atmospheres* no. 112 (D13). doi: 10.1029/2006JD007811.

Levy, Robert C., S. Mattoo, L. A. Munchak, L. A. Remer, A. M. Sayer, F. Patadia, and N. C. Hsu. 2013. "The Collection 6 MODIS aerosol products over land and ocean." *Atmospheric Measurement Techniques* no. 6 (11):2989-3034. doi: 10.5194/amt-6-2989-2013.

Li, Zhanqing, Jianping Guo, Aijun Ding, Hong Liao, Jianjun Liu, Yele Sun, Tijian Wang, Huiwen Xue, Hongsheng Zhang, and Bin Zhu. 2017. "Aerosol and boundary-layer interactions and impact on air quality." *National Science Review*. doi: 10.1093/nsr/nwx117.

Li, Zhanqing, Kwon-Ho Lee, Yuesi Wang, Jinyuan Xin, and Wei-Min Hao. 2010. "First observation-based estimates of cloud-free aerosol radiative forcing across China." *Journal of Geophysical Research: Atmospheres* no. 115 (D7). doi: 10.1029/2009JD013306.

Li, Zhe, Huiwen Xue, and Fan Yang. 2013. "A modeling study of ice formation affected by aerosols." *Journal of Geophysical Research: Atmospheres* no. 118 (19):11213-11227. doi: 10.1002/jgrd.50861.

Lin, Yun, Yuan Wang, Bowen Pan, Jiaxi Hu, Yangang Liu, and Renyi Zhang. 2016. "Distinct impacts of aerosols on an evolving continental cloud complex during the RACORO field campaign." *Journal of the Atmospheric Sciences* no. 73 (9). doi: 10.1175/JAS-D-15-0361.1.

MacGorman, Donald. R , and W. David Rust. 1998. *The electrical nature of storms*. New York: Oxford University Press.

Malkus, Joanne Starr. 1949. "Effects of wind shear on some aspects of convection." *Eos, Transactions American Geophysical Union* no. 30 (1):19-25. doi: 10.1029/TR030i001p00019.

Marshall, JS, and S Radhakant. 1978. "Radar precipitation maps as lightning indicators." *Journal of Applied Meteorology* no. 17 (2):206-212. doi: 10.1175/1520-0450(1978)017<0206:RPMALI>2.0.CO;2.

McCluskey, Christina S, Paul J DeMott, Anthony J Prenni, Ezra JT Levin, Gavin R McMeeking, Amy P Sullivan, Thomas CJ Hill, Shunsuke Nakao, Christian M Carrico, and Sonia M Kreidenweis. 2014. "Characteristics of atmospheric ice nucleating particles associated with biomass burning in the US: Prescribed burns and wildfires." *Journal of Geophysical Research: Atmospheres* no. 119 (17):10458-10470. doi: 10.1002/2014JD021980.

Murray, BJ, D O'sullivan, JD Atkinson, and ME Webb. 2012. "Ice nucleation by particles immersed in supercooled cloud droplets." *Chemical Society Reviews* no. 41 (19):6519-6554. doi: 10.1039/c2cs35200a.

Niu, Feng, and Zhanqing Li. 2012. "Systematic variations of cloud top temperature and precipitation rate with aerosols over the global tropics." *Atmospheric Chemistry and Physics* no. 12 (18):8491-8498. doi: 10.5194/acp-12-8491-2012.

Omar, Ali H, David M Winker, Mark A Vaughan, Yongxiang Hu, Charles R Trepte, Richard A Ferrare, Kam-Pui Lee, Chris A Hostetler, Chieko Kittaka, and Raymond R Rogers. 2009. "The CALIPSO automated aerosol classification and lidar ratio selection algorithm." *Journal of Atmospheric and Oceanic Technology* no. 26 (10):1994-2014. doi: 10.1175/2009JTECHA1231.1.

Phillips, JG, MA Cane, and C Rosenzweig. 1998. "ENSO, seasonal rainfall patterns and simulated maize yield variability in Zimbabwe." *Agricultural and Forest Meteorology* no. 90 (1):39-50. doi: 10.1016/S0168-1923(97)00095-6.

Proestakis, E, S Kazadzis, K Lagouvardos, V Kotroni, V Amiridis, E Marinou, C Price, and A Kazantzidis. 2016. "Aerosols and lightning activity: The effect of vertical profile and aerosol type." *Atmospheric Research* no. 182:243-255. doi: 10.1016/j.atmosres.2016.07.031.

Proestakis, E, S Kazadzis, K Lagouvardos, V Kotroni, and A Kazantzidis. 2016. "Lightning activity and aerosols in the Mediterranean region." *Atmospheric Research* no. 170:66-75. doi: 10.1016/j.atmosres.2015.11.010.

Randles, C. A., A. M. da Silva, V. Buchard, A. Darmenov, P. R. Colarco, V. Aquila, H. Bian, E. P. Nowottnick, X. Pan, A. Smirnov, H. Yu, and R. Govindaraju. 2016. "The MERRA-2 Aerosol Assimilation. Technical Report Series on Global Modeling and Data Assimilation." *NASA/TM–2016-104606* no. 45:139.

Reutter, Philipp, H Su, J Trentmann, Martin Simmel, Diana Rose, SS Gunthe, H Wernli, MO Andreae, and U Pöschl. 2009. "Aerosol-and updraft-limited regimes of cloud droplet formation: influence of particle number, size and hygroscopicity on the activation of cloud condensation nuclei (CCN)." *Atmospheric Chemistry and Physics* no. 9 (18):7067-7080. doi: 10.5194/acp-9-7067-2009.

Richardson, Mathews S, Paul J DeMott, Sonia M Kreidenweis, Daniel J Cziczo, Edward J Dunlea, Jose L Jimenez, David S Thomson, Lowell L Ashbaugh, Randolph D Borys, and Douglas L Westphal. 2007. "Measurements of heterogeneous ice nuclei in the western United States in springtime and their relation to aerosol characteristics." *Journal of*

Geophysical Research: Atmospheres (1984–2012) no. 112 (D2):D02209. doi: 10.1029/2006JD007500.

Rison, W, RJ Thomas, PR Krehbiel, T Hamlin, and J Harlin. 1999. "A GPS-based three-dimensional lightning mapping system: Initial observations in central New Mexico." *Geophysical Research Letters* no. 26 (23):3573-3576. doi: 10.1029/1999GL010856.

Roberts, P, and J Hallett. 1968. "A laboratory study of the ice nucleating properties of some mineral particulates." *Quarterly Journal of the Royal Meteorological Society* no. 94 (399):25-34. doi: 10.1002/qj.49709540317.

Rodriguez, Carlos A Morales, Rosmeri P da Rocha, and Rodrigo Bombardi. 2010. "On the development of summer thunderstorms in the city of São Paulo: Mean meteorological characteristics and pollution effect." *Atmospheric Research* no. 96 (2):477-488. doi: 10.1016/j.atmosres.2010.02.007.

Ropelewski, Chester F, and Michael S Halpert. 1996. "Quantifying southern oscillation-precipitation relationships." *Journal of Climate* no. 9 (5):1043-1059. doi: 10.1175/1520-0442(1996)009<1043:QSOPR>2.0.CO;2.

Rorig, Miriam L, and Sue A Ferguson. 1999. "Characteristics of lightning and wildland fire ignition in the Pacific Northwest." *Journal of Applied Meteorology* no. 38 (11):1565-1575. doi: 10.1175/1520-0450(1999)038<1565:COLAWF>2.0.CO;2.

Rosenfeld, D., U. Lohmann, G. B. Raga, C. D. O'Dowd, M. Kulmala, S. Fuzzi, A. Reissell, and M. O. Andreae. 2008. "Flood or drought: how do aerosols affect precipitation?" *Science* no. 321 (5894):1309-1313. doi: 10.1126/science.1160606.

Rosenfeld, Daniel, Baruch Fischman, Youtong Zheng, Tom Goren, and David Giguzin. 2014. "Combined satellite and radar retrievals of drop concentration and CCN at convective

cloud base." *Geophysical Research Letters* no. 41 (9):3259-3265. doi: 10.1002/2014GL059453.

Rosenfeld, Daniel, Youtong Zheng, Eyal Hashimshoni, Mira L Pöhlker, Anne Jefferson, Christopher Pöhlker, Xing Yu, Yannian Zhu, Guihua Liu, and Zhiguo Yue. 2016. "Satellite retrieval of cloud condensation nuclei concentrations by using clouds as CCN chambers." *Proceedings of the National Academy of Sciences*:201514044. doi: 10.1073/pnas.1514044113.

Rotunno, Richard, Joseph B Klemp, and Morris L Weisman. 1988. "A theory for strong, long-lived squall lines." *Journal of the Atmospheric Sciences* no. 45 (3):463-485. doi: 10.1175/1520-0469(1988)045<0463:ATFSLL>2.0.CO;2.

Saide, PE, SN Spak, RB Pierce, JA Otkin, TK Schaack, AK Heidinger, AM Silva, M Kacenelenbogen, J Redemann, and GR Carmichael. 2015. "Central American biomass burning smoke can increase tornado severity in the US." *Geophysical Research Letters* no. 42 (3):956-965. doi: 10.1002/2014GL062826.

Sassen, Kenneth, Paul J DeMott, Joseph M Prospero, and Michael R Poellot. 2003. "Saharan dust storms and indirect aerosol effects on clouds: CRYSTAL-FACE results." *Geophysical Research Letters* no. 30 (12):1633. doi: 10.1029/2003GL017371.

Saunders, CPR, H Bax-Norman, C Emersic, EE Avila, and NE Castellano. 2006. "Laboratory studies of the effect of cloud conditions on graupel/crystal charge transfer in thunderstorm electrification." *Quarterly Journal of the Royal Meteorological Society* no. 132 (621):2653-2673. doi: 10.1256/qj.05.218.

Schaefer, Vincent J. 1949. "The formation of ice crystals in the laboratory and the atmosphere." *Chemical Reviews* no. 44 (2):291-320. doi: 10.1021/cr60138a004.

Schultz, Christopher J, Lawrence D Carey, Elise V Schultz, and Richard J Blakeslee. 2017. "Kinematic and microphysical significance of lightning jumps versus nonjump increases in total flash rate." *Weather and Forecasting* no. 32 (1):275-288. doi: 10.1175/WAF-D-15-0175.1.

Schultz, Christopher J, Walter A Petersen, and Lawrence D Carey. 2011. "Lightning and severe weather: A comparison between total and cloud-to-ground lightning trends." *Weather and Forecasting* no. 26 (5):744-755. doi: 10.1175/WAF-D-10-05026.1.

Seinfeld, John H, Christopher Bretherton, Kenneth S Carslaw, Hugh Coe, Paul J DeMott, Edward J Dunlea, Graham Feingold, Steven Ghan, Alex B Guenther, and Ralph Kahn. 2016. "Improving our fundamental understanding of the role of aerosol−cloud interactions in the climate system." *Proceedings of the National Academy of Sciences* no. 113 (21):5781-5790. doi: 10.1073/pnas.1514043113.

Siu, Leong Wai, Kenneth P Bowman, and Craig C Epifanio. 2015. "Convective transport of trace species observed during the Stratosphere-Troposphere Analyses of Regional Transport 2008 experiment." *Journal of Geophysical Research: Atmospheres* no. 120 (19). doi: 10.1002/2015JD023645.

Stolz, Douglas C, Steven A Rutledge, and Jeffrey R Pierce. 2015. "Simultaneous influences of thermodynamics and aerosols on deep convection and lightning in the tropics." *Journal of Geophysical Research: Atmospheres* no. 120 (12):6207-6231. doi: 10.1002/2014JD023033.

Stolz, Douglas C, Steven A Rutledge, Jeffrey R Pierce, and Susan C Heever. 2017. "A global lightning parameterization based on statistical relationships among environmental factors,

aerosols, and convective clouds in the TRMM climatology." *Journal of Geophysical Research: Atmospheres* no. 122:7461–7492. doi: 10.1002/2016JD026220.

Storer, Rachel L, Susan C Van Den Heever, and Graeme L Stephens. 2010. "Modeling aerosol impacts on convective storms in different environments." *Journal of the Atmospheric Sciences* no. 67 (12):3904-3915. doi: 10.1175/2010JAS3363.1.

Storer, RL, SC Heever, and TS L'Ecuyer. 2014. "Observations of aerosol-induced convective invigoration in the tropical east Atlantic." *Journal of Geophysical Research: Atmospheres* no. 119 (7):3963-3975. doi: 10.1002/2013JD020272.

Takahashi, Tsutomu. 1978. "Riming electrification as a charge generation mechanism in thunderstorms." *Journal of the Atmospheric Sciences* no. 35 (8):1536-1548. doi: 10.1175/1520-0469(1978)035<1536:REAACG>2.0.CO;2.

Thomas, Ronald J, Paul R Krehbiel, William Rison, Steven J Hunyady, William P Winn, Timothy Hamlin, and Jeremiah Harlin. 2004. "Accuracy of the lightning mapping array." *Journal of Geophysical Research: Atmospheres* no. 109 (D14):D14207. doi: 10.1029/2004JD004549.

Thornton, Joel A, Katrina S Virts, Robert H Holzworth, and Todd P Mitchell. 2017. "Lightning enhancement over major oceanic shipping lanes." *Geophysical Research Letters* no. 44:9102-9111. doi: 10.1002/2017GL074982.

Torres, Omar, Aapo Tanskanen, Ben Veihelmann, Changwoo Ahn, Remco Braak, Pawan K Bhartia, Pepijn Veefkind, and Pieternel Levelt. 2007. "Aerosols and surface UV products from Ozone Monitoring Instrument observations: An overview." *Journal of Geophysical Research: Atmospheres* no. 112 (D24). doi: 10.1029/2007JD008809.

Tuttle, John D, VN Bringi, HD Orville, and FJ Kopp. 1989. "Multiparameter radar study of a microburst: Comparison with model results." *Journal of the Atmospheric Sciences* no. 46 (5):601-620. doi: 10.1175/1520-0469(1989)046<0601:MRSOAM>2.0.CO;2.

Twomey, S. 1959. "The nuclei of natural cloud formation part II: The supersaturation in natural clouds and the variation of cloud droplet concentration." *Pure and Applied Geophysics* no. 43 (1):243-249. doi: 10.1007/BF01993560.

van den Heever, Susan C, Gustavo G Carrió, William R Cotton, Paul J DeMott, and Anthony J Prenni. 2006. "Impacts of nucleating aerosol on Florida storms. Part I: Mesoscale simulations." *Journal of the Atmospheric Sciences* no. 63 (7):1752-1775. doi: 10.1175/JAS3713.1.

Van Donkelaar, Aaron, Randall V Martin, Robert C Levy, Arlindo M da Silva, Michal Krzyzanowski, Natalia E Chubarova, Eugenia Semutnikova, and Aaron J Cohen. 2011. "Satellite-based estimates of ground-level fine particulate matter during extreme events: A case study of the Moscow fires in 2010." *Atmospheric Environment* no. 45 (34):6225-6232. doi: 10.1016/j.atmosenv.2011.07.068.

Van Donkelaar, Aaron, Randall V Martin, and Rokjin J Park. 2006. "Estimating ground-level PM2.5 using aerosol optical depth determined from satellite remote sensing." *Journal of Geophysical Research: Atmospheres* no. 111 (D21). doi: 10.1029/2005JD006996.

Vaughan, Mark A, Kathleen A Powell, David M Winker, Chris A Hostetler, Ralph E Kuehn, William H Hunt, Brian J Getzewich, Stuart A Young, Zhaoyan Liu, and Matthew J McGill. 2009. "Fully automated detection of cloud and aerosol layers in the CALIPSO lidar measurements." *Journal of Atmospheric and Oceanic Technology* no. 26 (10):2034-2050. doi: 10.1175/2009JTECHA1228.1.

Wang, Yuan, Alexei Khalizov, Misti Levy, and Renyi Zhang. 2013. "New Directions: Light absorbing aerosols and their atmospheric impacts." *Atmospheric Environment* no. 81:713-715. doi: 10.1016/j.atmosenv.2013.09.034.

Weisman, Morris L, and Richard Rotunno. 2004. "“A theory for strong long-lived squall lines” revisited." *Journal of the Atmospheric Sciences* no. 61 (4):361-382. doi: 10.1175/1520-0469(2004)061<0361:ATFSLS>2.0.CO;2.

Wilcox, EM. 2010. "Stratocumulus cloud thickening beneath layers of absorbing smoke aerosol." *Atmospheric Chemistry and Physics* no. 10 (23):11769-11777. doi: 10.5194/acp-10-11769-2010.

Wilcox, Eric M, Rick M Thomas, Puppala S Praveen, Kristina Pistone, Frida A-M Bender, and Veerabhadran Ramanathan. 2016. "Black carbon solar absorption suppresses turbulence in the atmospheric boundary layer." *Proceedings of the National Academy of Sciences*:201525746. doi: 10.1073/pnas.1525746113.

Williams, E., D. Rosenfeld, N. Madden, J. Gerlach, N. Gears, L. Atkinson, N. Dunnemann, G. Frostrom, M. Antonio, B. Biazon, R. Camargo, H. Franca, A. Gomes, M. Lima, R. Machado, S. Manhaes, L. Nachtigall, H. Piva, W. Quintiliano, L. Machado, P. Artaxo, G. Roberts, N. Renno, R. Blakeslee, J. Bailey, D. Boccippio, A. Betts, D. Wolff, B. Roy, J. Halverson, T. Rickenbach, J. Fuentes, and E. Avelino. 2002. "Contrasting convective regimes over the Amazon: Implications for cloud electrification." *Journal of Geophysical Research: Atmospheres* no. 107 (D20):8082. doi: 10.1029/2001jd000380.

Williams, ER, and SJ Heckman. 1993. "The local diurnal variation of cloud electrification and the global diurnal variation of negative charge on the Earth." *Journal of Geophysical Research: Atmospheres* no. 98 (D3):5221-5234. doi: 10.1029/92JD02642.

Williams, ER, ME Weber, and RE Orville. 1989. "The relationship between lightning type and convective state of thunderclouds." *Journal of Geophysics Research* no. 94:13213-13220. doi: 10.1029/JD094iD11p13213.

Wilson, Theodore W, Luis A Ladino, Peter A Alpert, Mark N Breckels, Ian M Brooks, Jo Browse, Susannah M Burrows, Kenneth S Carslaw, J Alex Huffman, and Christopher Judd. 2015. "A marine biogenic source of atmospheric ice-nucleating particles." *Nature* no. 525 (7568):234-238. doi: 10.1038/nature14986.

Wu, Xiaoqing, and Michio Yanai. 1994. "Effects of vertical wind shear on the cumulus transport of momentum: Observations and parameterization." *Journal of the Atmospheric Sciences* no. 51 (12):1640-1660. doi: 10.1175/1520-0469(1994)051<1640:EOVWSO>2.0.CO;2.

Yu, Hongbin, SC Liu, and RE Dickinson. 2002. "Radiative effects of aerosols on the evolution of the atmospheric boundary layer." *Journal of Geophysical Research: Atmospheres* no. 107 (D12). doi: 10.1029/2001JD000754.

Yu, Hongbin, Yan Zhang, Mian Chin, Zhaoyan Liu, Ali Omar, Lorraine A Remer, Yuekui Yang, Tianle Yuan, and Jianglong Zhang. 2012. "An integrated analysis of aerosol above clouds from A-Train multi-sensor measurements." *Remote Sensing of Environment* no. 121:125-131. doi: 10.1016/j.rse.2012.01.011.

Yuan, T. L., L. A. Remer, H. S. Bian, J. R. Ziemke, R. Albrecht, K. E. Pickering, L. Oreopoulos, S. J. Goodman, H. B. Yu, and D. J. Allen. 2012. "Aerosol indirect effect on tropospheric ozone via lightning." *Journal of Geophysical Research-Atmospheres* no. 117:D18213. doi: 10.1029/2012jd017723.

Yuan, Tianle, Lorraine A Remer, Kenneth E Pickering, and Hongbin Yu. 2011. "Observational evidence of aerosol enhancement of lightning activity and convective invigoration." *Geophysical Research Letters* no. 38 (4):L04701. doi: 10.1029/2010GL046052.

Zhang, Y, Z Gao, D Li, Y Li, N Zhang, X Zhao, and J Chen. 2014. "On the computation of planetary boundary-layer height using the bulk Richardson number method." *Geoscientific Model Development* no. 7 (6):2599-2611. doi: 10.5194/gmd-7-2599-2014.

Zhao, Bin, Kuo-Nan Liou, Yu Gu, Jonathan H Jiang, Qinbin Li, Rong Fu, Lei Huang, Xiaohong Liu, Xiangjun Shi, and Hui Su. 2018. "Impact of aerosols on ice crystal size." *Atmospheric Chemistry and Physics* no. 18 (2):1065-1078. doi: 10.5194/acp-18-1065-2018.

Zhao, C., X. Liu, and L. R. Leung. 2012. "Impact of the Desert dust on the summer monsoon system over Southwestern North America." *Atmospheric Chemistry and Physics* no. 12 (8):3717-3731. doi: 10.5194/acp-12-3717-2012.

Zheng, Youtong, Daniel Rosenfeld, and Zhanqing Li. 2015. "Satellite inference of thermals and cloud-base updraft speeds based on retrieved surface and cloud-base temperatures." *Journal of the Atmospheric Sciences* no. 72 (6):2411-2428. doi: 10.1175/JAS-D-14-0283.1.

Zipser, Edward J. 1994. "Deep cumulonimbus cloud systems in the tropics with and without lightning." *Monthly Weather Review* no. 122 (8):1837-1851. doi: 10.1175/1520-0493(1994)122<1837:DCCSIT>2.0.CO;2.

Zipser, Edward J, and Kurt R Lutz. 1994. "The vertical profile of radar reflectivity of convective cells: A strong indicator of storm intensity and lightning probability?" *Monthly Weather*

Review no. 122 (8):1751-1759. doi: 10.1175/1520-0493(1994)122<1751:TVPORR>2.0.CO;2.

4. THE RESPONSE OF DEEP CONVECTION TO DAYTIME AEROSOL HEATING AT DIFFERENT HEIGHTS WITH AEROSOL CONCENTRATION PERTURBATIONS: A SENSITIVITY STUDY OVER NORTHERN ALABAMA

4.1. Introduction

Aerosols may invigorate or suppress convection through their microphysical and/or radiative effects (Altaratz et al. 2014; Fan et al. 2016; Lee, Tao, and Jung 2014; Rosenfeld et al. 2014; Tao et al. 2012). As thoroughly surveyed by previous studies (Altaratz et al. 2014; Fan et al. 2016; Lee, Tao, and Jung 2014; Rosenfeld et al. 2014; Tao et al. 2012), water-nucleating aerosols can enhance individual convective cells and perturb the spatiotemporal distribution of the moist static energy (MSE) of a storm system. Increased water-nucleating aerosols lead to increased cloud condensation nuclei (CCN), increased but smaller cloud water droplets, and slower droplet collection growth during the warm rain phase of a convective cloud (e.g. Albrecht 1989; Feingold 2003 et al.). Then, as the convective cloud grows deeper, more liquid water may be lifted above the freezing level, invigorating the convection through additional latent heat release (e.g. Andreae et al. 2004; Khain, Rosenfeld, and Pokrovsky 2005; Rosenfeld et al. 2008; van den Heever et al. 2006). In addition to the enhancement of single convective cells, previous modeling studies have also suggested the aerosol enhancement of an ensemble of clouds through enhanced low-level convergence and secondary convection (Khain, Rosenfeld, and Pokrovsky 2005; Lee et al. 2008; Lynn et al. 2005; Seifert and Beheng 2006; Tao et al. 2007). The enhanced low-level convergence in high CCN simulations appears to result from stronger evaporative cooling and downdrafts (Lee et al. 2008; Tao et al. 2007).

Whether aerosols invigorate or suppress convection is dependent upon environmental conditions (Fan et al. 2009; Fan et al. 2012; Khain, BenMoshe, and Pokrovsky 2008). Previous modeling studies have suggested that increased CCN tend to suppress convection in the presence of strong vertical wind shear and/or a dry environment, particularly for the cold cloud base convection (Fan et al. 2009; Fan et al. 2012; Khain, BenMoshe, and Pokrovsky 2008). In addition, the enhancement or suppression of convection by aerosols is often observed or simulated over a relatively small area and a relatively short period. However, the radiative-convective quasi equilibrium state of the system does not appear to be sensitive to CCN perturbations, if the aerosol impacts on convection are viewed over a relatively large area and a relatively long period (Grabowski & Morrison 2011; Stevens and Feingold 2009; van den Heever, Stephens, and Wood 2011). Stevens and Feingold (2009) call the cancellation or compensation of the changes in different parts and/or stages of a system a buffered effect, when the system is looked at as a whole. A recent study (Fan et al. 2018) suggested that the ultrafine aerosol particles (smaller than 50 nm) ingested into convective clouds may contribute to increased condensate and possibly enhance convection through additional latent heat release.

Absorbing aerosols—such as black carbon and dust—can absorb solar radiation and heat the layer of atmosphere with the absorbing aerosols (e.g. Huang et al. 2009; Li et al. 2010; Ramanathan et al. 2001). The perturbation of the atmospheric temperature structure by absorbing aerosols may enhance or suppress deep convection, depending on the height of the absorbing aerosol layer (Koch and Del Genio 2010; Li et al. 2017; Wang 2013). Yu, Liu, and Dickinson (2002) show that aerosol absorption near the surface increases the air temperature and weakens the capping inversion. On the contrary, aerosol absorption above the planetary boundary layer (PBL) enhances the capping inversion and reduces the height of PBL (Yu, Liu, and Dickinson

2002). Zhang et al. (2008) used the Abdus Salam Institute for Theoretical Physics Regional Climate Model, version 3 (RegCM3; Pal et al. 2007; Qian and Giorgi 1999) to further investigate the impact of the smoke shortwave radiative forcing on the diurnal features of PBL and clouds during the dry to wet transition season of the Amazon rain forest. They showed that strong aerosol absorption stabilized the 2-3 km layer right above the PBL and hence suppressed convection (Zhang et al. 2008).

Wu, Su, and Jiang (2011) used the chemistry version (Grell et al. 2005) of the Weather Research and Forecasting (Skamarock 2008) modeling system (WRF-Chem) to study the impact of biomass burning aerosols on convection during the dry season of South America. They found that increased biomass burning aerosols resulted in suppressed convection in the afternoon and enhanced convection at night, i.e. a suppression of diurnal amplitude of convection, which was primarily due to the aerosol radiative effect (Wu, Su, and Jiang 2011). The suppression of convection in the late afternoon and enhancement of convection in the nighttime and early morning by absorbing aerosols (dust aerosols) were also found during the monsoon season of West Africa by Zhao et al. (2011) using WRF-Chem. Based on a specified version of WRF-Chem (Skamarock et al. 2008; Zaveri et al. 2008; Zhao et al. 2010), Fan et al. (2015) found a similar feature over the Sichuan Basin in China. Aerosol absorption suppressed convection in the afternoon and resulted in stronger convection over the mountainous area at night when the accumulated instability was released through the orographical lifting (Fan et al. 2015). In addition, the enhancement of convection by absorbing aerosols are also suggested from the observations of more active lightning in the presence of absorbing aerosols (Altaratz et al. 2010; Kucienska, Raga, and Romero-Centeno 2012; Proestakis et al. 2016; Thornton et al. 2017).

As previously introduced, some WRF-Chem based studies of aerosol impacts on convection have taken both the aerosol microphysical and radiative effects into account altogether (e.g. Wu, Su, and Jiang 2011; Zhao et al. 2011). However, to the best of our knowledge, the response of deep convection to the heating of aerosol layers at different altitudes with perturbed CCN concentrations is still not clear. Microphysics and thermodynamics are coupled in the context of aerosol invigoration of convection (Altaratz et al. 2014). Whether convection becomes stronger or weaker as CCN increases in different aerosol-absorption-perturbed thermodynamic conditions is not conclusive. The objective of this study is to examine the response of deep convection to idealized daytime aerosol heating at different heights and aerosol concentration perturbations using sensitivity simulations, with a focus on updraft area that plays a key role in regulating the lightning flash rate (e.g. Deierling and Petersen 2008; Schultz et al. 2017). The experiment design is described in Section 4.4.2, followed by the results in Section 4.4.3. Discussion and conclusions are presented at last in Section 4.4.4.

4.2. Experiment Design

We selected a real case over northern Alabama, where correlations between satellite aerosol optical depth (AOD) retrievals and lightning flash rates have been reported in the previous Sections. The local standard time (LST) over northern Alabama is 6 hours behind the Coordinated Universal Time (UTC), i.e. LST = UTC - 6 h. In the control of a polar vortex centered over the southern Hudson Bay between Ontario and Quebec of Canada during 18–19 August 2012, the cold dry air was brought from high latitudes to the southern Great Plains and southeastern U.S., where it met the moist warm air coming from the sea. Consequently, a stationary front formed from central Texas to central Mississippi in the morning (07:30 LST) of 18 August. After lasting 9 hours, the front shifted northward when the warm front triumphed

over the cold front in the later afternoon (16:30 LST). Then, it became stationary again in the evening (19:30 LST) and lasted until the next morning (09:30 LST) from southern Kansas to the southern boundary of Tennessee. Influenced by the synoptic weather system, deep convective storms formed over northern Alabama during this period. This case was selected for our sensitivity study.

The version 3.8.1 of the WRF with Advanced Research WRF (ARW) dynamic solver (WRF-ARW; Skamarock and Klemp 2008) was integrated 36 hours from 00:00:00 UTC 18 August 2012 to 12:00:00 UTC 19 August 2012 over the domain as shown in Figure 27a. The simulation data from the sunrise (06:00 LST) of 18 August 2012 to the sunrise (06:00 LST) of 19 August 2012 were analyzed, with a focus on the responses of the storms in the afternoon and nighttime to the aerosol heating during the daytime of 18 August 2012 with CCN number concentration perturbations. The simulation domain features a two-way interactive nested grid. The parent (D01) and nested (D02) domains have horizontal resolutions of 9 km and 3 km, respectively. There are 29 layers assigned in the terrain-following hydrostatic-pressure vertical coordinate. The domain settings result in 71 × 70 × 29 and 102 × 102 × 29 grid points in the domains D01 and D02, respectively. The model was run using a 45 s time step in the domain D01, which then decreased to 15 s in the domain D02. The National Centers for Environmental Information (NCEI) North American Mesoscale Model (NAM) 6-hourly analysis fields were used to initialize and provide time-dependent lateral boundary conditions for the simulation runs.

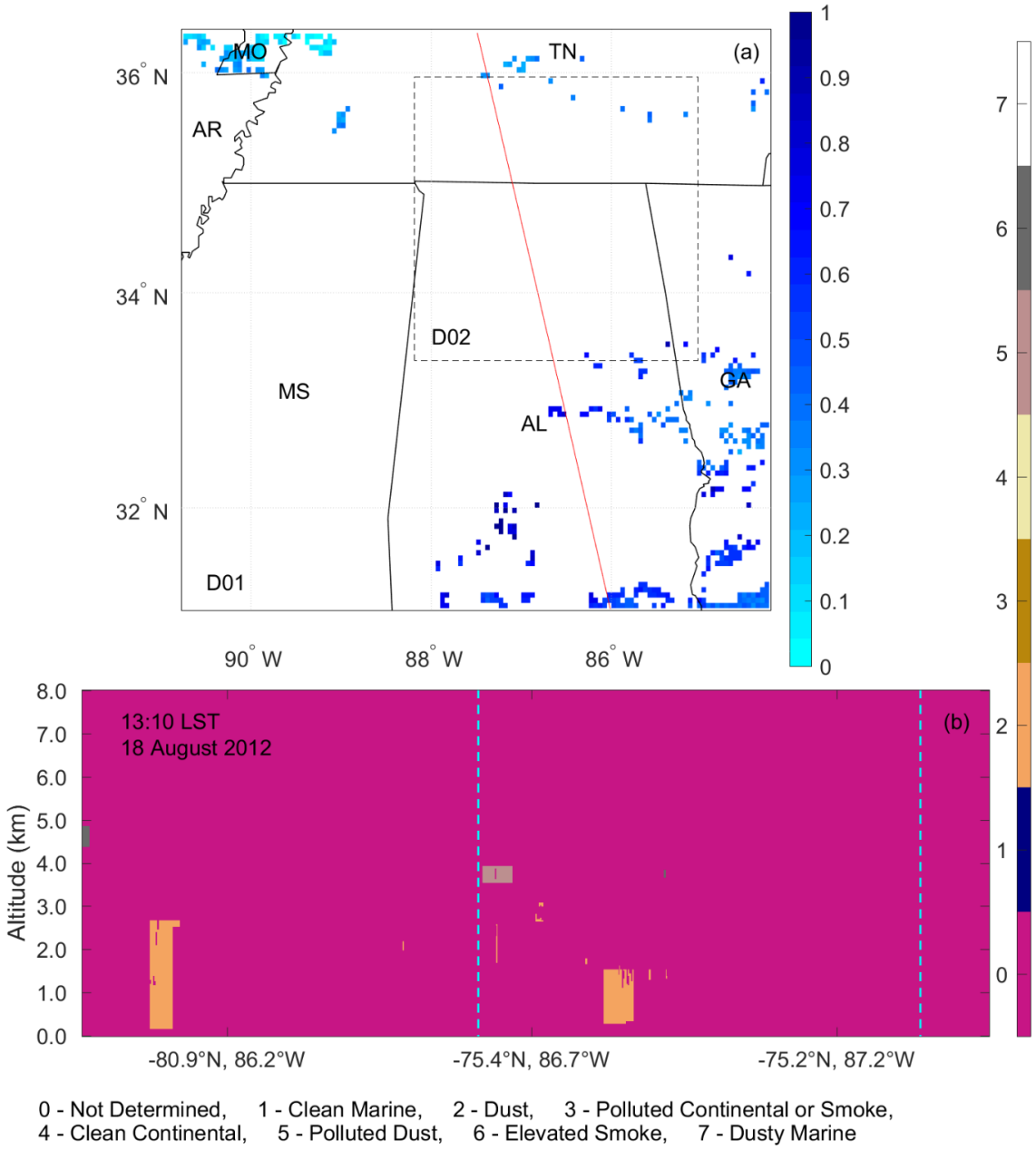

Figure 27. Map of the parent (D01) and nested (D02) domains in the model runs (a) and vertical profiles of aerosol types along the ground track of CALIOP over the simulation domains (b). The spatial distribution of the Aqua Moderate-resolution Imaging Spectroradiometer (MODIS) AOD retrievals (shaded) around the noon (11:30 – 13:30 LST) of 18 August 2012 is shown in the upper panel, where the red line marks the ground track of the lidar instrument on the CALIPSO (Cloud-Aerosol Lidar and Infrared Pathfinder Satellite Observations) satellite on the map. AL, GA, MS, and TN are short for Alabama, Georgia, Mississippi, and Tennessee, respectively. The two vertical dashed lines in the lower panel mark the northern and southern boundaries of the nested domain (D02).

The Dudhia shortwave (Dudhia 1989) and the rapid radiative transfer model (RRTMM; Mlawer et al. 1997) longwave radiation schemes were selected to calculate the upward and downward radiative fluxes. The land surface was represented by the unified Noah Land Surface Model (Chen and Dudhia 2001). The Monin-Obukhov (Janjić) scheme (Janjić 2002) was used to calculate surface layer fluxes. The subgrid boundary layer turbulence was parameterized using the Mellor-Yamada-Janjić scheme (MYJ; Janjić 2002). The Kain-Fritsch scheme (Kain 2004) was applied to the domain D01 to parameterize moist convection, which was resolved in the domain D02 without using a cumulus parameterization. The microphysical processes were parameterized using the Thompson aerosol-aware scheme (Thompson and Eidhammer 2014), which we call the Thompson scheme hereinafter. The Thompson scheme is a hybrid bulk microphysical scheme (Thompson et al. 2008; Thompson, Rasmussen, and Manning 2004), where water- and ice-nucleating aerosol number concentrations (N_{wa} and N_{ia}) are included (Thompson and Eidhammer 2014). Thompson scheme is currently the only available microphysics scheme in WRF where aerosol number concentration can be set and altered, though one can perturb the cloud droplet number concentration using other microphysical schemes in WRF to study the aerosol microphysical effect as well (e.g. White et al. 2017). Saide et al. (2016) suggested similar aerosol impacts on the near-storm environment between simulations using the Thompson scheme and the WRF-Chem. The model configuration and selected schemes are documented in Table 8.

Table 8. Model configuration and selected schemes.

Domain	Parent (D01)	Nested (D02)
Horizontal resolution (m)	9000	3000
Vertical layers	29	29
Horizontal grid points	71 × 70	102 × 102
Time step (s)	45	15
Initial-boundary conditions	40-km NCEI NAM	40-km NCEI NAM
Microphysics scheme	Thompson aerosol-aware	Thompson aerosol-aware
Shortwave radiation scheme	Dudhia	Dudhia
Longwave radiation scheme	RRTM	RRTM
Land surface model	Noah	Noah
Boundary layer scheme	MYJ	MYJ
Cumulus parameterization scheme	Kain-Fritsch	No

Figure 27a also shows the horizontal distribution of the Aqua Moderate-resolution Imaging Spectroradiometer (MODIS) AOD retrievals over the study area. The data are from the MODIS Level 2 Collection 6.1 that has a spatial resolution of 3 km (Levy and Hsu 2015; Levy et al. 2013). As shown in Figure 27a, the AODs over the southeastern part of the domain D01 (southern Alabama and western Georgia) were higher than those close to the northern boundary (southeastern Missouri and central Tennessee). The altitudes of the aerosol layers were captured by the Cloud-Aerosol Lidar with Orthogonal Polarization (CALIOP), the lidar instrument on the CALIPSO (Cloud-Aerosol Lidar and Infrared Pathfinder Satellite Observations) satellite (Omar

et al. 2009; Vaughan et al. 2009). Figure 27b shows vertical profiles of the CALIOP aerosol type retrievals from the Version 4.10 Level 2 vertical feature mask products (Winker 2016). Originally, based on the volume depolarization ratio measurements and associated extinction-to-backscatter ratios (lidar ratios) of the CALIOP, seven pre-defined aerosol types (1) Clean Marine, (2) Dust, (3) Polluted Continental or Smoke, (4) Clean Continental, (5) Polluted Dust, (6) Elevated Smoke, and (7) Dusty Marine were identified (Omar et al. 2009) in the latest version (Version 4.10).

As shown in Figure 27b, a dust layer below 2 km was detected over northern Alabama (around 34.2 ˚N); another thicker dust layer from surface to around 2.7 km was detected over southern Alabama (around 31.5 ˚N). In addition, a thin polluted dust layer around 4 km was detected near the southern boundary of the domain D02. The CALIOP-identified dust and polluted dust layers suggest the presence of absorbing aerosols during the daytime of 18 August 2012 over the study area. Central American biomass burning aerosols that are absorbing aerosols have been observed to be transported to the south central and southeast U.S. (e.g. Saide et al. 2015; Wang, Van den Heever, and Reid 2009) and may have an impact on severe weather, including tornados (Saide et al. 2015) and lightning (Wang, Van den Heever, and Reid 2009). In addition, African mineral dust aerosols that are also absorbing aerosols have been observed to travel a long distance and reach the southeast U.S. (e.g. Prospero 1999; Sassen et al. 2003). To test the storm responses to the daytime heating from absorbing aerosols at different heights, we conducted two experiment runs, Exp750hPa and Exp900hPa, where the temperature profiles were perturbed during the daytime as if a homogeneous absorbing aerosol layer were present over the entire domain.

Huang et al. (2009) suggested daily mean heating rates of 1, 2, and 3 K day^{-1} for the light, moderate, and heavy dust layers from the Taklimakan desert, respectively. The warming of the dust aerosols peaked at the dust layer and decreased above and below the layer (Huang et al. 2009). As shown in Figure 28, the vertical profile of temperature perturbation in the experiment runs was assumed satisfy a normal distribution with respect to the pressure level: $\Delta T(p) = A \times \exp[-(p - \mu)^2/2\sigma^2]$, where ΔT is temperature perturbation, A is amplitude, p is pressure, μ is mean, and σ is standard deviation. In the Exp750hPa run, μ was set to 750 hPa and σ was set to 50 hPa; in the Exp900hPa run, μ was set to 900 hPa and σ was set to 100 hPa. A was fixed to 1 K in both runs. The boundary conditions at each step in the WRF runs were prepared by interpolation of the forcing fields at the two nearest times. The temperature perturbation was added to the 6-hourly NAM forcing fields at noon (12:00 LST) of 18 August 2012. Thus, the temperature profiles on the boundary of the domain D01 are warmed at each time step from the sunrise (06:00 LST) to the sunset (18:00 LST) with a peak at the noon. It should be noted that the heating layer added as such avoids the interactions between horizontal inhomogeneity of absorbing aerosols and synoptic-scale flows (e.g. Jin et al. 2015; Lau et al. 2008; Menon et al. 2002; Zhao, Liu, and Leung 2012), making the experiment focus on addressing the local radiative effects of absorbing aerosols.

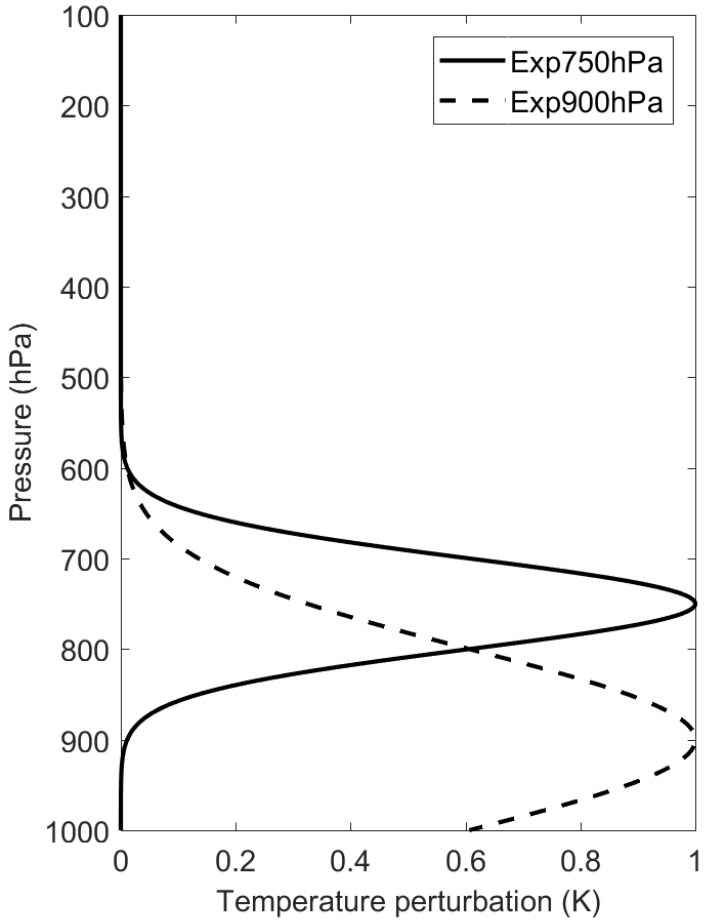

Figure 28. Temperature perturbations in the two experimental runs, Exp750hPa and Exp900hPa.

In the Thompson scheme, the aerosol vertical profiles can be fixed over all horizontal model grid points or read from auxiliary aerosol climatology datasets. For the fixed case, the near surface and free atmospheric water-nucleating aerosol number concentrations ($N_{wa,0}$ and $N_{wa,1}$) can be set to determine the shape of the N_{wa} vertical profile; the near surface and free atmospheric ice-nucleating aerosol number concentrations ($N_{ia,0}$ and $N_{ia,1}$) can be set to determine the shape of the N_{ia} vertical profile. The N_{wa} and N_{ia} vertical profiles are assumed decrease exponentially with height and scaled using the ratios of $N_{wa,1}$ to $N_{wa,0}$ and $N_{ia,1}$ to $N_{ia,0}$,

respectively. The horizontal grid points over the whole domain were initialized to have same vertical profiles of N_{wa} and N_{ia} in this study. We performed 7 different runs for each of the Control, Exp750hPa, and Exp900hPa simulations with initial $N_{wa,0}$ set to 75, 150, 300, 600, 1200, 2400, and 4800 # cm^{-3}, respectively. $N_{wa,1}$ was fixed to its default value 50 # cm^{-3}. Figure 29 shows the resultant N_{wa} initial vertical profiles, proxies for the cleanest to the most polluted environments in reality. In each of the runs, $N_{ia,1}$ and $N_{ia,0}$ were set to their default values 0.5 and 1.5 # cm^{-3}, respectively, making the experiment preclude the impacts of ice nuclei. It should be noted that a number of previous studies have suggested the potential influence of ice-nucleating aerosols on convection as surveyed by Fan et al. (2016). Only water-nucleating aerosol concentrations were perturbed in this study to avoid this complexity.

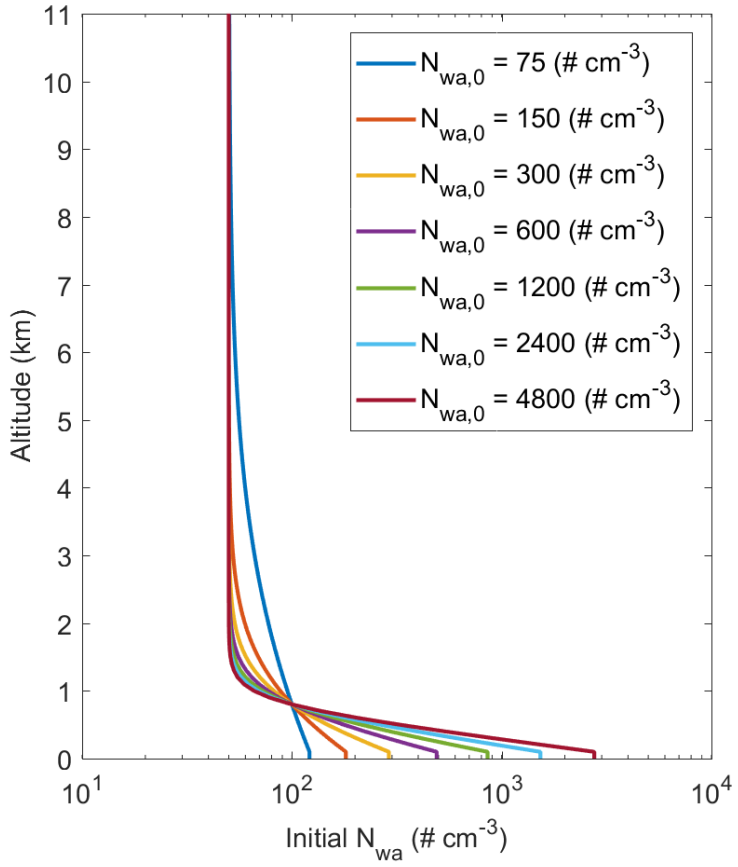

Figure 29. Initial number concentrations of water-nucleating aerosols (N_{wa}, # cm^{-3}) specified in different runs.

The simulation results are first compared to the Level 2 radar data from the Hytop, Alabama (34.927 N, 86.080 W) KHTX WSR-88D (Section 4.3.1). Then, the differences in the updraft area in domain D02 between the control and experimental runs are shown (Section 4.3.2). Previous studies have chosen vertical wind speed thresholds to define the updraft horizontal grid points (Fan et al. 2008; Lee et al. 2008; Morrison 2012; Tao et al. 2007; Wang 2005). A vertical wind speed threshold of 3 m s^{-1} (Lee et al. 2008) was adopted in this study; all the horizontal grid points in domain D02 where maximum vertical wind speeds exceed 3 m s^{-1} are regarded as updraft grid points. Next, the differences in the mean convective available

potential energy (CAPE) over domain D02 and the mean low-level vertical wind shear (LLVWS) over the updraft area between the control and experimental runs are examined (Section 4.3.3). The presence of absorbing aerosols may result in increased CAPE (Wang et al. 2013) and LLVWS (Saide et al. 2015), which in turn are linked to the intensification (Emanuel 1994) and organization (Rotunno, Klemp, and Weisman 1988; Weisman and Rotunno, 2004) of convection. Absorbing aerosols can cause a capping inversion that inhibits convection, and consequently CAPE is gradually accumulated and the convection becomes stronger when it occurs later (Wang et al. 2013). Absorbing aerosols on top of the PBL can suppress the turbulent mixing within PBL (Ding et al. 2016; Dong et al. 2017; Li et al. 2017; Wilcox et al. 2016), leading to enhanced LLVWS that may have an impact on thunderstorms (Saide et al. 2015). The zonal and meridional components of horizontal winds at 1 km were first obtained by linear interpolation. Then, the vector difference between the horizontal winds at 1 km and 10 m at each grid point was taken as the LLVWS. Last, the differences in hydrometeors averaged over the updraft area—including mixing ratios of water vapor (q_v), cloud water (q_c), rain water (q_r), ice (qi), snow (q_s), and graupel (q_g)—between the control and experimental runs are shown (Section 4.3.4). Thirty minute running mean was applied to the 5-minute time series of updraft area, CAPE, LLVWS, and hydrometeor simulations to smooth out the high frequency variations.

4.3. Results

4.3.1. Comparison with radar observation

Figure 30 shows a comparison of the model simulated and observational composite radar reflectivity over the domain D02. Since there were no aerosol number concentration measurements for the selected case, the Control run with an initial $N_{wa,0}$ of the default value 300 # cm^{-3} was chosen as the counterpart of radar observations in Figure 30. The spatial patterns of

the composite radar reflectivity among the Control runs with different near-surface water-nucleating aerosol number concentrations are similar (not shown). As shown by the radar observations (Figure 30), small isolated convective cells started to form over western and central Alabama in the early afternoon of 18 August 2012. In the later afternoon, the storms merged to a west-east line across Alabama. After that, the convective system continued to develop; the storm area became more widespread and reached a maximum around 20:00 LST. The convective system moved eastward and gradually dissipated during the decaying stage at night. Around 00:00 LST 19 August 2012, a smaller storm formed over the northern Alabama and lasted until the sunrise.

Overall, the simulated spatial patterns of radar reflectivity resemble those from radar observations. The simulation results fail to reproduce the instantaneous locations of convective cores. This model drawback has been widely documented (e.g. McCaul Jr et al. 2009; Wong, Barth, and Noone 2013). The simulated nighttime convective system became most widespread about 2 hours later than observed. Model simulations underestimate the radar reflectivity during the early stage of the convective system (16:00–20:00 LST) and overestimate the radar reflectivity during the mature and decaying stages of the convective system (00:00–06:00 LST). Previous studies have reported radar reflectivity overestimation by models during the mature and decaying stages of storms, particularly in the middle and upper troposphere (e.g. Blossey et al. 2007; Li et al. 2008; Matsui et al. 2009). The overly high radar reflectivity simulated by models is due to the overly strong simulated updrafts (e.g. Fan et al. 2017; Varble et al. 2014) and overly high simulated cloud ice contents (Lang et al. 2007; Matsui et al. 2009; Stanford et al. 2017; Varble et al. 2011).

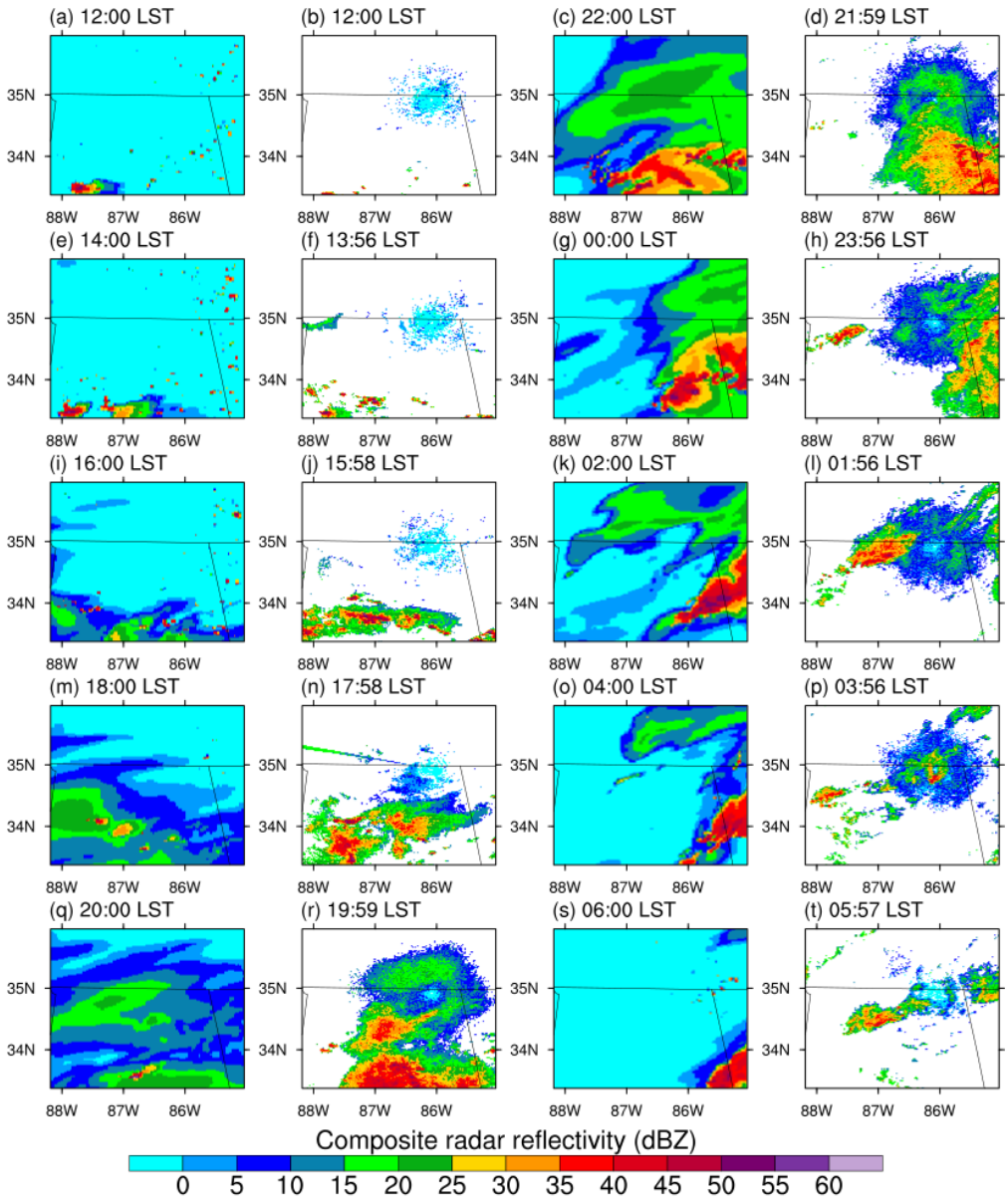

Figure 30. Composite radar reflectivity over the domain D02 from 12:00 LST 18 August 2012 to 06:00 LST 19 August 2012. The 1st and 3rd columns are from the Control run with an initial $N_{wa,0}$ of 300 # cm^{-3}. The 2nd and 4th columns are from radar Level 2 data.

4.3.2. Updraft area

The time sequence of the updraft area over the domain D02 from the Control run (Figure 31a) is consistent with the development of storms shown by the composite radar reflectivity

sequence in Figure 30. In the Control runs, relatively weak storms were present right before noon and last to the later afternoon with a maximum updraft area of about 200 km^2 around noon. Strong storms swept over the area from the evening of 18 August 2012 to the sunrise of 19 August 2012 with two updraft area peaks of up to about 1000 and 800 km^2 at around 22:00 and 03:00 LST, respectively. The nighttime storms occurred 0.5–1.5 hours later in the more polluted conditions ($N_{wa,0}$ = 1200, 2400, and 4800 # cm^{-3}) than in the cleaner conditions ($N_{wa,0}$ = 75, 150, and 300 # cm^{-3}). van den Heever and Cotton (2007) suggested that the suppression of the warm-rain process by increased N_{wa} delays the downdraft development and makes increased smaller cloud and rain droplets stay longer within the clouds, which in turn delays the condensation of supercooled water and associated latent heat release. As a consequence, the updraft enhancement through latent heat release is delayed (van den Heever and Cotton 2007). However, the strength of the nighttime deep convection in terms of the two updraft area maxima did not appear to be monotonic with respect to N_{wa} (Figure 31a).

In the Exp750hPa runs where a heating layer that peaked at 750 hPa was added (Figure 28), the early afternoon storms were suppressed and the evening storms were enhanced (Figure 31b and 31c). The suppression of convection in the afternoon and enhancement of convection at night by absorbing aerosols are in agreement with previous studies (Wu, Su, and Jiang 2011; Zhao et al. 2011). Fan et al. (2008) also suggested the suppression of daytime deep convection by absorbing aerosols. The overall net enhancement of the storms over domain D02 during the sunrise of 18 August 2012 to the sunrise of 19 August 2012 did not appear to be monotonic to N_{wa} (Table 9). The enhancement of updraft area by the heating layer at 750 hPa in the most polluted case ($N_{wa,0}$ = 4800 # cm^{-3}) was more than double that in the cleanest case ($N_{wa,0}$ = 75 # cm^{-3}; Table 9), suggesting potentially greater impact of absorbing aerosols on storms over the

most polluted metropolitans in the world, such as the urban areas in China (Wang et al. 2016). The nighttime storms also generally occurred later in the more polluted conditions ($N_{wa,0}$ = 1200, 2400, and 4800 # cm^{-3}) than in the cleaner conditions ($N_{wa,0}$ = 150, 300, and 600 # cm^{-3}) in the Exp750hPa runs (Figure 31c). The updraft area was larger in the cleaner cases than in the more polluted cases at the first peak around 22:00–23:00 LST (Figure 31c); the second peak of updraft area around 03:00 LST disappeared in the cleaner cases (Figure 31c). The result suggests a slower release of accumulated conditional instability in high N_{wa} conditions.

In the Exp900hPa runs where a heating layer that peaked at 900 hPa was added (Figure 28), the nighttime storms were also enhanced, but the two peaks in updraft area became one peak around 00:00 LST (Figure 31d and 31e). The updraft area maxima in the Exp900hPa runs with $N_{wa,0}$ of 600 and 1200 # cm^{-3} were greater than their counterparts in the Exp750hPa runs (Figure 31c and 31e). The rapid release of accumulated conditional instability in the Exp900hPa runs with $N_{wa,0}$ of 600 and 1200 # cm^{-3} resemble the case reported by Fan et al. (2015) over the Sichuan Basin of China. The delayed updraft area peak in the Exp900hPa runs might be due to the enhanced evaporation of cloud water droplets, which is discussed more in Section 4.3.4. Shi et al. (2014) suggested that the radiative effect of mineral dust aerosols delayed the nighttime onset of a mesoscale convective system that passed through the Niamey, Niger area in August by 2 hours. The overall net enhancement of storms during the sunrise of 18 August 2012 to the sunrise of 19 August 2012 in the Exp900hPa runs was also not monotonic to $N_{wa,0}$ (Table 9). The net enhancement of storms in the Exp900hPa runs was less great than that in the Exp750hPa runs (Table 9). The enhancement of storms in the most polluted case ($N_{wa,0}$ = 4800 # cm^{-3}) was more than 50% greater than that in the cleaner cases ($N_{wa,0}$ = 75, 150, and 300 # cm^{-3}), which again is

suggestive of potentially greater impact of absorbing aerosols on storms over the most polluted urban areas.

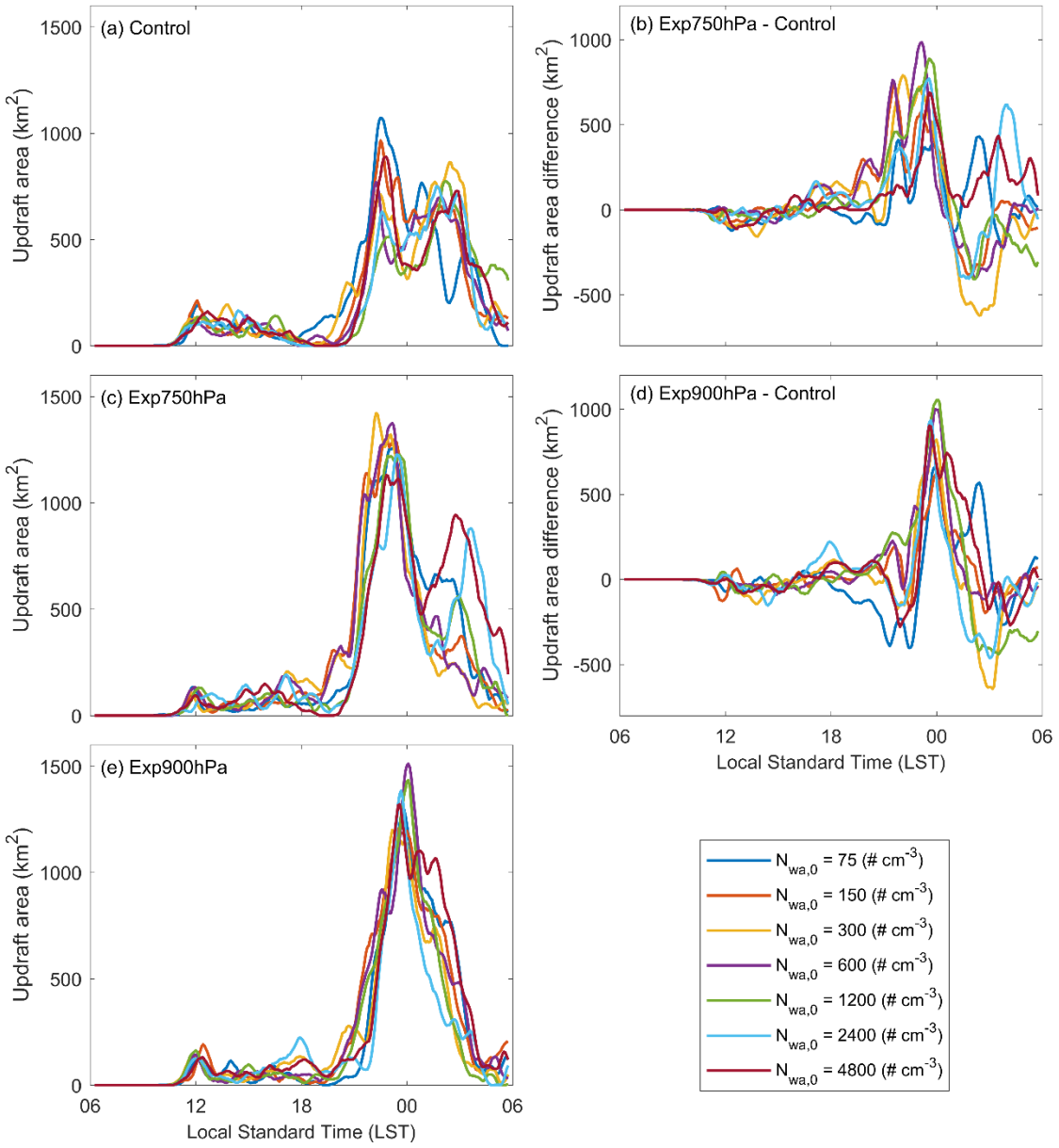

Figure 31. Time series of updraft area from control and experimental runs, (a), (c), and (e); and time series of the difference in updraft area between control and experimental runs, (b) and (d).

Table 9. Time mean difference in the updraft area (A) in domain D02 between the experimental runs and the control run during 06:00 LST 18 August 2012–06:00 LST 19 August 2012.

$N_{wa,0}$ (# cm^{-3})	$A_{Exp750hPa}$ - $A_{control}$ (km^2)	$A_{Exp900hPa}$ - $A_{control}$ (km^2)
75	31.3	6.2
150	51.4	38.8
300	18.4	-0.3
600	65.4	60.1
1200	48.6	33.3
2400	67.1	8.5
4800	83.9	58.8

4.3.3. CAPE and low-level vertical wind shear

As shown in Figure 32, after the sunrise, the mean CAPE over the domain D02 started to increase; it increased from below 400 J kg^{-1} to a maximum of around 800 J kg^{-1} at the noon. After that, CAPE began to decrease as convection occurred; it decreased fastest between 18:00 and 00:00 LST when the strong nighttime storms swept over the domain D02. The presence of weak and isolated convection in the afternoon and strong storms at night is not uncommon. Lin et al. (2016) studied a similar case over the U.S. Southern Great Plain (SGP) on 25–26 May 2009. The two simulation ensembles whose respective layers of heating peaked at 750 and 900hPa both showed increased maximum CAPE at noon as compared to the Control runs (Figure 32), suggesting that absorbing aerosols at 750 and 900hPa contributed to the accumulation of convective instability. CAPE decreased more slowly in the Exp750hPa runs than in the Control and Exp900hPa runs during 12:00–15:00 LST, consistent with the suppression of convection in

the Exp750hPa runs during this period as shown in Figure 31b and 31c. The suppression of convection with increased CAPE by the heating layer at 750hPa above the PBL and subsequently enhanced storms agree with Wang et al. (2013). The Exp900hPa runs showed more rapid decrease of CAPE right before the updraft maxima at 00:00 LST, particularly for the two runs with $N_{wa,0}$ of 600 and 1200 # cm^{-3} (Figure 32d), in agreement with the fastest development of storms for the two runs (Figure 31d).

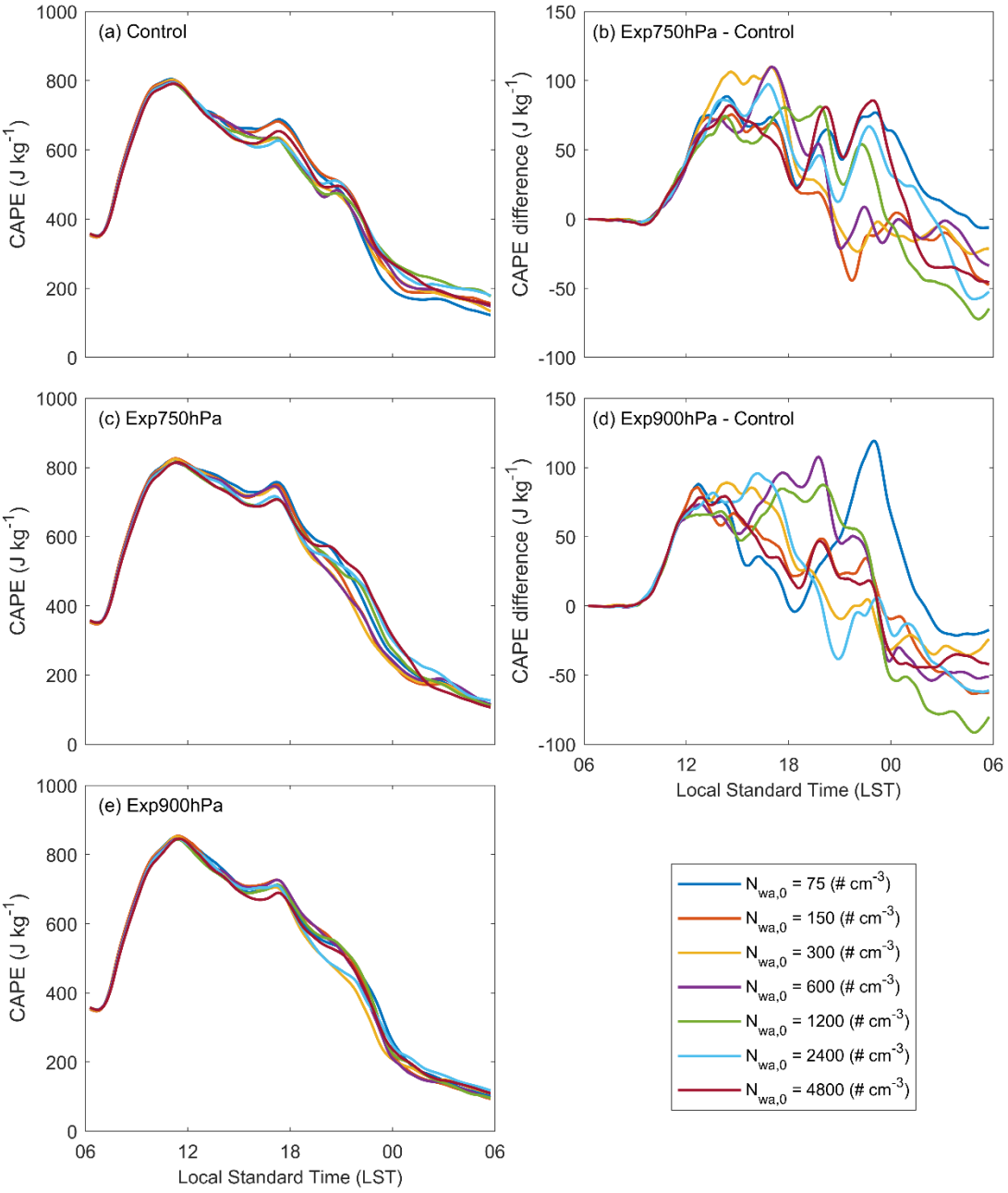

Figure 32. Time series of the mean CAPE over the domain D02 from control and experimental runs, (a), (c), and (e); and time series of the difference in the mean CAPE over the domain D02 between control and experimental runs, (b) and (d).

Saide et al. (2015) suggested that absorbing aerosols result in enhanced LLVWS in an environment that is already conducive to severe weather. The simulation results in this study

agree with Saide et al. (2015). The mean LLVWSs over the updraft areas in the experimental runs exceeded those in the control runs by up to and more than 5 m s^{-1} during the development of the nighttime storm system around 00:00 LST (Figure 33). The overall net enhancement of the LLVWS over the updraft area during 06:00 LST 18 August 2012–06:00 LST 19 August 2012 was not monotonic with respect to N_{wa} (Table 10); the enhancement by the heating layer above the PBL (Exp750 hPa) was greater than that by the heating layer within the PBL (Exp900 hPa). Previous studies have suggested a key role of enhanced LLVWS and cold pool in new cell formations of convective systems (Knupp and Cotton 1982; Rotunno, Klemp, and Weisman 1988; Weisman and Rotunno 2004). However, the duration of the nighttime convective system in this study did not appear to be longer in the presence of enhanced LLVWS (Figure 31). The 3 km spacing of horizontal grid points may be too coarse to resolve cold pools (Del Genio, Wu, and Chen 2012). Moreover, we cannot tell the cause and effect between the enhanced updraft area and the enhanced mean LLVWS over the updraft area in the experimental runs of this study.

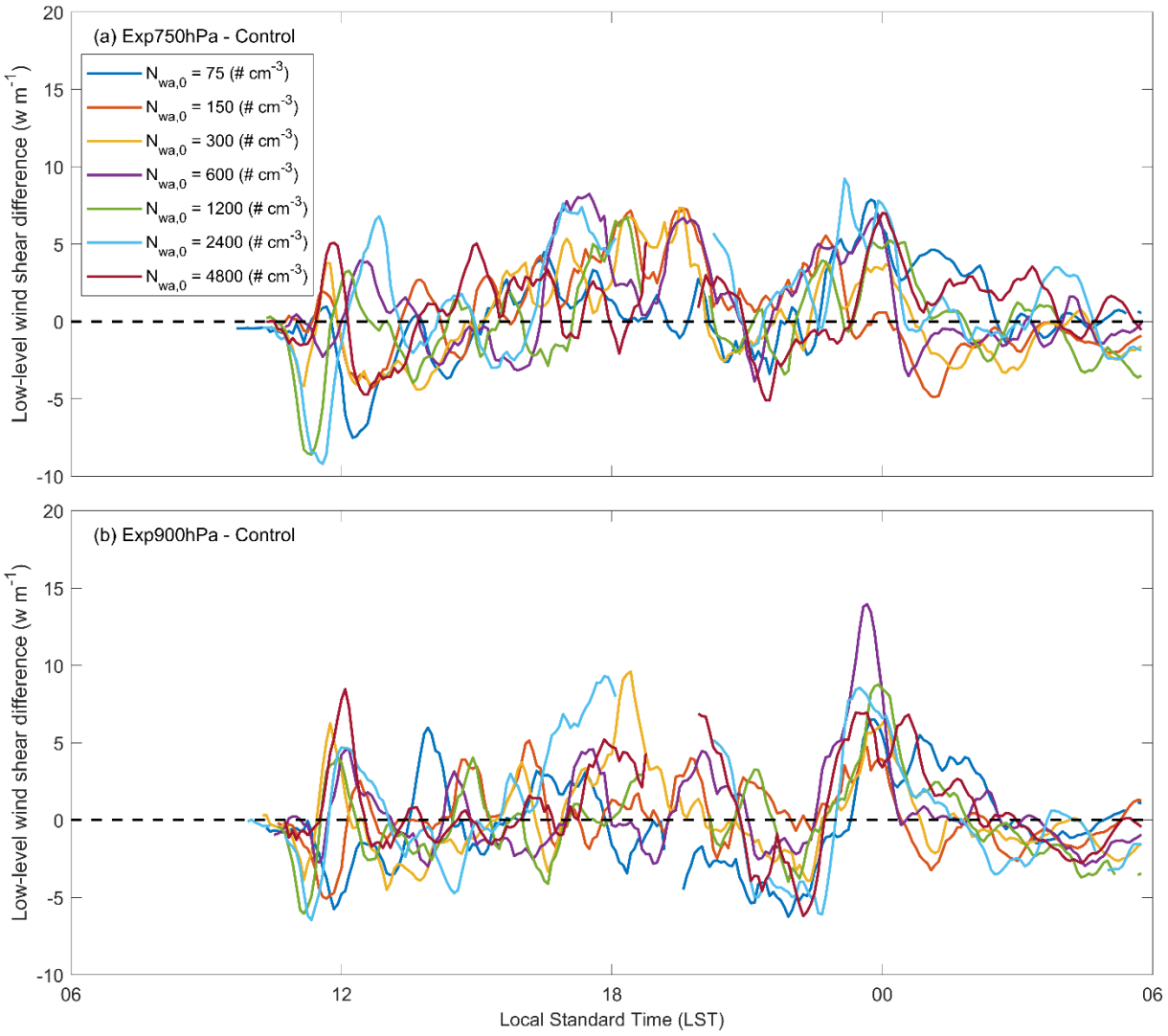

Figure 33. Time series of difference in the low-level vertical wind shear averaged over the updraft area between control and experimental runs.

Table 10. Time mean difference in the low-level vertical wind shear (LLVWS) in domain D02 between the experimental runs and the control run during 06:00 LST 18 August 2012–06:00 LST 19 August 2012.

$N_{wa,0}$ (# cm^{-3})	$LLVWS_{Exp750hPa} - LLVWS_{control}$ (m s^{-1})	$LLVWS_{Exp900hPa} - LLVWS_{control}$ (m s^{-1})
75	0.45	-0.26
150	0.73	0.22
300	0.17	0.14
600	1.11	0.60
1200	0.00	-0.08
2400	1.11	0.41
4800	0.81	0.85

4.3.4. Hydrometeors

The updraft area enhancement by the heating layers at 750 and 900 hPa in the experimental runs was associated with increased mean mixing ratios of cloud ice particles over the updraft area in the middle and upper troposphere (Figure 34) and increased mean mixing ratios of condensate particles over the updraft area in the lower and middle troposphere (Figure 35) in general. The excessive frozen condensates over the updraft area reached maxima in the evening during 20:00–00:00 LST in the Exp750hPa runs (Figure 34) and at night around 00:00 LST in the Exp900hPa runs (Figure 35). The excess maxima of cloud ice content were followed by the deficit maxima during 01:00– 04:00 LST in the Exp750hPa runs (Figure 34), suggesting more intense deep convection enhancement of the nighttime storms during the first wax and

wane of the updraft area than the second (Figure 31). The deficits of cloud and rain water mixing ratios were present right before the delayed enhancement of the nighttime storms in the Exp900hPa runs (Figures 32 and 36), suggesting enhanced evaporation of cloud and rain droplets or enhanced evaporation of cloud droplets and suppressed cloud autoconversion in the presence of the heating layer within the PBL. The delayed onset of the nighttime storms in the Exp900hPa runs (Figure 31) might be contributed by the cloud water deficits (Figure 35), which limited the amount of supercooled water above the freezing level that was needed to trigger the enhancement of updrafts through the release of latent heating.

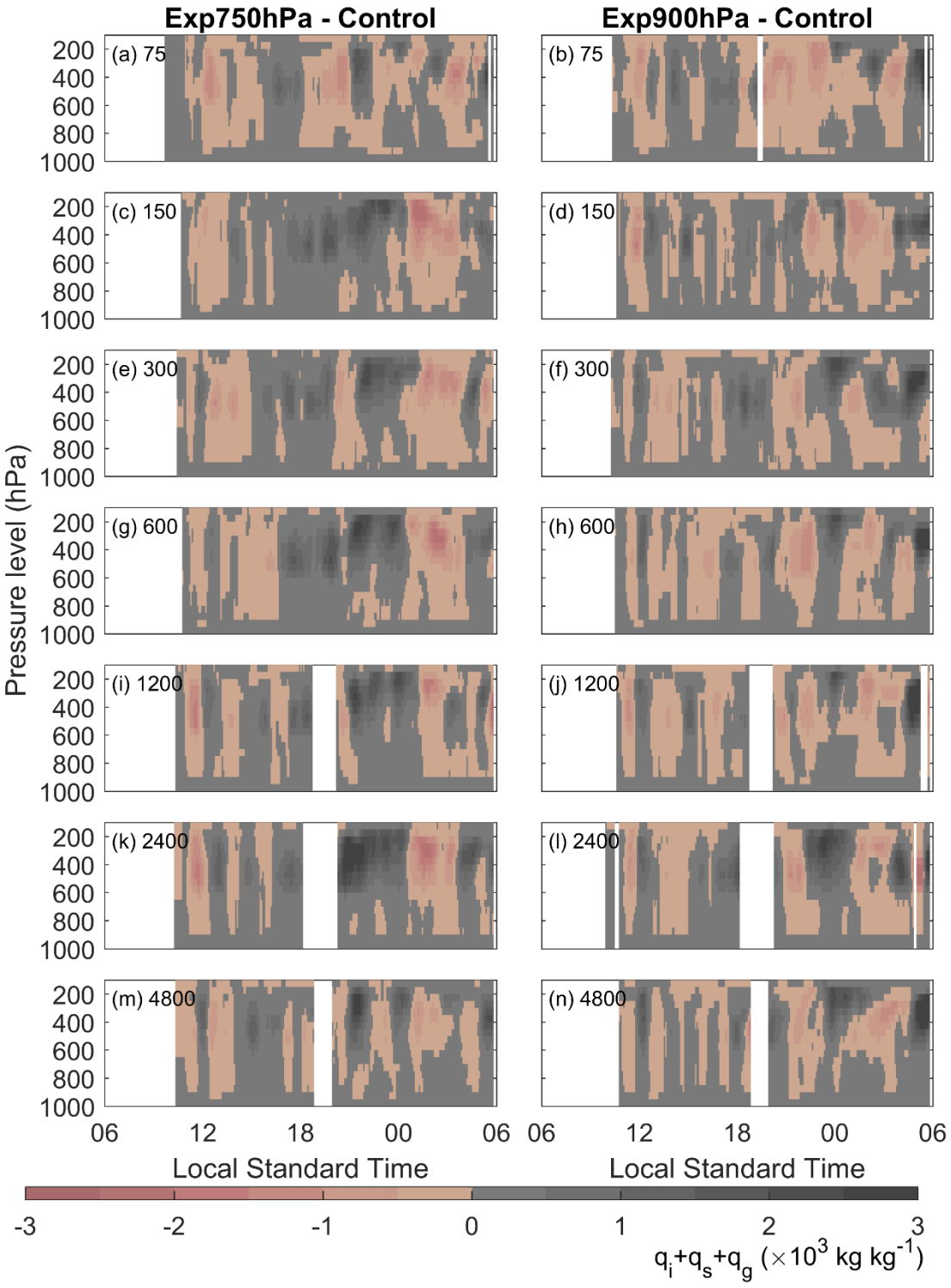

Figure 34. Time series of the difference in the mean vertical profile of cloud ice content ($q_i+q_s+q_g$; kg kg^{-1}) over the updraft area between control and experimental runs. The number on the upper left corner of each panel is the initial $N_{wa,0}$ in # cm^{-3}.

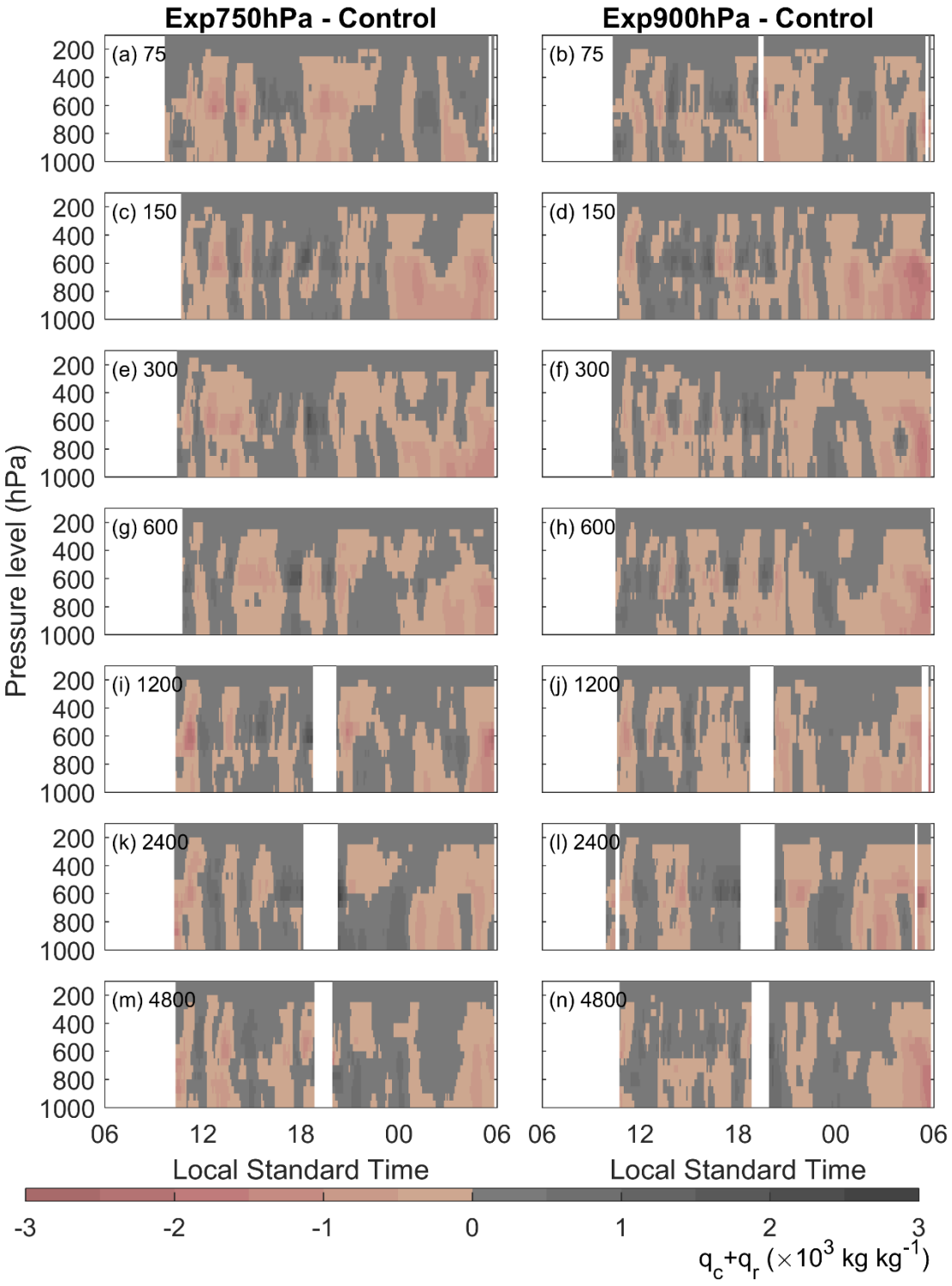

Figure 35. Time series of the difference in the mean vertical profile of cloud water content (q_c+q_r; kg kg^{-1}) over the updraft area between control and experimental runs. The number on the upper left corner of each panel is the initial $N_{wa,0}$ in # cm^{-3}.

Overall, the net mean cloud ice contents over the updraft areas during 06:00 LST 18 August 2012–06:00 LST 19 August 2012 in the experiment runs area were greater than those in the control runs (Figure 36) except for the cleanest case ($N_{wa,0}$ = 75 # cm^{-3}). The increased cloud ice contents over the updraft areas in the experimental runs suggested enhanced updraft wind speeds and lightning activity (Deierling and Petersen 2008; Deierling et al. 2008; Lynn and Yair, 2010; Yair et al. 2010) by the heating layers. The excessive frozen condensates over the updraft areas were not monotonic with respect to $N_{wa,0}$ (Figure 36). Overall, the cloud and rain water contents over the updraft areas below 700 hPa were depleted in the Exp900hPa runs (Figure 36h and 36i), suggestive of enhanced evaporation of condensates and suppressed cloud autoconversion by absorbing aerosols within the PBL. However, the water vapor mixing ratio over the updraft area did not appear to increase below 700 hPa but increase between around 650 and 400 hPa in the Exp900hPa runs (Figure 36g), suggesting an overall more buoyant convective environment in the middle troposphere. The cloud and rain water mixing ratios over the updraft areas in the middle troposphere did not appear to increase (Figure 36b, 36c, 36h, and 36i) in the experimental runs. Perhaps, the excessive supercooled water brought by the enhanced updrafts in the experimental runs froze into cloud ice and graupel rapidly.

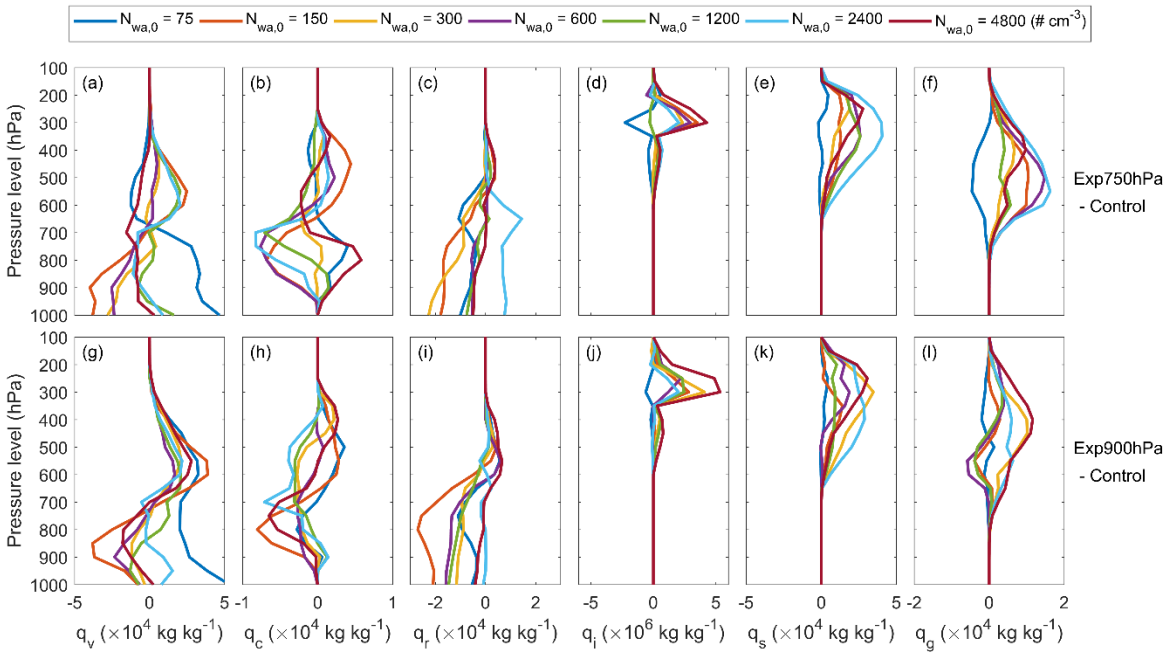

Figure 36. Time mean of the difference in the mean vertical profiles of the mixing ratios of water vapor (q_v), cloud water (q_c), rain water (q_r), ice (qi), snow (q_s), and graupel (q_g) over the updraft area between control and experimental runs during 06:00 LST 18 August 2012–06:00 LST 19 August 2012.

4.4. Discussion and Conclusions

The impact of absorbing aerosols on convection is sensitive to the height of aerosol layer (Koch and Del Genio 2010; Li et al. 2017; Wang 2013). The sensitivity of deep convection to aerosol daytime heating at different heights with aerosol number concentration perturbations is studied by conducting idealized WRF experiments. The simulations focus on the updraft area that is closely linked to lightning activity (e.g. Deierling and Petersen 2008; Schultz et al. 2017), the enhancement of which by absorbing aerosols has been suggested (Altaratz et al. 2010; Kucienska, Raga, and Romero-Centeno 2012; Proestakis et al. 2016; Thornton et al. 2017). The results suggest that homogenous heating layers above or within the PBL both result in enhanced updrafts and cloud ice content over the updraft areas of the nighttime storms. The enhancements

of updraft area, cloud ice content, and LLVWS by the heating layers do not appear to be monotonic with respect to the water-nucleating aerosol number concentration. The updraft area enhancement in the most polluted case is greater than in the cleanest cases, suggestive of a potentially greater impact of absorbing aerosols on the storms over the most polluted urban areas in the world. The heating layer above the PBL suppresses isolated convective cells in the early afternoon and results in stronger storms with enhanced LLVWS in the evening and at night when the accumulated convective instability is released. The heating layer within the PBL results in a delayed onset of the enhanced nighttime storms, which may be due in part to the enhanced evaporation of cloud and rain water right before the onset of the nighttime storms. The cloud water deficit may limit the supercooled water brought above the freezing level that is needed to enhance convective updrafts through the latent heat release.

We used the Thompson scheme that is a bulk microphysics scheme in this study. However, as thoroughly surveyed by Khain et al. (2015), cloud-resolving simulations using spectral bin schemes generally agree better with observations than those using bulk schemes, though there are also studies that have suggested small differences using the two different kinds of microphysics schemes (e.g. Iguchi et al. 2008). Moreover, in the Thompson scheme, the CCN activation fraction is parameterized as a function of water-nucleating aerosol number concentration, temperature, hygroscopicity parameter (κ; Petters and Kreidenweis 2007), vertical velocity, and aerosol mean radius (Eidhammer, DeMott, and Kreidenweis 2009; Feingold and Heymsfield 1992; Thompson and Eidhammer 2014), where κ is fixed to 0.4 and aerosol mean radius is fixed to 0.04 μm in the current version. However, the microphysical effects of aerosols are sensitive to the chemical composition of aerosols (Wang 2005). How the results in this study vary with different chemical compositions of aerosols remains unclear. Furthermore, it should be

noted that only the daytime heating of absorbing aerosols is considered in this study. However, the longwave warming effect of absorbing aerosols during the nighttime may be greater than that during the daytime (Zhao et al. 2011).

4.5. References

Albrecht, Bruce A. 1989. "Aerosols, cloud microphysics, and fractional cloudiness." *Science* no. 245 (4923):1227-1230. doi: 10.1126/science.245.4923.1227.

Altaratz, O, I Koren, LA Remer, and E Hirsch. 2014. "Cloud invigoration by aerosols—Coupling between microphysics and dynamics." *Atmospheric Research* no. 140:38-60. doi: 10.1016/j.atmosres.2014.01.009.

Altaratz, Orit, Ilan Koren, Yoav Yair, and Colin Price. 2010. "Lightning response to smoke from Amazonian fires." *Geophysical Research Letters* no. 37:L07801. doi: 10.1029/2010gl042679.

Andreae, M. O., D. Rosenfeld, P. Artaxo, A. A. Costa, G. P. Frank, K. M. Longo, and M. A. F. Silva-Dias. 2004. "Smoking rain clouds over the Amazon." *Science* no. 303 (5662):1337-1342. doi: 10.1126/science.1092779.

Blossey, Peter N, Christopher S Bretherton, Jasmine Cetrone, and Marat Kharoutdinov. 2007. "Cloud-resolving model simulations of KWAJEX: Model sensitivities and comparisons with satellite and radar observations." *Journal of the Atmospheric Sciences* no. 64 (5):1488-1508. doi: 10.1175/JAS3982.1.

Chen, Fei, and Jimy Dudhia. 2001. "Coupling an advanced land surface–hydrology model with the Penn State–NCAR MM5 modeling system. Part I: Model implementation and sensitivity." *Monthly Weather Review* no. 129 (4):569-585. doi: 10.1175/1520-0493(2001)129<0569:CAALSH>2.0.CO;2.

Deierling, Wiebke, and Walter A Petersen. 2008. "Total lightning activity as an indicator of updraft characteristics." *Journal of Geophysical Research: Atmospheres* no. 113 (D16). doi: 10.1029/2007JD009598.

Deierling, Wiebke, Walter A Petersen, John Latham, Scott Ellis, and Hugh J Christian. 2008. "The relationship between lightning activity and ice fluxes in thunderstorms." *Journal of Geophysical Research: Atmospheres* no. 113 (D15). doi: 10.1029/2007JD009700.

Del Genio, Anthony D, Jingbo Wu, and Yonghua Chen. 2012. "Characteristics of mesoscale organization in WRF simulations of convection during TWP-ICE." *Journal of Climate* no. 25 (17):5666-5688. doi: 10.1175/JCLI-D-11-00422.1.

Ding, AJ, X Huang, W Nie, JN Sun, V-M Kerminen, T Petäjä, H Su, YF Cheng, X-Q Yang, and MH Wang. 2016. "Enhanced haze pollution by black carbon in megacities in China." *Geophysical Research Letters* no. 43 (6):2873-2879. doi: 10.1002/2016GL067745.

Dong, Zipeng, Zhanqing Li, Xing Yu, Maureen Cribb, Xingmin Li, and Jin Dai. 2017. "Opposite long-term trends in aerosols between low and high altitudes: a testimony to the aerosol–PBL feedback." *Atmospheric Chemistry and Physics* no. 17 (12):7997-8009. doi: 10.5194/acp-17-7997-2017.

Dudhia, Jimy. 1989. "Numerical study of convection observed during the winter monsoon experiment using a mesoscale two-dimensional model." *Journal of the Atmospheric Sciences* no. 46 (20):3077-3107. doi: 10.1175/1520-0469(1989)046<3077:NSOCOD>2.0.CO;2.

Eidhammer, Trude, Paul J DeMott, and Sonia M Kreidenweis. 2009. "A comparison of heterogeneous ice nucleation parameterizations using a parcel model framework."

Journal of Geophysical Research: Atmospheres no. 114 (D6). doi: 10.1029/2008JD011095.

Emanuel, Kerry A. 1994. *Atmospheric convection*. New York: Oxford University Press.

Fan, J. W., D. Rosenfeld, Y. N. Ding, L. R. Leung, and Z. Q. Li. 2012. "Potential aerosol indirect effects on atmospheric circulation and radiative forcing through deep convection." *Geophysical Research Letters* no. 39. doi: 10.1029/2012gl051851.

Fan, Jiwen, Bin Han, Adam Varble, Hugh Morrison, Kirk North, Pavlos Kollias, Baojun Chen, Xiquan Dong, Scott E Giangrande, and Alexander Khain. 2017. "Cloud-resolving model intercomparison of an MC3E squall line case: Part I—Convective updrafts." *Journal of Geophysical Research: Atmospheres* no. 122 (17):9351-9378. doi: 10.1002/2017JD026622.

Fan, Jiwen, Daniel Rosenfeld, Yan Yang, Chun Zhao, L Ruby Leung, and Zhanqing Li. 2015. "Substantial contribution of anthropogenic air pollution to catastrophic floods in Southwest China." *Geophysical Research Letters* no. 42 (14):6066-6075. doi: 10.1002/2015GL064479.

Fan, Jiwen, Daniel Rosenfeld, Yuwei Zhang, Scott E Giangrande, Zhanqing Li, Luiz AT Machado, Scot T Martin, Yan Yang, Jian Wang, and Paulo Artaxo. 2018. "Substantial convection and precipitation enhancements by ultrafine aerosol particles." *Science* no. 359 (6374):411-418.

Fan, Jiwen, Yuan Wang, Daniel Rosenfeld, and Xiaohong Liu. 2016. "Review of aerosol–cloud interactions: mechanisms, significance, and challenges." *Journal of the Atmospheric Sciences* no. 73 (11):4221-4252. doi: 10.1175/JAS-D-16-0037.1.

Fan, Jiwen, Tianle Yuan, Jennifer M Comstock, Steven Ghan, Alexander Khain, L Ruby Leung, Zhanqing Li, Vanderlei J Martins, and Mikhail Ovchinnikov. 2009. "Dominant role by vertical wind shear in regulating aerosol effects on deep convective clouds." *Journal of Geophysical Research: Atmospheres* no. 114 (D22):D22206. doi: 10.1029/2009JD012352.

Fan, Jiwen, Renyi Zhang, Wei-Kuo Tao, and Karen I Mohr. 2008. "Effects of aerosol optical properties on deep convective clouds and radiative forcing." *Journal of Geophysical Research: Atmospheres* no. 113 (D8). doi: 10.1029/2007JD009257.

Feingold, Graham, Wynn L. Eberhard, Dana E. Veron, and Michael Previdi. 2003. "First measurements of the Twomey indirect effect using ground-based remote sensors." *Geophysical Research Letters* no. 30 (6):1287. doi: 10.1029/2002gl016633.

Feingold, Graham, and Andrew J Heymsfield. 1992. "Parameterizations of condensational growth of droplets for use in general circulation models." *Journal of the Atmospheric Sciences* no. 49 (23):2325-2342. doi: 10.1175/1520-0469(1992)049<2325:POCGOD>2.0.CO;2.

Grabowski, Wojciech W, and Hugh Morrison. 2011. "Indirect impact of atmospheric aerosols in idealized simulations of convective–radiative quasi equilibrium. Part II: Double-moment microphysics." *Journal of Climate* no. 24 (7):1897-1912. doi: 10.1175/2010JCLI3647.1.

Grell, Georg A, Steven E Peckham, Rainer Schmitz, Stuart A McKeen, Gregory Frost, William C Skamarock, and Brian Eder. 2005. "Fully coupled “online” chemistry within the WRF model." *Atmospheric Environment* no. 39 (37):6957-6975. doi: 10.1016/j.atmosenv.2005.04.027.

Huang, J., Q. Fu, J. Su, Q. Tang, P. Minnis, Y. Hu, Y. Yi, and Q. Zhao. 2009. "Taklimakan dust aerosol radiative heating derived from CALIPSO observations using the Fu-Liou radiation model with CERES constraints." *Atmospheric Chemistry and Physics* no. 9:4011-4021. doi: 10.5194/acp-9-4011-2009.

Iguchi, Takamichi, Teruyuki Nakajima, Alexander P Khain, Kazuo Saito, Toshihiko Takemura, and Kentaroh Suzuki. 2008. "Modeling the influence of aerosols on cloud microphysical properties in the east Asia region using a mesoscale model coupled with a bin-based cloud microphysics scheme." *Journal of Geophysical Research: Atmospheres* no. 113 (D14). doi: 10.1029/2007JD009774.

Janjić, Zaviša I. 2002. *Nonsingular implementation of the Mellor-Yamada level 2.5 scheme in the NCEP Meso model*: US Department of Commerce, National Oceanic and Atmospheric Administration, National Weather Service, National Centers for Environmental Prediction.

Jin, Q., J. Wei, Z.-L. Yang, B. Pu, and J. Huang. 2015. "Consistent response of Indian summer monsoon to Middle East dust in observations and simulations." *Atmospheric Chemistry and Physics* no. 1680:7324. doi: 10.5194/acp-15-9897-2015.

Kain, John S. 2004. "The Kain–Fritsch convective parameterization: an update." *Journal of Applied Meteorology* no. 43 (1):170-181. doi: 10.1175/1520-0450(2004)043<0170:TKCPAU>2.0.CO;2.

Khain, A, D Rosenfeld, and A Pokrovsky. 2005. "Aerosol impact on the dynamics and microphysics of deep convective clouds." *Quarterly Journal of the Royal Meteorological Society* no. 131 (611):2639-2663. doi: doi: 10.1256/qj.04.62.

Khain, AP, KD Beheng, A Heymsfield, A Korolev, SO Krichak, Z Levin, M Pinsky, Vaughan Phillips, T Prabhakaran, and A Teller. 2015. "Representation of microphysical processes in cloud-resolving models: Spectral (bin) microphysics versus bulk parameterization." *Reviews of Geophysics* no. 53 (2):247-322. doi: 10.1002/2014RG000468.

Khain, AP, N BenMoshe, and A Pokrovsky. 2008. "Factors determining the impact of aerosols on surface precipitation from clouds: An attempt at classification." *Journal of the Atmospheric Sciences* no. 65 (6):1721-1748. doi: 10.1175/2007JAS2515.1.

Knupp, Kevin R, and William R Cotton. 1982. "An intense, quasi-steady thunderstorm over mountainous terrain. Part II: Doppler radar observations of the storm morphological structure." *Journal of the Atmospheric Sciences* no. 39 (2):343-358.

Koch, D, and AD Del Genio. 2010. "Black carbon semi-direct effects on cloud cover: review and synthesis." *Atmospheric Chemistry and Physics* no. 10 (16):7685-7696. doi: 10.5194/acp-10-7685-2010.

Kucienska, B, GB Raga, and R Romero-Centeno. 2012. "High lightning activity in maritime clouds near Mexico." *Atmospheric Chemistry and Physics* no. 12 (17):8055-8072. doi: 10.5194/acp-12-8055-2012.

Lang, S, WK Tao, J Simpson, R Cifelli, S Rutledge, W Olson, and J Halverson. 2007. "Improving simulations of convective systems from TRMM LBA: Easterly and westerly regimes." *Journal of the Atmospheric Sciences* no. 64 (4):1141-1164. doi: 10.1175/JAS3879.1.

Lau, KM, SC Tsay, C Hsu, M Chin, V Ramanathan, GX Wu, Z Li, R Sikka, B Holben, and D Lu. 2008. "The Joint Aerosol–Monsoon Experiment: A new challenge for monsoon

climate research." *Bulletin of the American Meteorological Society* no. 89 (3):369-383. doi: 10.1175/BAMS-89-3-369.

Lee, S. S., L. J. Donner, V. T. J. Phillips, and Y. Ming. 2008. "Examination of aerosol effects on precipitation in deep convective clouds during the 1997 ARM summer experiment." *Quarterly Journal of the Royal Meteorological Society* no. 134 (634):1201-1220. doi: 10.1002/qj.287.

Lee, Seoung-Soo, Wei-Kuo Tao, and Chang-Hoon Jung. 2014. "Aerosol effects on instability, circulations, clouds, and precipitation." *Advances in Meteorology* no. 2014. doi: 10.1155/2014/683950.

Levy, R., and C. Hsu. 2015. MODIS Atmosphere L2 Aerosol Product. NASA MODIS Adaptive Processing System, Goddard Space Flight Center, USA: http://dx.doi.org/10.5067/MODIS/MYD04_L2.006.

Levy, Robert C., S. Mattoo, L. A. Munchak, L. A. Remer, A. M. Sayer, F. Patadia, and N. C. Hsu. 2013. "The Collection 6 MODIS aerosol products over land and ocean." *Atmospheric Measurement Techniques* no. 6 (11):2989-3034. doi: 10.5194/amt-6-2989-2013.

Li, Yaping, Edward J Zipser, Steven K Krueger, and Mike A Zulauf. 2008. "Cloud-resolving modeling of deep convection during KWAJEX. Part I: Comparison to TRMM satellite and ground-based radar observations." *Monthly Weather Review* no. 136 (7):2699-2712. doi: 10.1175/2007MWR2258.1.

Li, Zhanqing, Jianping Guo, Aijun Ding, Hong Liao, Jianjun Liu, Yele Sun, Tijian Wang, Huiwen Xue, Hongsheng Zhang, and Bin Zhu. 2017. "Aerosol and boundary-layer

interactions and impact on air quality." *National Science Review*. doi: 10.1093/nsr/nwx117.

Li, Zhanqing, Kwon-Ho Lee, Yuesi Wang, Jinyuan Xin, and Wei-Min Hao. 2010. "First observation-based estimates of cloud-free aerosol radiative forcing across China." *Journal of Geophysical Research: Atmospheres* no. 115 (D7). doi: 10.1029/2009JD013306.

Lin, Yun, Yuan Wang, Bowen Pan, Jiaxi Hu, Yangang Liu, and Renyi Zhang. 2016. "Distinct impacts of aerosols on an evolving continental cloud complex during the RACORO field campaign." *Journal of the Atmospheric Sciences* no. 73 (9). doi: 10.1175/JAS-D-15-0361.1.

Lynn, B, and Y Yair. 2010. "Prediction of lightning flash density with the WRF model." *Advances in Geosciences* no. 23:11-16. doi: 10.5194/adgeo-23-11-2010.

Lynn, Barry H, Alexander P Khain, Jimy Dudhia, Daniel Rosenfeld, Andrei Pokrovsky, and Axel Seifert. 2005. "Spectral (bin) microphysics coupled with a mesoscale model (MM5). Part II: Simulation of a CaPE rain event with a squall line." *Monthly Weather Review* no. 133 (1):59-71. doi: 10.1175/MWR-2841.1.

Matsui, Toshihisa, Xiping Zeng, Wei-Kuo Tao, Hirohiko Masunaga, William S Olson, and Stephen Lang. 2009. "Evaluation of long-term cloud-resolving model simulations using satellite radiance observations and multifrequency satellite simulators." *Journal of Atmospheric and Oceanic Technology* no. 26 (7):1261-1274. doi: 10.1175/2008JTECHA1168.1.

McCaul Jr, Eugene W, Steven J Goodman, Katherine M LaCasse, and Daniel J Cecil. 2009. "Forecasting lightning threat using cloud-resolving model simulations." *Weather and Forecasting* no. 24 (3):709-729. doi: 10.1175/2008WAF2222152.1.

Menon, Surabi, James Hansen, Larissa Nazarenko, and Yunfeng Luo. 2002. "Climate Effects of Black Carbon Aerosols in China and India." *Science* no. 297 (5590):2250-2253. doi: 10.1126/science.1075159.

Mlawer, Eli J, Steven J Taubman, Patrick D Brown, Michael J Iacono, and Shepard A Clough. 1997. "Radiative transfer for inhomogeneous atmospheres: RRTM, a validated correlated-k model for the longwave." *Journal of Geophysical Research: Atmospheres* no. 102 (D14):16663-16682. doi: 10.1029/97JD00237

Morrison, Hugh. 2012. "On the robustness of aerosol effects on an idealized supercell storm simulated with a cloud system-resolving model." *Atmospheric Chemistry and Physics* no. 12 (16):7689-7705. doi: 10.5194/acp-12-7689-2012.

Omar, Ali H, David M Winker, Mark A Vaughan, Yongxiang Hu, Charles R Trepte, Richard A Ferrare, Kam-Pui Lee, Chris A Hostetler, Chieko Kittaka, and Raymond R Rogers. 2009. "The CALIPSO automated aerosol classification and lidar ratio selection algorithm." *Journal of Atmospheric and Oceanic Technology* no. 26 (10):1994-2014. doi: 10.1175/2009JTECHA1231.1.

Pal, Jeremy S, Filippo Giorgi, Xunqiang Bi, Nellie Elguindi, Fabien Solmon, Xuejie Gao, Sara A Rauscher, Raquel Francisco, Ashraf Zakey, and Jonathan Winter. 2007. "Regional climate modeling for the developing world: the ICTP RegCM3 and RegCNET." *Bulletin of the American Meteorological Society* no. 88 (9):1395-1410. doi: 10.1175/BAMS-88-9-1395.

Petters, MD, and SM Kreidenweis. 2007. "A single parameter representation of hygroscopic growth and cloud condensation nucleus activity." *Atmospheric Chemistry and Physics* no. 7 (8):1961-1971. doi: 10.5194/acp-7-1961-2007.

Proestakis, E, S Kazadzis, K Lagouvardos, V Kotroni, V Amiridis, E Marinou, C Price, and A Kazantzidis. 2016. "Aerosols and lightning activity: The effect of vertical profile and aerosol type." *Atmospheric Research* no. 182:243-255. doi: 10.1016/j.atmosres.2016.07.031.

Prospero, Joseph M. 1999. "Long-range transport of mineral dust in the global atmosphere: Impact of African dust on the environment of the southeastern United States." *Proceedings of the National Academy of Sciences* no. 96 (7):3396-3403. doi: 10.1073/pnas.96.7.3396.

Qian, Yun, and Filippo Giorgi. 1999. "Interactive coupling of regional climate and sulfate aerosol models over eastern Asia." *Journal of Geophysical Research: Atmospheres* no. 104 (D6):6477-6499. doi: 10.1029/98JD02347

Ramanathan, VCPJ, PJ Crutzen, JT Kiehl, and Dm Rosenfeld. 2001. "Aerosols, climate, and the hydrological cycle." *Science* no. 294 (5549):2119-2124. doi: 10.1126/science.1064034.

Rosenfeld, D., U. Lohmann, G. B. Raga, C. D. O'Dowd, M. Kulmala, S. Fuzzi, A. Reissell, and M. O. Andreae. 2008. "Flood or drought: how do aerosols affect precipitation?" *Science* no. 321 (5894):1309-1313. doi: 10.1126/science.1160606.

Rosenfeld, Daniel, Meinrat O Andreae, Ari Asmi, Mian Chin, Gerrit Leeuw, David P Donovan, Ralph Kahn, Stefan Kinne, Niku Kivekäs, and Markku Kulmala. 2014. "Global observations of aerosol-cloud-precipitation-climate interactions." *Reviews of Geophysics* no. 52:750 – 808. doi: 10.1002/2013RG000441.

Rotunno, Richard, Joseph B Klemp, and Morris L Weisman. 1988. "A theory for strong, long-lived squall lines." *Journal of the Atmospheric Sciences* no. 45 (3):463-485. doi: 10.1175/1520-0469(1988)045<0463:ATFSLL>2.0.CO;2.

Saide, Pablo E, Gregory Thompson, Trude Eidhammer, Arlindo M Silva, R Bradley Pierce, and Gregory R Carmichael. 2016. "Assessment of biomass burning smoke influence on environmental conditions for multiyear tornado outbreaks by combining aerosol-aware microphysics and fire emission constraints." *Journal of Geophysical Research: Atmospheres* no. 121 (17). doi: 10.1002/2016JD025056.

Saide, PE, SN Spak, RB Pierce, JA Otkin, TK Schaack, AK Heidinger, AM Silva, M Kacenelenbogen, J Redemann, and GR Carmichael. 2015. "Central American biomass burning smoke can increase tornado severity in the US." *Geophysical Research Letters* no. 42 (3):956-965. doi: 10.1002/2014GL062826.

Sassen, Kenneth, Paul J DeMott, Joseph M Prospero, and Michael R Poellot. 2003. "Saharan dust storms and indirect aerosol effects on clouds: CRYSTAL-FACE results." *Geophysical Research Letters* no. 30 (12):1633. doi: 10.1029/2003GL017371.

Schultz, Christopher J, Lawrence D Carey, Elise V Schultz, and Richard J Blakeslee. 2017. "Kinematic and microphysical significance of lightning jumps versus nonjump increases in total flash rate." *Weather and Forecasting* no. 32 (1):275-288. doi: 10.1175/WAF-D-15-0175.1.

Seifert, A, and KD Beheng. 2006. "A two-moment cloud microphysics parameterization for mixed-phase clouds. Part 2: Maritime vs. continental deep convective storms." *Meteorology and Atmospheric Physics* no. 92 (1-2):67-82. doi: 10.1007/s00703-005-0113-3.

Shi, JJ, T Matsui, W-K Tao, Q Tan, C Peters-Lidard, M Chin, K Pickering, N Guy, S Lang, and EM Kemp. 2014. "Implementation of an aerosol-cloud-microphysics-radiation coupling into the NASA unified WRF: Simulation results for the 6–7 August 2006 AMMA special observing period." *Quarterly Journal of the Royal Meteorological Society* no. 140 (684):2158-2175. doi: 10.1002/qj.2286.

Skamarock, W. C., J. B. Klemp, J. Dudhia, D. O. Gill, D. M. Barker, M. G. Duda, X.-Y. Huang, W. Wang, and J. G. Powers. 2008. "A description of theadvanced research WRF version 3." *NCAR Tech. Note NCAR/TN–475+STR*:1-96.

Skamarock, William C, and Joseph B Klemp. 2008. "A time-split nonhydrostatic atmospheric model for weather research and forecasting applications." *Journal of Computational Physics* no. 227 (7):3465-3485. doi: 10.1016/j.jcp.2007.01.037.

Stanford, McKenna W, Adam Varble, Ed Zipser, J Walter Strapp, Delphine Leroy, Alfons Schwarzenboeck, Rodney Potts, and Alain Protat. 2017. "A ubiquitous ice size bias in simulations of tropical deep convection." *Atmospheric Chemistry and Physics* no. 17 (15):9599. doi: 10.5194/acp-17-9599-2017.

Stevens, Bjorn, and Graham Feingold. 2009. "Untangling aerosol effects on clouds and precipitation in a buffered system." *Nature* no. 461 (7264):607. doi: 10.1038/nature08281.

Tao, Wei-Kuo, Jen-Ping Chen, Zhanqing Li, Chien Wang, and Chidong Zhang. 2012. "Impact of aerosols on convective clouds and precipitation." *Reviews of Geophysics* no. 50 (2). doi: 10.1029/2011RG000369

Tao, Wei-Kuo, Xiaowen Li, Alexander Khain, Toshihisa Matsui, Stephen Lang, and Joanne Simpson. 2007. "Role of atmospheric aerosol concentration on deep convective

precipitation: Cloud-resolving model simulations." *Journal of Geophysical Research: Atmospheres* no. 112 (D24). doi: 10.1029/2007JD008728.

Thompson, Gregory, and Trude Eidhammer. 2014. "A study of aerosol impacts on clouds and precipitation development in a large winter cyclone." *Journal of the Atmospheric Sciences* no. 71 (10):3636-3658.

Thompson, Gregory, Paul R Field, Roy M Rasmussen, and William D Hall. 2008. "Explicit forecasts of winter precipitation using an improved bulk microphysics scheme. Part II: Implementation of a new snow parameterization." *Monthly Weather Review* no. 136 (12):5095-5115. doi: 10.1175/2008MWR2387.1.

Thompson, Gregory, Roy M Rasmussen, and Kevin Manning. 2004. "Explicit forecasts of winter precipitation using an improved bulk microphysics scheme. Part I: Description and sensitivity analysis." *Monthly Weather Review* no. 132 (2):519-542. doi: 10.1175/1520-0493(2004)132<0519:EFOWPU>2.0.CO;2.

Thornton, Joel A, Katrina S Virts, Robert H Holzworth, and Todd P Mitchell. 2017. "Lightning enhancement over major oceanic shipping lanes." *Geophysical Research Letters* no. 44:9102-9111. doi: 10.1002/2017GL074982.

van den Heever, Susan C, Gustavo G Carrió, William R Cotton, Paul J DeMott, and Anthony J Prenni. 2006. "Impacts of nucleating aerosol on Florida storms. Part I: Mesoscale simulations." *Journal of the Atmospheric Sciences* no. 63 (7):1752-1775. doi: 10.1175/JAS3713.1.

van den Heever, Susan C, and William R Cotton. 2007. "Urban aerosol impacts on downwind convective storms." *Journal of Applied Meteorology and Climatology* no. 46 (6):828-850. doi: 10.1175/JAM2492.1.

van den Heever, Susan C, Graeme L Stephens, and Norman B Wood. 2011. "Aerosol indirect effects on tropical convection characteristics under conditions of radiative–convective equilibrium." *Journal of the Atmospheric Sciences* no. 68 (4):699-718.

Varble, Adam, Ann M Fridlind, Edward J Zipser, Andrew S Ackerman, Jean-Pierre Chaboureau, Jiwen Fan, Adrian Hill, Sally A McFarlane, Jean-Pierre Pinty, and Ben Shipway. 2011. "Evaluation of cloud-resolving model intercomparison simulations using TWP-ICE observations: Precipitation and cloud structure." *Journal of Geophysical Research: Atmospheres* no. 116 (D12). doi: 10.1029/2010JD015180.

Varble, Adam, Edward J Zipser, Ann M Fridlind, Ping Zhu, Andrew S Ackerman, Jean-Pierre Chaboureau, Scott Collis, Jiwen Fan, Adrian Hill, and Ben Shipway. 2014. "Evaluation of cloud-resolving and limited area model intercomparison simulations using twp-ice observations: 1. Deep convective updraft properties." *Journal of Geophysical Research: Atmospheres* no. 119 (24). doi: 10.1002/2013JD021372.

Vaughan, Mark A, Kathleen A Powell, David M Winker, Chris A Hostetler, Ralph E Kuehn, William H Hunt, Brian J Getzewich, Stuart A Young, Zhaoyan Liu, and Matthew J McGill. 2009. "Fully automated detection of cloud and aerosol layers in the CALIPSO lidar measurements." *Journal of Atmospheric and Oceanic Technology* no. 26 (10):2034-2050. doi: 10.1175/2009JTECHA1228.1.

Wang, Chien. 2005. "A modeling study of the response of tropical deep convection to the increase of cloud condensation nuclei concentration: 1. Dynamics and microphysics." *Journal of Geophysical Research: Atmospheres* no. 110 (D21). doi: 10.1029/2004JD005720.

Wang, Chien. 2013. "Impact of anthropogenic absorbing aerosols on clouds and precipitation: A review of recent progresses." *Atmospheric Research* no. 122:237-249. doi: 10.1016/j.atmosres.2012.11.005.

Wang, Gehui, Renyi Zhang, Mario E Gomez, Lingxiao Yang, Misti Levy Zamora, Min Hu, Yun Lin, Jianfei Peng, Song Guo, and Jingjing Meng. 2016. "Persistent sulfate formation from London Fog to Chinese haze." *Proceedings of the National Academy of Sciences* no. 113 (48):13630-13635. doi: 10.1073/pnas.1616540113.

Wang, Jun, Susan C Van den Heever, and Jeffrey S Reid. 2009. "A conceptual model for the link between Central American biomass burning aerosols and severe weather over the south central United States." *Environmental Research Letters* no. 4 (1):015003. doi: 10.1088/1748-9326/4/1/015003.

Wang, Yuan, Alexei Khalizov, Misti Levy, and Renyi Zhang. 2013. "New Directions: Light absorbing aerosols and their atmospheric impacts." *Atmospheric Environment* no. 81:713-715. doi: 10.1016/j.atmosenv.2013.09.034.

Weisman, Morris L, and Richard Rotunno. 2004. "“A theory for strong long-lived squall lines” revisited." *Journal of the Atmospheric Sciences* no. 61 (4):361-382. doi: 10.1175/1520-0469(2004)061<0361:ATFSLS>2.0.CO;2.

White, Bethan, Edward Gryspeerdt, Philip Stier, Hugh Morrison, Gregory Thompson, and Zak Kipling. 2017. "Uncertainty from choice of microphysics scheme in convection-permitting models significantly exceeds aerosol effects." *Atmospheric Chemistry and Physics* no. 17:12145-12175. doi: 10.5194/acp-17-12145-2017.

Wilcox, Eric M, Rick M Thomas, Puppala S Praveen, Kristina Pistone, Frida A-M Bender, and Veerabhadran Ramanathan. 2016. "Black carbon solar absorption suppresses turbulence

in the atmospheric boundary layer." *Proceedings of the National Academy of Sciences*:201525746. doi: 10.1073/pnas.1525746113.

Winker, D. 2016. CALIPSO LID_L2_VFM-Standard HDF File - Version 4.10 [Data set]. NASA Langley Atmospheric Science Data Center DAAC. https://doi.org/10.5067/caliop/calipso/lid_l2_vfm-standard-v4-10.

Wong, J, MC Barth, and D Noone. 2013. "Evaluating a lightning parameterization based on cloud-top height for mesoscale numerical model simulations." *Geoscientific Model Development* no. 6 (2):429. doi: 10.5194/gmd-6-429-2013.

Wu, Longtao, Hui Su, and Jonathan H Jiang. 2011. "Regional simulations of deep convection and biomass burning over South America: 2. Biomass burning aerosol effects on clouds and precipitation." *Journal of Geophysical Research: Atmospheres* no. 116 (D17). doi: 10.1029/2011JD016106.

Yair, Yoav, Barry Lynn, Colin Price, Vassiliki Kotroni, Konstantinos Lagouvardos, Efrat Morin, Alberto Mugnai, and Maria del Carmen Llasat. 2010. "Predicting the potential for lightning activity in Mediterranean storms based on the Weather Research and Forecasting (WRF) model dynamic and microphysical fields." *Journal of Geophysical Research: Atmospheres* no. 115 (D4). doi: 10.1029/2008JD010868.

Yu, Hongbin, SC Liu, and RE Dickinson. 2002. "Radiative effects of aerosols on the evolution of the atmospheric boundary layer." *Journal of Geophysical Research: Atmospheres* no. 107 (D12). doi: 10.1029/2001JD000754.

Zaveri, Rahul A, Richard C Easter, Jerome D Fast, and Leonard K Peters. 2008. "Model for simulating aerosol interactions and chemistry (MOSAIC)." *Journal of Geophysical Research: Atmospheres* no. 113 (D13). doi: 10.1029/2007JD008782.

Zhang, Yan, Rong Fu, Hongbin Yu, Robert E Dickinson, Robinson Negron Juarez, Mian Chin, and Hui Wang. 2008. "A regional climate model study of how biomass burning aerosol impacts land-atmosphere interactions over the Amazon." *Journal of Geophysical Research: Atmospheres* no. 113 (D14). doi: 10.1029/2007JD009449.

Zhao, C., X. Liu, and L. R. Leung. 2012. "Impact of the Desert dust on the summer monsoon system over Southwestern North America." *Atmospheric Chemistry and Physics* no. 12 (8):3717-3731. doi: 10.5194/acp-12-3717-2012.

Zhao, Chun, Xiaohong Liu, LR Leung, Ben Johnson, Sally A McFarlane, WI Gustafson Jr, Jerome D Fast, and R Easter. 2010. "The spatial distribution of mineral dust and its shortwave radiative forcing over North Africa: modeling sensitivities to dust emissions and aerosol size treatments." *Atmospheric Chemistry and Physics* no. 10 (18):8821-8838. doi: 10.5194/acp-10-8821-2010.

Zhao, Chun, Xiaohong Liu, L Ruby Leung, and S Hagos. 2011. "Radiative impact of mineral dust on monsoon precipitation variability over West Africa." *Atmospheric Chemistry and Physics* no. 11 (5):1879-1893. doi: 10.5194/acp-11-1879-2011.

5. SUMMARY

Through analyzing data from satellite, sun photometer, radar, reanalysis, lightning mapping array, and model simulations, we find satellite AOD retrievals become more useful in lightning predictions in particular meteorological conditions including the low CAPE regime. The correlation between AOD and lightning FR rises in the presence of absorbing aerosols, especially in the low CAPE regime. In addition, in the presence of absorbing aerosols, AOD and CAPE show an increased positive correlation; AOD and PBLH show a more negative correlation. The positive correlation between AOD and lightning FR is contributed by the association between AOD and storm area. However, the mean flash rate per unit storm area does not appear to correlate with AOD. Aerosol lightning enhancement may be associated with enhanced low-level vertical wind shear and secondary convection, which results from both the radiative and microphysical effects of aerosols. Based on idealized model experiments, we further show that daytime homogeneous heating layers above or within the planetary boundary layer (PBL) result in enhanced updrafts and cloud ice content over the updraft areas of the nighttime storms. A heating layer above the PBL suppresses deep convection in the early afternoon and enhances nighttime storms with stronger LLVWS when the accumulated CAPE is released. A heating layer within the PBL delays the onset of the nighttime storms and may result in a faster development of the storms at night. The enhanced evaporation of cloud and rain water droplets right before the onset of nighttime storms in the presence of the heating layer within the PBL may contribute to the onset delay. Overall, the enhancements of updraft area, cloud ice content, and LLVWS by the heating layers are not monotonic with respect to the water-nucleating aerosol number concentration. The updraft area enhancement in the most polluted

case is greater than those in the cleanest cases, suggesting a potentially stronger impact of absorbing aerosols on the deep convection over the most pollution urban areas in the world.

The increased correlation between AOD and lightning FR in particular meteorological regimes suggest the potential of applying AOD retrievals from geostationary satellites—such as GOES-R and Fengyun-4 satellites—in improved predictions of enhanced lightning in these meteorological regimes. In addition, lightning activity is closely related to nitrogen oxides and ozone in the atmosphere, which in turn play a role in determining the life time of atmospheric methane that is an important greenhouse gas (Schumann and Huntrieser 2007, Fiore et al. 2006). The increased correlation between AOD and lightning FR in the presence of absorbing aerosols suggests the importance of studying the influence of anthropogenic biomass burning on lightning activity and atmospheric methane concentration in the future. The observational and modeling results that support the CAPE- and PBL-mechanisms suggest additional thought and discussions on whether aerosol radiative and microphysical effects need to be taken into consideration in cumulus parameterization schemes.

5.1. References

Fiore, Arlene M, Larry W Horowitz, Edward J Dlugokencky, and J Jason West. 2006. "Impact of meteorology and emissions on methane trends, 1990–2004." *Geophysical Research Letters* no. 33 (12). doi: 10.1029/2006GL026199.

Schumann, Ulrich, and Heidi Huntrieser. 2007. "The global lightning-induced nitrogen oxides source." *Atmospheric Chemistry and Physics* no. 7 (14):3823-3907. doi: 10.5194/acp-7-3823-2007.